Multifunctional Catalysts for Ring-Opening Copolymerizations

Claire A. L. Lidston,[†] Sarah M. Severson,[†] Brooks A. Abel, and Geoffrey W. Coates*

ABSTRACT: The ring-opening copolymerization (ROCOP) of epoxides with CO_2 or cyclic anhydrides is a versatile route toward synthesizing a wide range of polycarbonate and polyester copolymers. ROCOP most commonly uses binary catalyst systems comprising separate Lewis acid and nucleophilic cocatalyst components. However, the dependence on two discrete catalyst components leads to low activities at low loadings, and binary catalyst systems are prone to numerous side reactions. It was therefore proposed that covalently tethering the Lewis acid catalyst and cocatalyst together would increase both catalyst activity and selectivity in epoxide ROCOP. Since these initial efforts, many multifunctional catalysts featuring covalently tethered cationic or Lewis base cocatalyst(s) have been developed for epoxide ROCOP. This review examines multifunctional catalysts that have been developed for copolymerization of epoxides with CO_2, cyclic anhydrides, carbonyl sulfide (COS), and cyclic thioanhydrides. In particular, we will assess how multifunctional catalysts' mechanisms of operations lead to improved activity and selectivity in ROCOP.

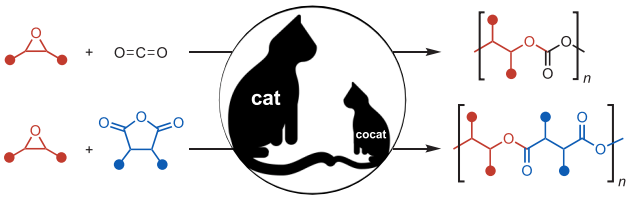

KEYWORDS: *multifunctional catalysts, epoxides, cyclic anhydrides, CO_2, ring-opening copolymerization, polyesters, polycarbonates*

1. INTRODUCTION

1.1. Background. The development of efficient and selective multifunctional catalysts for the alternating copolymerization of epoxides with either carbon dioxide (CO_2) or cyclic anhydrides has provided a controlled, versatile route toward semiaromatic and aliphatic polycarbonates and polyesters, respectively. Polycarbonates and polyesters are important classes of commodity plastics used extensively in packing, fiber, and film applications due to their mechanical strength and chemical resistance.[1] Aliphatic polycarbonates or polyesters can biodegrade into benign byproducts, enabling their use as sustainable alternatives to petroleum-derived and nondegradable plastics.[2−10]

Generally, commercial polycarbonates and polyesters are synthesized via step-growth condensation polymerizations.[1] While condensation approaches take advantage of the wide range of commercially available diols and diacids, the generation of water, alcohol, or acid condensation byproducts requires elevated temperatures and reduced pressures to achieve the high conversions needed to access high molecular weight materials. Also, the use of comonomers such as phosgene for polycarbonate synthesis introduces additional challenges due to its toxicity and corrosiveness.

Chain-growth polymerizations are atom economical alternatives to step-growth condensation reactions and enable molecular weight control based on the monomer to initiator ratio and percent conversion, with improved access to high molecular weight polymers with low dispersities. Furthermore, the use of controlled or "living" chain-growth polymerizations allows for the synthesis of more complex polymer architectures such as block copolymers. Chain-growth methods of polycarbonate synthesis include ring-opening polymerization (ROP) of cyclic carbonates and ring-opening copolymerization (ROCOP) of epoxides and CO_2.[11] Polyesters can be analogously synthesized from either ROP of lactones or ROCOP of epoxides and cyclic anhydrides.[2] Although ROP of cyclic carbonates or lactones enables molecular weight control and the synthesis of block copolymers, the functionalities and properties of the resulting materials are limited by the narrower monomer scope.[12]

1.2. Epoxide Copolymerization. The copolymerizations of epoxides and CO_2 or epoxides and cyclic anhydrides not only demonstrate controlled or "living" behavior but also enable the synthesis of a wide range of polycarbonates and polyesters owing to the diverse scope of readily available epoxides and cyclic anhydrides, many of which are renewably sourced (Scheme 1).[13,14] CO_2 is also an ideal and sustainable comonomer for polycarbonate synthesis owing to its low cost, low toxicity, and natural abundance. Sulfur-containing polymers can be synthesized by ROCOP using carbonyl sulfide (COS) and/or cyclic thioanhydrides as monomers,

Scheme 1. Generalized Copolymerization of Epoxides with (a) CO_2 and (b) Cyclic Anhydrides

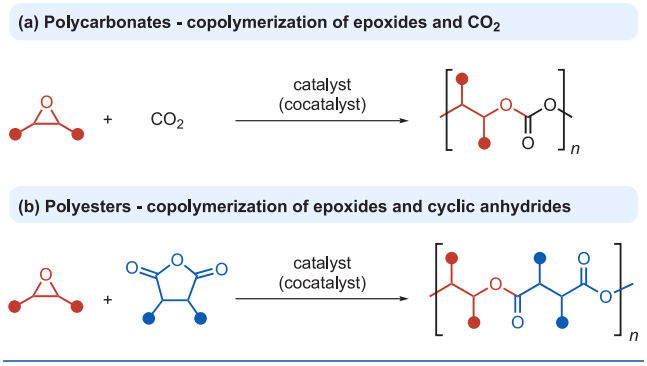

which react similarly to their oxygenated analogues.[15−17] The wide range of properties afforded by polyesters, polycarbonates, polythioesters, and polythiocarbonates are summarized in several reviews and will not be examined in further detail here.[18−23] Rather, we will focus on efficient and selective polymerization approaches toward these materials, with a strong emphasis on the use of multifunctional catalysts and their mechanisms of operation.

1.3. Catalyst Development. Early examples of epoxide copolymerization were catalyzed by metal alkoxides and amine initiators, but these polymerizations were plagued by low catalytic activity, significant polyether formation, and limited control over molecular weight and dispersity.[24−28] Inoue and co-workers first demonstrated in 1969 that a catalyst system based upon a mixture of diethyl zinc ($ZnEt_2$) and water could control the ROCOP of propylene oxide (PO) and CO_2.[29] Inoue and co-workers also used this catalyst system to synthesize polyesters by ROCOP of phthalic anhydride (PA) with various epoxides.[30] Foreshadowing current mechanistic understanding of ROCOP catalyst systems, zinc alkoxide and carboxylate intermediates were observed during the copolymerizations.[31]

Since these early discoveries, many heterogeneous and homogeneous catalyst systems have been developed for ROCOP. Heterogeneous catalysts such as zinc carboxylates and double metal cyanide complexes (DMCC) often require harsh reaction conditions and permit polyether formation; further, their polymerization mechanism is not well understood.[32−34] Most advancements in catalyst development have therefore focused on the development of homogeneous single-site Lewis acid catalysts. Inoue and co-workers developed the first single-site catalyst, an Al catalyst featuring a tetraphenylporphyrin (TPP) ligand framework, which was active for epoxide/CO_2 copolymerization when 1-methylimidazole (MeIm) was added as an exogenous cocatalyst.[35,36] Inspired by the success of *N*,*N*′-bis(salicylidene)ethylenediamine (salen) chromium catalysts in the asymmetric ring-opening of epoxides, Jacobsen and co-workers demonstrated the use of salen(Cr) catalysts in epoxide/CO_2 copolymerization.[37] Since these initial discoveries, many metal porphyrin complexes, metal salen-type catalysts, and organocatalysts have been developed for epoxide copolymerization with either CO_2 or cyclic anhydrides.[38−45] These single-site complexes commonly require the use of a nucleophilic cocatalyst, which include onium salts such as bis(triphenylphosphine)iminium chloride ([PPN]Cl) and nucleophilic bases such as 4-dimethylaminopyridine (DMAP) or phosphines.

A significant drawback to such binary ROCOP catalyst systems is decreased catalytic efficiency at low loadings, necessitating the use of elevated catalyst concentrations which precludes synthesis of high molecular weight polymers and increases overall cost. The decreased catalyst activity is predominately due to the second-order dependence of polymerization rate on binary catalyst/cocatalyst concentration, leading to an exponential decrease in activity with decreasing loading.

In 2006, Nozaki and co-workers proposed that covalently linking the Lewis acid and cocatalyst would subvert dilution effects on ROCOP catalyst activity. They showed that a multifunctional *N*,*N*′-bis(salicylidene)cyclohexanediamine (salcy)Co(III) catalyst system with a pendant protonated piperidinium cocatalyst maintained catalyst activity at low loadings during epoxide/CO_2 ROCOP. Further, the multifunctional (salcy)Co(III) complex limited side reactions such as cyclic carbonate formation as compared to analogous binary catalyst/cocatalyst systems.[46] Lee[47] and Lu[48] similarly proposed that multifunctional catalysts would maintain proximity between propagating chains and the Lewis acid, preventing catalyst deactivation at low loadings. These hypotheses have since led to the development of numerous multifunctional catalysts that maintain high catalyst activity at low loadings while improving molecular weight control and preventing side reactions.

In this review, we will discuss the development of multifunctional catalysts for ROCOP, focusing on mechanistic functions that guide their improved catalytic activity and selectivity. We will categorize multifunctional catalysts into two general classes: multifunctional catalysts with tethered cations (Chart 1) and multifunctional catalysts with tethered Lewis bases (Chart 2). Although heterobimetallic catalysts also eliminate the need for an exogenous cocatalyst and differentiate the roles of epoxide activation and chain-end control, many excellent reviews have already detailed their development, and we will therefore not discuss them herein.[49−53]

2. MECHANISTIC CONSIDERATIONS OF MULTIFUNCTIONAL CATALYSTS

Extensive mechanistic studies have elucidated the roles of coordination complexes and organocatalysts in ring-opening copolymerizations. As all multifunctional catalysts reported to date incorporate a Lewis acid center, mechanistic discussion will focus on these systems.

During ROCOP, the Lewis acid/nucleophilic cocatalyst pair initiates polymerization, activates epoxide toward ring-opening, and modulates the reactivity of the propagating chain ends. In general, ring-opening of metal-bound epoxide by cocatalyst-associated carbonate or carboxylate chain ends is rate-limiting. Dilution of the catalyst/cocatalyst pair distances the cocatalyst-associated propagating chains from catalyst-activated epoxide, thereby inhibiting epoxide ring-opening (Scheme 2a). Lee[47] and Lu[48] proposed that covalently tethering the Lewis acid and cocatalyst would prevent the growing polymer chain from diffusing away from the Lewis acid, thereby promoting intramolecular epoxide ring-opening (Scheme 2b). While this hypothesis proved sensitive to cocatalyst identity and stoichiometry (vide infra), various multifunctional salen[54−66] and porphyrin[67−69] complexes exhibit improved catalytic activity at decreased loadings as compared to their binary analogues.

Chart 1. Cationic Multifunctional ROCOP Catalysts

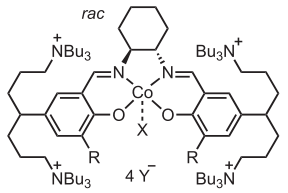

cat1: R = Me, X = Y = DNP
cat2: R = ^{t}Bu, X = Y = DNP
cat3: R = Me, X = Y = BF_4
cat4: R = ^{t}Bu, X = Y = BF_4

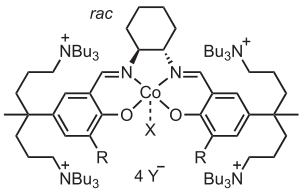

cat5: X = BF_4, Y = DNP, R = Me
cat6: X = OAc, Y = NO_3, R = Me
cat7: X = Cl, Y = TCP, R = Me
cat8: X = Y = TCP, R = ^{t}Bu
cat9: X = Y = TCP, R = Me
cat10: X = DNP, Y = DCP, R = Me

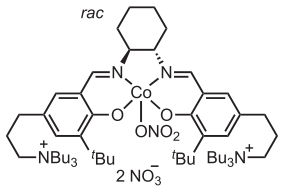

cat11

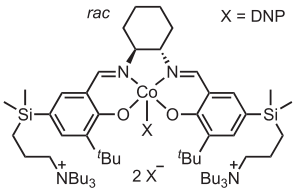

cat12

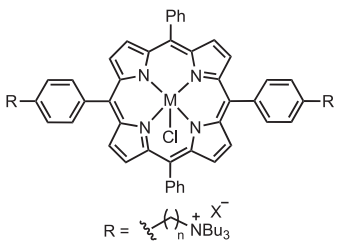

cat13: M = Al, X = Br, n = 2
cat14: M = Al, X = Br, n = 3
cat15: M = Al, X = Br, n = 4
cat16: M = Al, X = Br, n = 5
cat17: M = Al, X = Br, n = 6
cat18: M = Co, X = NO_3, n = 3

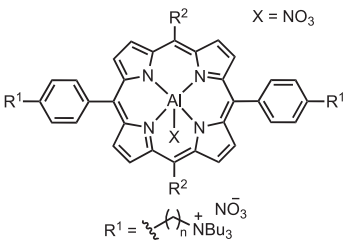

cat19: n = 6, R^2 = Ph
cat20: n = 6, R^2 = *p*-BrPh
cat21: n = 6, R^2 = *p*-OMePh
cat22: n = 3, R^2 = Ph
cat23: n = 3, R^2 = *p*-^{t}BuPh
cat24: n = 3, R^2 = C_6F_5

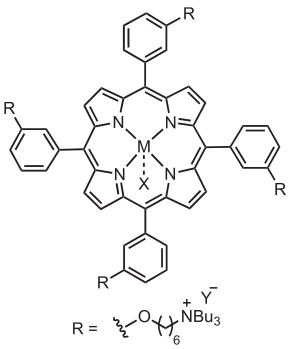

cat25: M = Al, X = Y = Cl
cat26: M = Al, X = Y = Br
cat27: M = Mg, X = N/A, Y = Cl
cat28: M = Mg, X = N/A, Y = Br
cat29: M = Zn, X = N/A, Y = Cl
cat30: M = Zn, X = N/A, Y = Br

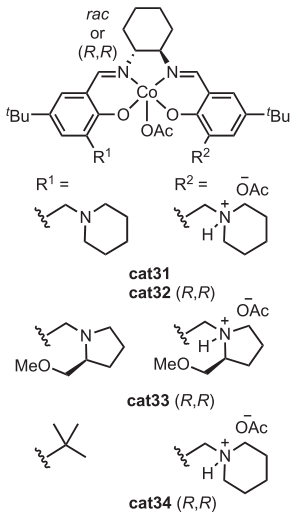

cat31
cat32 (*R*,*R*)
cat33 (*R*,*R*)
cat34 (*R*,*R*)

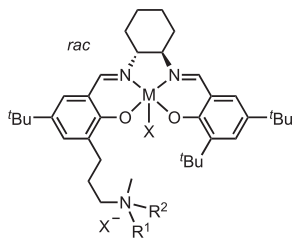

cat35: M = Co, X = DNP, R^1 = Et, R^2 = Et
cat36: M = Co, X = DNP, R^1 = Cy, R^2 = Me
cat37: M = Cr, X = N_3, R^1 = Cy, R^2 = Me

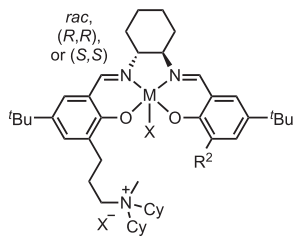

cat38: M = Cr, X = N_3, R = ^{t}Bu
cat39: M = Co, X = DNP, R = ^{t}Bu
cat40: M = Co, X = DNP, R = ^{t}Bu)
cat41: M = Co, X = DNP, R = Ad

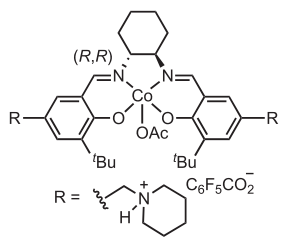

cat42

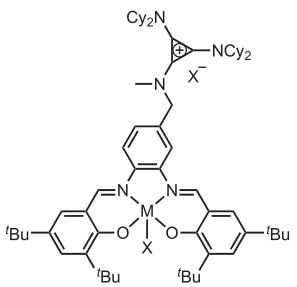

cat43: M = Al, X = Cl
cat44: M = Cr, X = Cl
cat45: M = Co, X = OAc
cat46: M = Fe, X = Cl
cat47: M = Zn, X = Cl
cat48: M = Mn, X = OAc

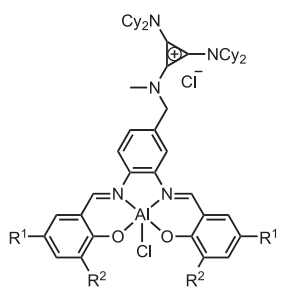

cat49: R^1 = ^{t}Bu, R^2 = Me
cat50: R^1 = ^{t}Bu, R^2 = Ad
cat51: R^1 = F, R^2 = ^{t}Bu
cat52: R^1 = OMe, R^2 = ^{t}Bu

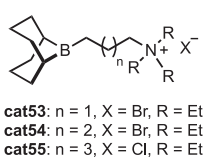

cat53: n = 1, X = Br, R = Et
cat54: n = 2, X = Br, R = Et
cat55: n = 3, X = Cl, R = Et
cat56: n = 3, X = Br, R = Et
cat57: n = 3, X = Br, R = Bu
cat58: n = 3, X = I, R = Et
cat59: n = 4, X = Br, R = Et
cat60: n = 5, X = Br, R = Et

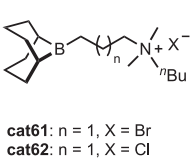

cat61: n = 1, X = Br
cat62: n = 1, X = Cl
cat63: n = 2, X = Br
cat64: n = 3, X = Cl
cat65: n = 3, X = Br
cat66: n = 3, X = I
cat67: n = 4, X = Br

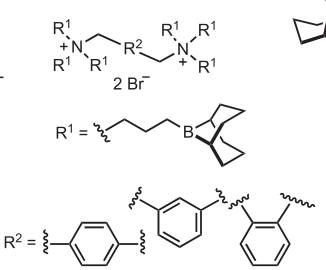

cat68 **cat69** **cat70**

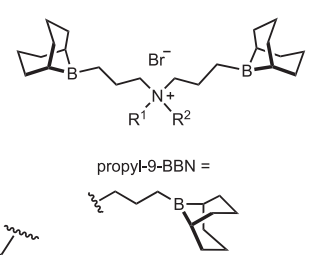

cat71: R^1 = R^2 = propyl-9-BBN
cat72: R^1 = ^{n}Bu, R^2 = propyl-9-BBN
cat73: R^1 = ^{n}Bu, R^2 = Me

2.1. Tethered Cationic Cocatalysts. Lu and co-workers compared the kinetics of epoxide/CO_2 coupling catalyzed by (salcy)Co(III) complexes featuring either a tethered or untethered ammonium cocatalyst using in situ infrared (IR) spectroscopy (Figure 1).[54] The binary (salcy)CoDNP/[TBA]-DNP (DNP = 2,4-dinitrophenol, TBA = tetrabutylammonium) catalyst system exhibited an experimental reaction order of 1.61, consistent with a bimolecular pathway in which the polymerization rate depends on the concentrations of both the (salcy)CoDNP Lewis acid and ammonium cocatalyst. Deviation from the expected second-order behavior was attributed to reduction of Co(III) to inactive Co(II). By contrast, polymerizations catalyzed by multifunctional **cat35** exhibited a first-order rate dependence on catalyst concentration, consistent with intramolecular epoxide ring-opening. Good agreement between the experimental and theoretical

Chart 2. Non-ionic Multifunctional ROCOP Catalysts

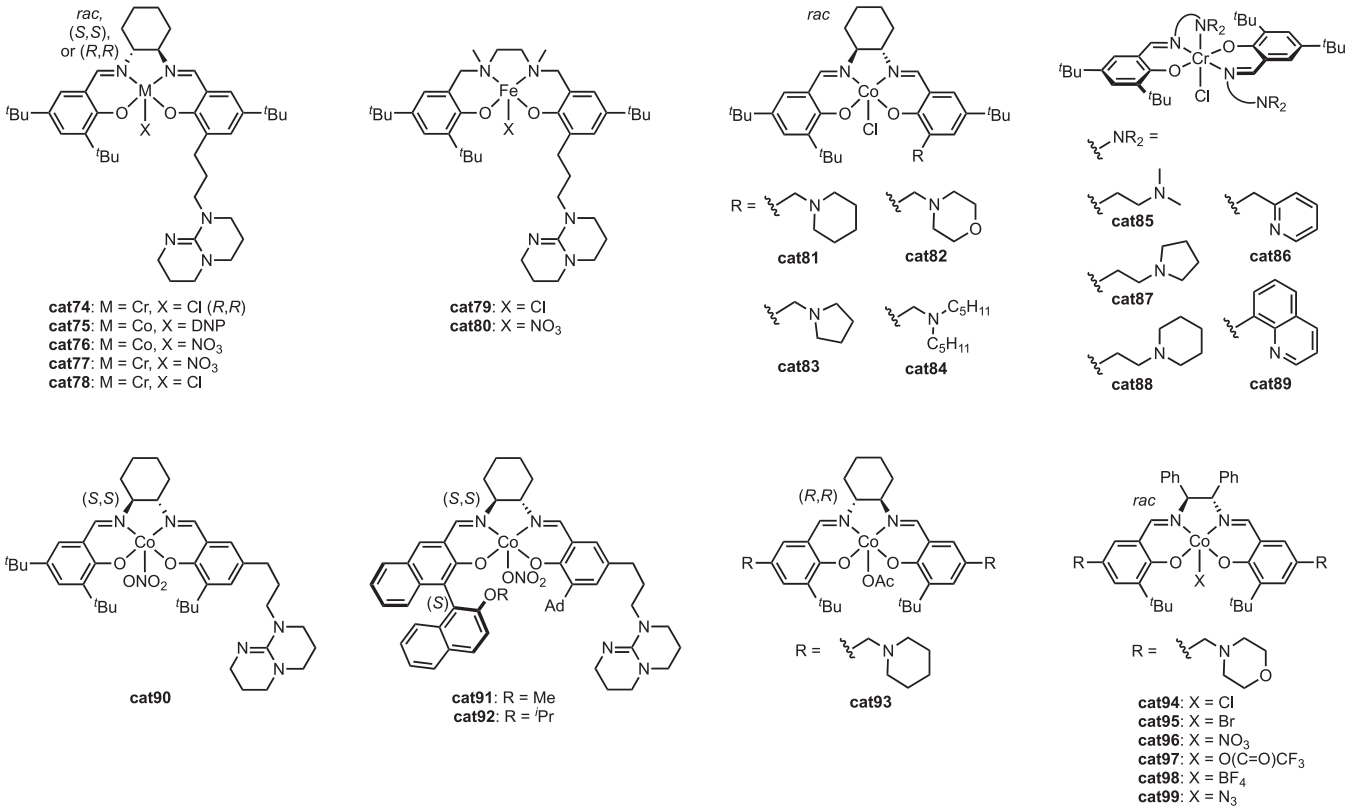

Scheme 2. Generalized Overview of Multifunctional and Binary Catalysts

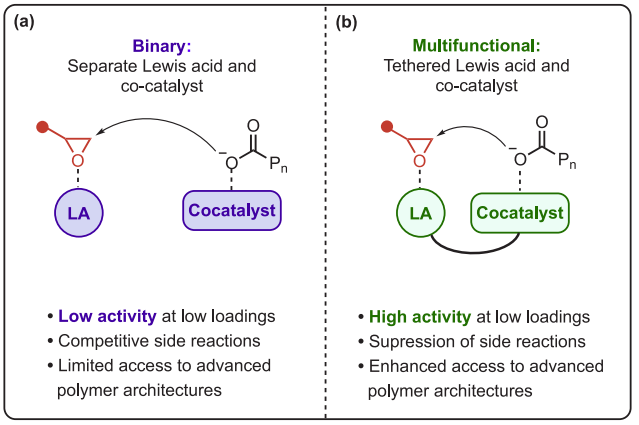

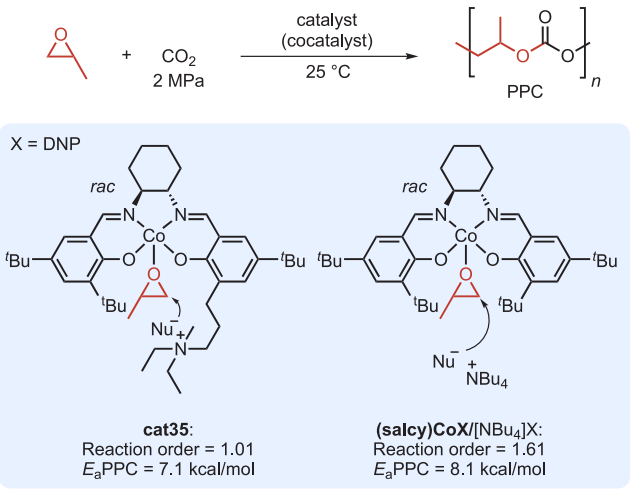

Figure 1. Kinetics of epoxide ring-opening with **cat35** and (salcy)CoX/[Bu_4N]X.

reaction orders suggests that the multifunctional catalyst system is less prone to catalyst deactivation via reduction. Enforcing intramolecular epoxide ring-opening was associated with a 1.02 kcal/mol decrease in the energy of activation for copolymer formation relative to the intermolecular process. Intriguingly, the multifunctional catalyst also eliminated the induction period observed at low loadings in the binary catalyst system.

Hasegawa, Nozaki, Ema, and co-workers recently reported aluminum porphyrin complexes **cat25** and **cat26** bearing four tethered quaternary ammonium cocatalysts that exhibited excellent activity and selectivity for the copolymerization of cyclohexene oxide (CHO) and CO_2 (TOF = 10 000 h^{-1} at 2.0 MPa and T = 120 °C, $[catalyst]_0$:$[CHO]_0$ = 1:40 000, >99% polycarbonate).[70] By contrast, a binary analogue (TPP)AlCl/[PPN]Cl achieved a TOF of only 1600 h^{-1} under the same conditions. Detailed kinetic studies via in situ Fourier-transform (FT) IR spectroscopy revealed a first-order dependence on the concentration of **cat25** and first-order dependence on the concentration of CHO. Polymerization rates were invariant with CO_2 pressure, suggesting zero-order behavior. These reaction orders are consistent with rate-limiting epoxide ring-opening by a carbonate chain end. Repeating experiments at various reaction temperatures afforded an experimental activation energy of 13.2 kcal/mol for polycarbonate formation using multifunctional **cat25**. The

activation energy in the binary (TPP)AlCl/[PPN]Cl system was higher at 16.2 kcal/mol, accounting for the observed lower catalyst activities toward CHO/CO_2 ROCOP. Density functional theory (DFT) calculations using a variant of the multifunctional aluminum porphyrin complex with a single tethered ammonium cocatalyst validated that epoxide ring-opening is rate limiting (E_a = 14.6 kcal/mol), while the barrier to CO_2 insertion is lower (E_a = 7.2 kcal/mol). The Nozaki group has previously proposed that catalytic activity is inversely related to the energetic difference between bound carbonate and bound epoxide;[71] in this system, aluminum's high relative affinity for epoxide makes this exchange thermodynamically favorable. The authors also observed that transition state structures were stabilized by the pendant ammonium cations, corroborating the utility of a tethered cocatalyst. Calculations revealed that carbonate dissociation is 18 kcal/mol more favorable with the multifunctional catalyst than with the binary system.

Coates and co-workers developed a multifunctional *N*,*N*′-bis(salicylidene)phenylenediamine (salph) AlCl catalyst featuring an aminocyclopropenium cocatalyst (**cat43**) that exhibited first-order behavior in the copolymerization of epoxides and cyclic anhydrides. Previously, a detailed mechanistic study of epoxide/cyclic anhydride copolymerization by the Tolman, Cramer, and Coates groups initially suggested a first-order dependence on the concentration of the binary (salph)AlCl/[PPN]Cl system when using a 1 mol % catalyst loading.[72] However, subsequent investigation revealed that this pseudo-first-order kinetic behavior was a feature of high catalyst loadings; at lower catalyst loadings (≤0.083 mol %), time normalization kinetic analysis[73] revealed second-order behavior due to dilution of the active species. By contrast, **cat43** afforded first-order behavior at all loadings studied (0.5−0.025 mol %) (Scheme 3).[56] A first-order dependence on epoxide concentration and a zero-order dependence on cyclic anhydride concentration are consistent with pre-equilibrium epoxide binding and rate-limiting ring-opening. Unlike previously reported complexes featuring onium cocatalysts pendant to the salicylidene moiety, the aminocyclopropenium cocatalyst is installed via the salph backbone; this change in geometry significantly streamlines catalyst synthesis and derivatization without affecting the intramolecular ring-opening mechanism.

Scheme 3. Proposed ROCOP Mechanism Using Multifunctional cat43

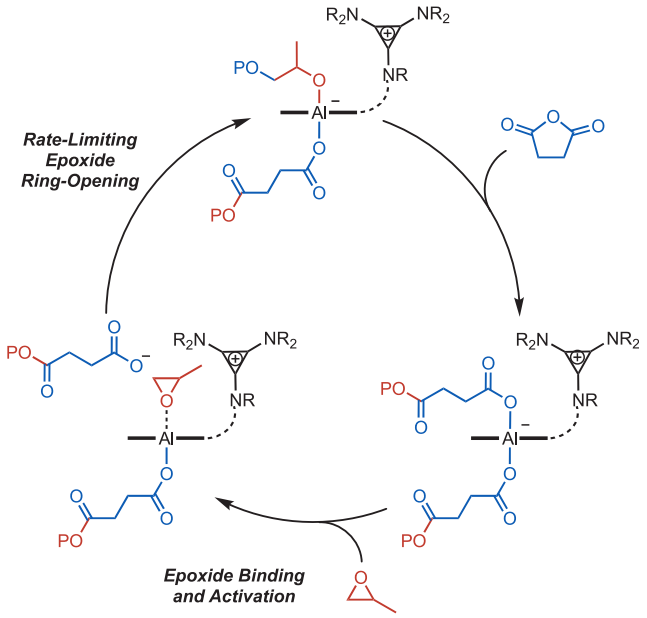

Incorporating a cationic unit to yield a multifunctional catalyst has improved activity in some systems by enforcing intramolecular ring-opening; yet in other cases, multifunctionality prompts a change in the coordination mode of the Lewis acid to afford increased activity. The Lee group reported that increasing the number of ammonium cocatalysts per Co center from two to four increased activity in multifunctional (salcy)CoDNP complexes **cat1** and **cat2** (Figure 2).[65] This result may be attributed to the additional cocatalyst-associated propagating chains accelerating rate-limiting epoxide ring-opening. Presumably, these catalysts, which incorporate up to six covalently tethered ammonium units, facilitate intramolecular epoxide ring-opening to accelerate polymerization at low catalyst loadings. However, Lee and co-workers have further proposed that incorporating multiple covalently tethered ammonium cocatalysts engenders an unusual salen binding geometry in which the Co resides outside the ONNO binding pocket, coordinated by the salen phenoxides and dinitrophenolate (DNP) counterions.[66,74,75] DFT calculations corroborated that the κ^2 imine-uncoordinated structure is energetically favorable. Complexes featuring large *ortho* substituents or sterically encumbered diamine backbones achieved lower polymerization rates than those incorporating less sterically demanding substituents; the authors proposed that the larger substituents enforce the less active κ^4−O,N,N,O-coordinated catalyst geometry.

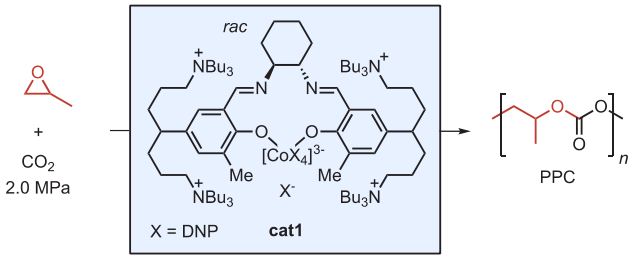

High activity at low catalyst loadings

[PO]:[cat1]	time (min)	TOF (h^{-1})
25,000:1	15	26,000
50,000:1	30	26,000
100,000:1	60	22,000
150,000:1	150	12,400

T = 80 °C

Catalyst recycling

run	time (min)	TOF (h^{-1})	M_n (kDa)
1	65	19,400	296
2	85	14,800	172
3	85	14,800	176
4	80	15,800	190
5	90	13,300	210

[PO]:[**cat1**] = 100,000:1, *T* = 70–77 °C

Figure 2. Activity and recyclability of **cat1** in PO/CO_2 ROCOP.

Wu and co-workers recently developed tethered organocatalysts featuring a 9-borabicyclo(3.3.1)nonane (9-BBN) functionality tethered to an ammonium cation.[76,77] Notably, **cat56** demonstrates high activity for CHO/CO_2 copolymerization across a range of temperatures, reaching a TOF of 4900 h^{-1} at 150 °C. At 80 °C, **cat56** (Figure 3a) maintains a TOF of 710 h^{-1} for the copolymerization of CHO and CO_2, whereas the corresponding binary system consisting of hexyl-9-BBN and butyltriethylammonium bromide (BTEAB) as a cocatalyst

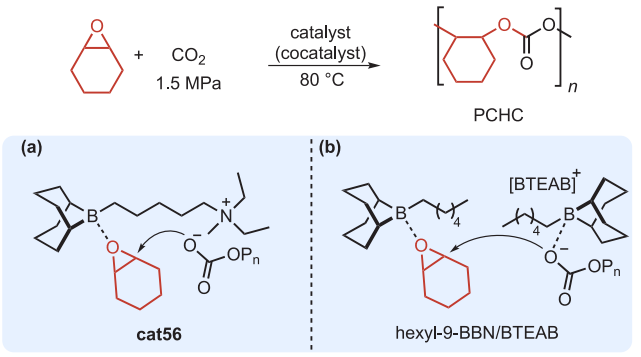

Figure 3. Epoxide ring-opening in CHO/CO_2 ROCOP using multifunctional **cat56** and binary hexyl-9-BBN/BTEAB.

only maintained a TOF of 12 h^{-1}. Consistent with previous reports of epoxide/CO_2 copolymerization mediated by 2 equiv of Et_3B and 1 equiv of [PPN]Cl, the hexyl-9-BBN/BTEAB binary system demonstrated increased activity (TOF = 330 h^{-1}) when a second equiv of hexyl-9-BBN was used (Figure 3b).[78] In contrast, the multifunctional system exhibits a first-order dependence on **cat56** and CHO, and a zero-order dependence on CO_2, consistent with rate-limiting epoxide ring-opening by a carbonate chain end. An experimental activation energy of 13.7 kcal/mol was determined for synthesis of poly(cyclohexene carbonate) (PCHC) by **cat56**. The authors proposed that the multifunctional system's dependence on only one catalytic unit is due to an intramolecular synergistic effect between the boron center and ammonium salt. X-ray crystallographic analysis of **cat56** in DMF identified a flexible pocket within the multifunctional catalyst having a B−N bond distance of 7.025 Å. In the absence of DMF, it is likely that the Br anion may be located within this flexible pocket and may weakly interact with the boron center.[79] Interestingly, DFT analysis suggests that the ammonium cation distributes its positive charge across the hydrogen atoms of the linker carbons, enabling these electropositive α-hydrogens to further stabilize the Br anion. Finally, ^{11}B NMR analysis of **cat56** indicates a broad resonance only present for the multifunctional catalyst, which the authors attribute to an intramolecular synergistic effect between the boron center and ammonium salt. Wu and co-workers proposed that the introduction of CHO displaces the stabilized Br anion, inducing ring-opening by the Br anion and producing a boron-stabilized alkoxide that can readily undergo CO_2 insertion.

2.2. Tethered Lewis Bases. While the majority of ROCOP cocatalysts are based on onium salts comprising a nucleophilic counteranion, organic bases such as 4-dimethylaminopyridine (DMAP)[80] and 7-methyl-1,5,7-triazabicyclo[4.4.0]dec-5-ene (Me-TBD)[81] have also been used successfully as nucleophilic cocatalysts albeit with distinct catalytic behavior. Lu and co-workers published an elegant ESI/MS study investigating the ROCOP behavior of a (salcy)$CoNO_3$ complex with covalently tethered TBD unit (**cat76**).[48] Combining **cat76** and PO resulted in epoxide ring-opening by the TBD group followed by coordination of the resulting TBD^+-alkoxide to the Co center with concomitant dissociation of the original nitrate X-type ligand. Pressurizing the system with CO_2 promoted formation of the tethered Co(III)carbonate, which is the active catalyst for PO/CO_2 copolymerization (Scheme 4a). The 5-coordinate Co(III)-

Scheme 4. (a) Activation of the TBD-Tethered (salcy)$CoNO_3$ Catalyst cat76 via Sequential PO and CO_2 Insertion. (b) ROCOP Catalyzed by the Active Complex

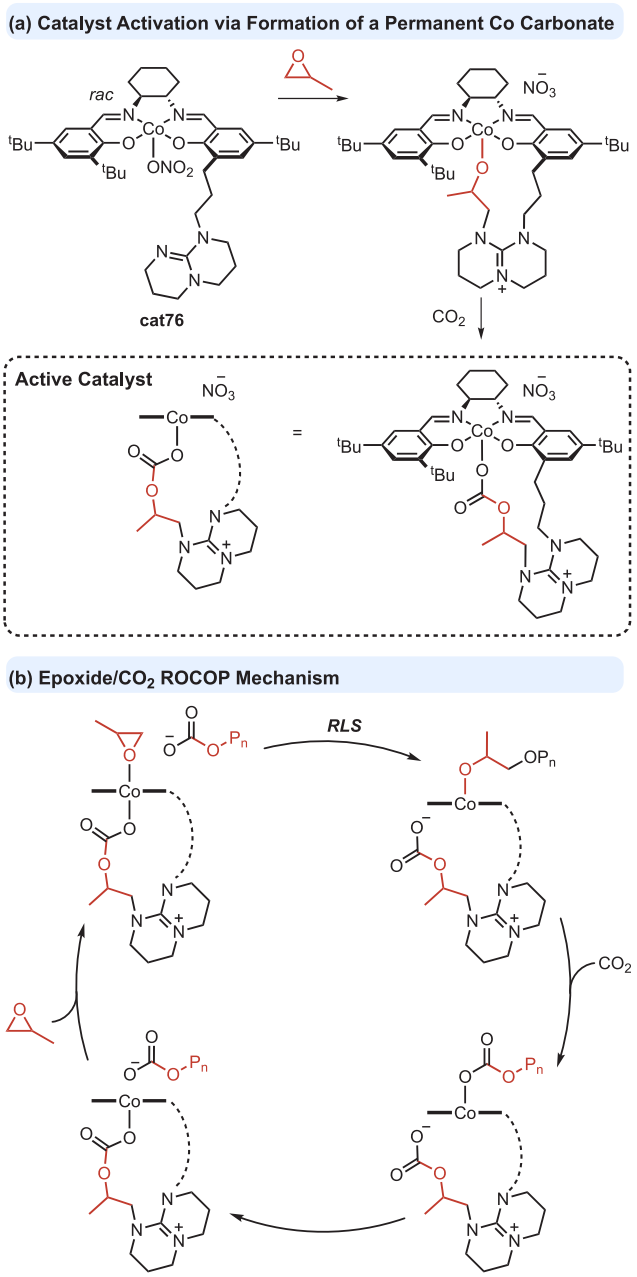

carbonate axially coordinates epoxide, which is ring-opened first by the nitrate anion to initiate polymerization and subsequently by a carbonate chain end during propagation. Formation of the Co(III)alkoxide prompts the tethered TBD^+-carbonate unit to dissociate. CO_2 insertion into the Co(III)-alkoxide bond is rapid, regenerating a carbonate chain end (Scheme 4b). While both the propagating carbonate chain end and the tethered TBD^+-carbonate ligand have similar binding affinities for Co, intramolecular coordination is favored; dissociation of the propagating carbonate chain end turns over the catalytic cycle to afford an open coordination site for epoxide binding. This chelation effect, in fact, precludes catalysis by a (salcy)CoX complex with two tethered TBD units, as intramolecular carbonate coordination produces a coordinatively saturated 6-coordinate Co center that blocks

epoxide binding and activation. The tethered TBD cocatalyst therefore performs a distinct function from tethered cationic (e.g., onium and aminocyclopropenium) cocatalysts: rather than delivering the nucleophilic chain end, the TBD^+-carbonate reversibly dissociates to modulate the electron density at the Co center. The authors further hypothesized that reversible coordination of the TBD^+-carbonate stabilizes the active Co(III) complex against reductive deactivation (vide infra).

Covalently tethered Lewis bases can also serve to directly stabilize the metal center without first reacting with epoxide/CO_2 to form the corresponding carbonate species. Masdeu-Bultó and co-workers developed tridentate NN′O-donor ligands that incorporate pendant Lewis basic trialkylamine (**cat85**), pyridyl (**cat86**), pyrrolidinyl (**cat87**), piperidinyl (**cat88**), or quinolyl (**cat89**) units.[82] Two ligand equivalents in κ^3-N,N,O and κ^2-N,O coordination support a hexacoordinate Cr(III)Cl Lewis acid center and a pendant Lewis base (Figure 4). Only the complex featuring a tethered 2-pyridyl moiety

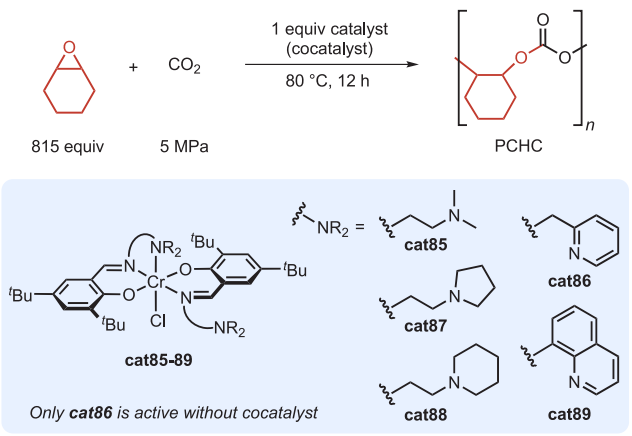

Figure 4. Amine-tethered Cr(III) complexes **cat85**–**cat89**.

(**cat86**) achieved any conversion to polycarbonate in the absence of exogenous cocatalyst (7% conversion of CHO, $[Cr]_0$:$[CHO]_0$ = 1:815, 12 h at 80 °C, 5 MPa, TOF = 5 h^{-1}). The authors proposed that the chloride and pyridyl ligands of **cat86** are sufficiently labile to ring-open chromium-bound epoxide. By contrast, the complexes with other pendant Lewis bases may adopt a coordinatively saturated bis(chelate) $[Cr(NN'O)_2]^+Cl^-$ geometry. These species are consequently unable to activate epoxide toward nucleophilic attack, similar to Lu's coordinatively saturated complex featuring two TBD groups.[48] Even for **cat86**, exogenous DMAP or [PPN]Cl cocatalyst was necessary to promote reasonable activity (up to 95% conversion in 12 h at 80 °C, 5 MPa, TOF < 66 h^{-1}). Presumably, additional cocatalyst accelerates epoxide ring-opening and facilitates formation of an open coordination site at Cr. As observed in other binary catalyst systems, dilution of the Cr Lewis acid and added cocatalyst reduced catalyst activity.

3. CATALYST STABILITY

Multifunctional complexes have demonstrated distinct mechanistic advantages over their binary analogues that enable unprecedentedly low catalyst loadings. However, even moderate catalyst degradation can have a significant impact on polymerization control when reactions are performed at low catalyst concentrations. Accordingly, the catalyst must remain stable against deactivation under a wide range of reaction conditions. Some of the highest activities observed for epoxide/CO_2 and epoxide/cyclic anhydride ROCOP were achieved using multifunctional (salen)Co(III) complexes (vide supra). However, Co(III) complexes are prone to reductive deactivation to form inactive Co(II) species.[83] High temperatures are often used to increase polymerization rates but reportedly also accelerate Co(III) reduction.[84−88] This section will discuss the factors contributing to reduction of Co(III) catalysts and multifunctional strategies to stabilize Co(III) species.

3.1. Reductive Deactivation of Binary Porphyrin and Salen Co ROCOP Catalysts. In a 1985 report, Nishinaga and co-workers demonstrated that (salen)Co(III)OH complexes quantitatively oxidized alcohol substrates to aldehydes or ketones with concomitant reduction to (salen)Co(II).[89] The authors proposed the reaction proceeds via β-hydrogen elimination from a Co-alkoxide to form the corresponding carbonyl compound and a Co(III)-hydride, which performs a hydrogen transfer to afford the (salen)Co(II) and water. Expanding on these results, Reiger and co-workers examined reductive deactivation of Co(III) porphyrin and salen catalysts under epoxide/CO_2 copolymerization conditions.[90] Monitoring a mixture of (TPP)CoCl and PO by UV−vis spectroscopy revealed a decrease in the Soret band associated with the Co(III) parent complex and growth of a new band associated with the Co(II) species. As the reaction was performed in the absence of CO_2, the authors proposed that reduction occurs from the Co-alkoxide (Scheme 5). Indeed, a model (TPP)Co-

Scheme 5. Co(III) Reduction Pathways with Binary Co Catalysts

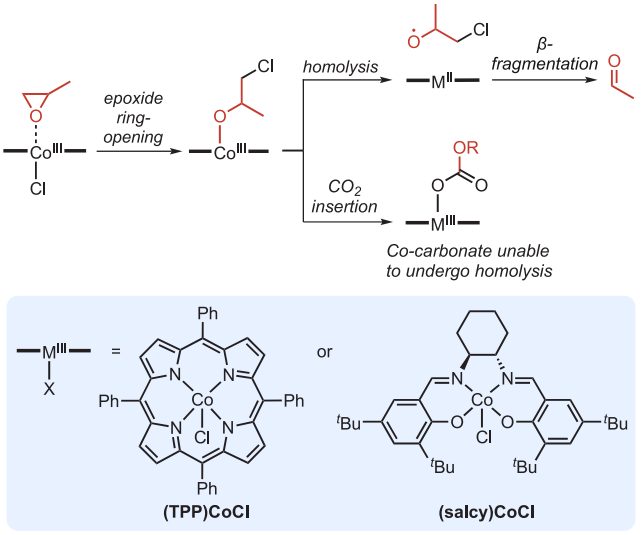

methoxide complex obtained by mixing (TPP)CoCl and NaOMe also underwent reduction. Reiger and co-workers also observed similar rapid reduction upon treating (salcy)CoCl with PO or with NaO^iPr. Interestingly, acetaldehyde was detected alongside catalyst reduction. The authors therefore proposed that cobalt reduction occurs via homolysis of the Co−O bond to generate Co(II) and an alkoxy radical that can then undergo β-fragmentation to produce acetaldehyde (Scheme 5). The second product produced by β-fragmentation was not discussed by the authors. Notably, mixtures of

(TPP)CoCl and NaO_2COCH_3 afforded Co(III)-carbonates that were stable against reduction due to the inability for homolysis to occur. Co(III) reduction also decelerated when (TPP)CoCl was mixed with PO in the presence of CO_2 due to the rapid insertion of CO_2 to form the more stable Co-carbonate resting state. The authors therefore proposed that favoring the carbonate resting state will trap the autoreducible Co(III)-alkoxide as a more stable carbonate, therefore improving catalytic activity.

3.2. Tethered Lewis Bases. In addition to promoting an unusual polymerization mechanism, **cat76** with tethered TBD unit reported by Lu and co-workers (Scheme 4) is highly stable against reduction.[48] To assess the role of the tethered TBD^+-carbonate ligand in suppressing Co(III) reduction, the authors varied the covalent tether length and epoxide comonomer. A variant of **cat76** with a short methylene linker was unable to form the inserted TBD^+-carbonate due to geometric constraints; lacking the intramolecular carbonate ligand, this complex underwent rapid reduction under polymerization conditions. Exchanging PO for CHO also resulted in rapid reduction of **cat76**. Presumably, the intramolecular TBD group is unable to ring-open the more sterically hindered CHO, precluding formation of the inserted TBD^+-alkoxide and TBD^+-carbonate species. Pretreating **cat76** with PO prior to the addition of CHO affords polymerization to PCHC. Similarly, mixtures of CHO and trace PO are readily copolymerized with CO_2. These results demonstrate that the tethered TBD group alone is unable to stabilize the Co(III) center, and that the intramolecular, reversible Co−carbonate linkage is required. The unprecedented stability of **cat76** helps to preserve its high activity at low loadings (TOF = 7100 h^{-1}, 90 °C, 2 MPa, 0.004 mol % **cat76**).

3.3. Tethered Cations. In an early report on multifunctional ROCOP catalysts, Lee and co-workers proposed that cationic cocatalysts anchored to the ligand framework would maintain proximity of chain ends with the Co(III) center, thereby stabilizing the catalyst against reductive deactivation.[47] Indeed, **cat12**-mediated PO/CO_2 ROCOP maintains a TOF of 3500 h^{-1} at 90 °C, whereas the analogous binary system produces no polymer at this temperature, presumably due to reduction of Co(III) (Figure 5). Similarly, a porphyrin Co

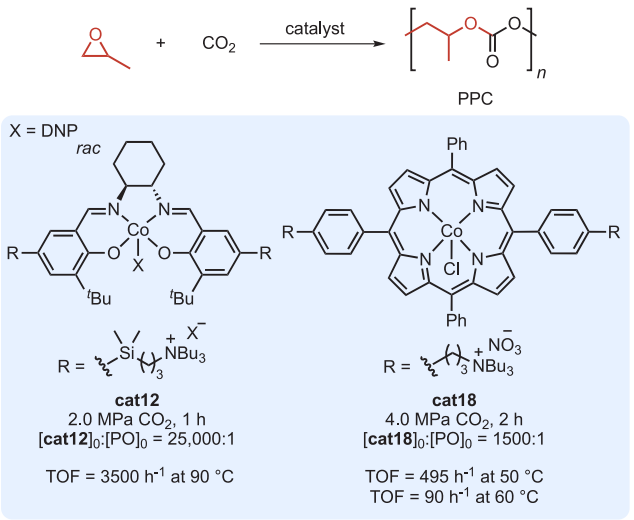

Figure 5. Multifunctional cobalt catalysts **cat12** and **cat18** used in PO/CO_2 ROCOP.

complex with two pendant ammonium cocatalysts (**cat18**) exhibited improved thermal stability as compared to its binary (TPP)CoCl/[PPN]Cl analogue.[67] However, increasing the reaction temperature from 50 °C to 60 °C resulted in a significant decrease in the activity of **cat18** from 495 h^{-1} to 90 h^{-1} which the authors attributed to reductive deactivation. Similarly, when reactions were performed at 100 °C, **cat12** lost activity due to catalyst degradation.

On the basis of NMR studies, Lee and co-workers proposed that the tetraammonium-tethered complex **cat3** bearing less bulky *o*-Me substituents on the salicylidene moiety exhibits an unusual coordination mode in which the salicylidene nitrogen atoms are not coordinated to Co; the resulting κ^2-bisphenoxide complex is proposed to be both more stable and more catalytically active than the typical κ^4-O,N,N,O coordinated cobalt complexes.[66] By contrast, the bulkier *o*-^{t}Bu substituents of **cat4** enforce the standard κ^4-O,N,N,O geometry, providing a standard for comparison (Chart 3). However, the NMR

Chart 3. Redox Behavior of κ^4 and κ^2 Multifunctional (salcy)CoX Complexes cat3 and cat4

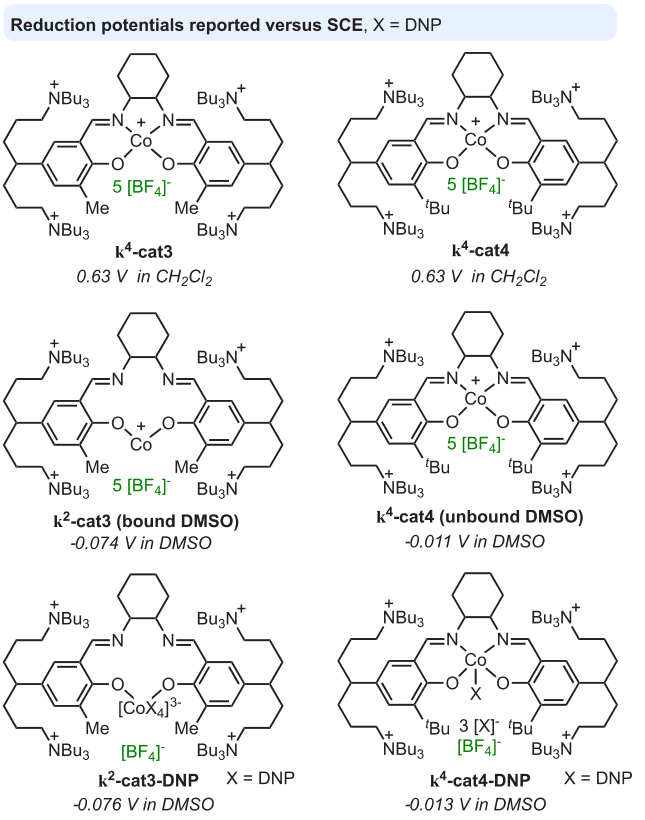

studies were performed in DMSO-d_6; coordination under catalytic conditions may therefore be different.[66,74] Cyclic voltammetry of κ^4-O,N,N,O and κ^2-bisphenoxide complexes revealed the relative redox stabilities afforded by these geometries (Chart 3). The authors first considered complexes bearing *o*-Me and *o*-^{t}Bu substituents with noncoordinating BF_4^- anions (**cat3** and **cat4**, respectively); both variants should adopt the standard κ^4 coordination mode in noncoordinating solvents, as neither the BF_4 ion nor the solvent should bind Co(III) more strongly than the salicylidene ONNO binding pocket. Both BF_4 complexes exhibit the same $E_{1/2}$ value (0.63 V relative to SCE) in noncoordinating CH_2Cl_2, consistent with

their similar geometries and substitution patterns. In strongly donating DMSO solvent, **cat4** (DMSO) and **cat3** (DMSO) exhibit significantly different reduction potentials ($E_{1/2}$ = −0.011 for **cat4** and −0.074 V for **cat3** relative to SCE); the authors attribute this discrepancy to the *o*-Me complex adopting the κ^2-bisphenoxide geometry in DMSO.

Exchanging the noncoordinating BF_4^- anions of **cat3** and **cat4** for strongly donating 2,4-dinitrophenolate anions afforded nearly identical reduction potentials in DMSO solvent as DMSO solvent alone ($E_{1/2}$ = −0.013 V for **cat4**−DNP and −0.076 V for **cat3**−DNP relative to SCE). This result corroborates that strongly donating DMSO solvent can also engender the κ^2 geometry. Moreover, the significant difference in reduction potentials (0.063 V) of the κ^4 *o*-^{t}Bu complex and κ^2 *o*-Me complex corresponds to a 10-fold difference in Co(III)/Co(II) ratio at a given electrochemical potential. Accordingly, the κ^2 *o*-Me complex should be significantly more stable than the κ^4 *o*-^{t}Bu analogue in polymerizations at elevated temperature. Indeed, the κ^2 *o*-Me complexes featuring a DNP anion was more active than its κ^4 *o*-^{t}Bu analogue at 70−75 °C, though the authors do not attribute this discrepancy specifically to differences in redox stabilities. In an effort to replace the DNP counteranion which could be prone to energetic decomposition, Lee and co-workers also prepared a series of catalysts incorporating 2,4,5-trichlorophenolate (TCP), 2,4,6-TCP, or 2,4-dichlorophenolate (DCP) anions (**cat7**−**cat10**).[74] In further support of the hypothesis that the uncoordinated geometry contributes to increased activity, the κ^2-2,4,5−TCP complex (**cat7**) with *o*-Me salicylidene substituents exhibited excellent catalytic activity (TOF = 10 000 h^{-1}), whereas the κ^4-2,4,5−TCP complex (**cat8**) with *o*-^{t}Bu substituents was inactive.

3.4. Multifunctional Complexes Incorporating Redox-Stable Lewis Acids. Multifunctional catalysts incorporating Cr, Al, Fe, Mg, Zn, and B Lewis acid centers have been reported for epoxide/CO_2 and epoxide/cyclic anhydride ROCOP. These complexes are less prone to reductive deactivation but are generally less active than their Co analogues.

Darensbourg and co-workers compared the activities and thermal stabilities of Cr and Co salcy complexes bearing a pendant ammonium cocatalyst in the copolymerization of cyclopentene oxide (CPO) and CO_2 (Figure 6).[91] At 70 °C, the Co complex **cat36** was significantly more active (TOF = 57 h^{-1}) than the Cr complex **cat37** (TOF = 2.2 h^{-1}). Decreasing [**cat36**] by 50% preserved the TOF at 70 °C, suggesting that reduction is not significant at this temperature. However, increasing the reaction temperature to 100 °C halved the TOF of **cat36**, with concomitant loss of poly(cyclopentene carbonate) (PCPC) selectivity (62% at 100 °C from >99% at 70 °C). In the **cat37**-catalyzed system, the same temperature increase afforded a 25-fold increase in activity (TOF = 50 h^{-1} at 100 °C) with excellent PCPC selectivity (>99%), demonstrating the resilience of the Cr center against deactivation at higher temperatures. Notably, the stability, activity, and selectivity of **cat37** at 100 °C matches those of **cat36** at 70 °C.

While Cr multifuncional complexes are stable against reduction and generally afford activities comparable to Co, metal toxicity of Cr-based reagents and residues is a concern. Efforts toward redox innocent nontoxic Lewis acids have identified Al as a promising alternative to metals such as Cr. Coates and co-workers prepared a range of multifunctional

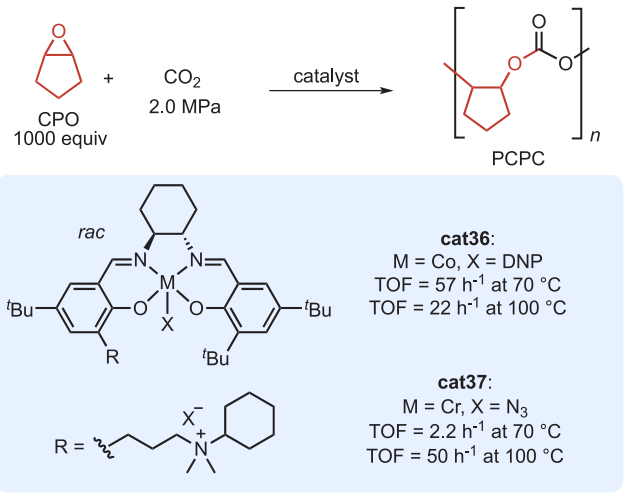

Figure 6. Activity of Co and Cr multifunctional catalysts **cat36** and **cat37** in CPO/CO_2 ROCOP.

catalysts incorporating Al (**cat43**), Fe (**cat46**), Zn (**cat47**), and Mn (**cat48**) metal centers to use in epoxide/anhydride copolymerization. While **cat46**−**cat48** exhibited low catalytic activities, the aminocyclopropenium-tethered (salph)AlCl catalyst **cat43** exhibited similar activities to those of the chromium analogue (**cat44**) (TOFs = 93 and 111 h^{-1}, respectively) in ROCOP of PO and carbic anhydride (CPMA) ([catalyst]$_0$:[CPMA]$_0$ = 1:400 at 60 °C).[56] While polymerizations using the cobalt analogue (**cat45**) slowed significantly at low loadings due to reductive deactivation, **cat43** exhibited similar TOFs at all loadings studied (0.5−0.025 mol %). At 100 °C, the activity of **cat43** (TOF = 466 h^{-1}) surpassed that of a Co analogue (**cat45**) at 60 °C (TOF = 376 h^{-1}) (Figure 7). Coates and co-workers also prepared a range of catalysts featuring Me (**cat49**), Ad (**cat50**), F (**cat51**), and OMe (**cat52**) substituents, although **cat43** still maintained the highest activity.

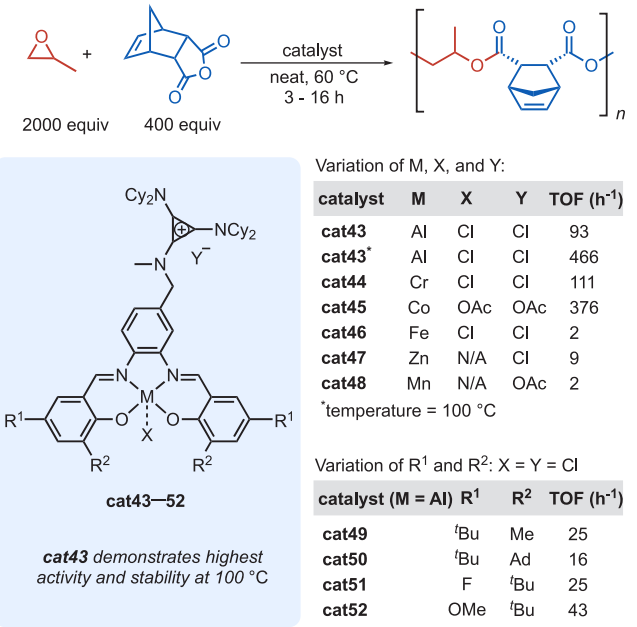

Variation of M, X, and Y:

catalyst	M	X	Y	TOF (h^{-1})
cat43	Al	Cl	Cl	93
cat43*	Al	Cl	Cl	466
cat44	Cr	Cl	Cl	111
cat45	Co	OAc	OAc	376
cat46	Fe	Cl	Cl	2
cat47	Zn	N/A	Cl	9
cat48	Mn	N/A	OAc	2

*temperature = 100 °C

Variation of R^1 and R^2: X = Y = Cl

catalyst (M = Al)	R^1	R^2	TOF (h^{-1})
cat49	^{t}Bu	Me	25
cat50	^{t}Bu	Ad	16
cat51	F	^{t}Bu	25
cat52	OMe	^{t}Bu	43

Figure 7. Catalytic activity in PO/CPMA ROCOP with **cat43**−**cat52**.

A handful of multifunctional Al complexes that demonstrate good activities and excellent selectivity for polycarbonate have recently been reported for epoxide/CO_2 ROCOP. Citing concern over toxic metal residue in hydrolytically degradable polycarbonates, Wang and co-workers developed a series of aluminum porphyrin complexes with two tethered ammonium cocatalysts with NO_3 counteranions (Figure 8).[68,69] At 70 °C

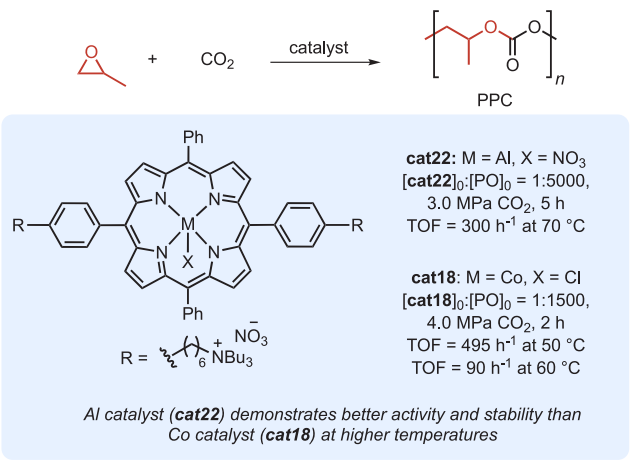

Figure 8. Catalytic activities of **cat22** and **cat18** at various temperatures.

and 90 °C, **cat22** achieved moderate TOFs (305 and 985 h^{-1}, respectively, 3 MPa CO_2, [**cat22**]$_0$:[PO]$_0$ = 1:5000). Increasing the polymerization temperature to 110 °C accelerated polymerization rates (TOF = 3400 h^{-1}, 3 MPa CO_2, [**cat22**]$_0$:[PO]$_0$ = 1:20 000). The cobalt analogue **cat18** began to undergo reduction at only 50 °C (TOF = 495 h^{-1}) with catalytic activity significantly dropping at 60 °C (TOF = 90 h^{-1}).[67] Notably, **cat22** maintained activity even at extremely low catalyst loadings (TOF = 3100 h^{-1}, [**cat22**]$_0$:[PO]$_0$ = 1:100 000, T = 110 °C, 3 MPa CO_2), suggesting no significant catalyst deactivation. Ema, Nozaki, Hasegawa, and co-workers recently reported **cat25**, an aluminum porphyrin complex with four tethered quaternary ammonium salts that achieves TOFs up to 10 000 h^{-1} ([Al]$_0$:[CHO]$_0$ = 1:40 000, 2 MPa CO_2) at 120 °C.[70] Decreasing the catalyst loading decreased activity (TOF = 1875 h^{-1} at [Al]$_0$:[CHO]$_0$ = 1:100 000, T = 120 °C, 2 MPa CO_2), which the authors attribute to the increased viscosity of the reaction mixture rather than catalyst deactivation.

Although Cr and Al complexes typically require higher temperatures to achieve activities similar to those of their Co analogues, eliminating catalyst deactivation provides better control over reaction kinetics and living chain-end retention. Catalysts incorporating other redox-stable metals have generally exhibited lower TOFs in both polyester and polycarbonate synthesis. Substituting Al with Mg (**cat27**) or Zn (**cat29**) in Nozaki and Ema's porphyrin catalysts afforded TOFs of 27 h^{-1} and 48 h^{-1}, respectively ([cat]$_0$:[CHO]$_0$ = 1:40 000, 2.0 MPa CO_2, T = 120 °C) (Figure 9). Lower catalyst activities (TOFs < 10 h^{-1}) have also been observed in PO/CPMA copolymerizations using multifunctional tris(dialkylamino)cyclopropenium (TDAC) (salph)MX complexes **cat46**–**cat48** (M = Fe, Zn, and Mn).[56] A notable exception to this trend is COS/epoxide copolymerizations: both Cr and Fe catalysts have demonstrated higher activities

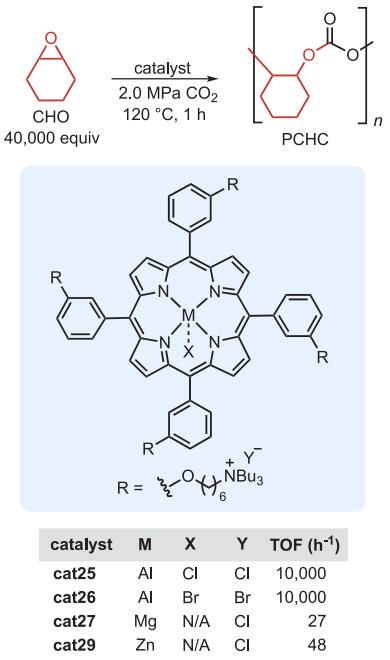

catalyst	M	X	Y	TOF (h^{-1})
cat25	Al	Cl	Cl	10,000
cat26	Al	Br	Br	10,000
cat27	Mg	N/A	Cl	27
cat29	Zn	N/A	Cl	48

Figure 9. Catalytic activity of multifunctional porphyrin catalysts in CHO/CO_2 ROCOP.

than a Co analogue, even at temperatures that do not promote Co(III) reduction (25 °C).[92,93]

4. ROCOP SELECTIVITY AND SIDE REACTIONS

A long-standing objective in ROCOP is to develop catalysts that are highly active toward alternating copolymerization while suppressing side reactions such as transesterification, epimerization, and backbiting, among others. These deleterious reactions influence molecular weight control and thermomechanical properties and reduce reaction efficiency. This section will discuss the thermodynamic and kinetic origins of ROCOP side reactions and highlight the features of multifunctional ROCOP catalysts that enable the synthesis of near defect-free polycarbonates and polyesters.

4.1. Polycarbonate vs Cyclic Carbonate Selectivity during Epoxide-CO_2 ROCOP. ROCOP of epoxides and CO_2 is a useful method of converting CO_2 into value-added materials such as polycarbonates. Since Inoue's pioneering work on catalyst-mediated epoxide CO_2 coupling reactions,[29−31] extensive progress has been made toward developing highly active and selective catalysts for the ROCOP of epoxides and CO_2. Particular attention has been given toward the prevention of cyclic carbonate formation during ROCOP. This side reaction consumes epoxide monomer, makes purification difficult due to the high boiling point of cyclic carbonate byproducts, and can limit molecular weight due to irreversible depolymerization.

Cyclic carbonate formation occurs when carbonate (Scheme 6b) or alkoxide (Scheme 6c) chain ends backbite via S_N2 or transesterification mechanisms, respectively. Typically, cyclic carbonate formation proceeds via backbiting of dissociated polymer chains which have increased nucleophilicity relative to metal-bound carbonate or alkoxide chain ends.[94] Under nonlimiting CO_2 conditions, most chain ends reside as the carbonate due to rate-limiting epoxide ring-opening, and therefore backbiting occurs predominately by carbonate attack. This insight has led to the design of multifunctional catalysts

Scheme 6. (a) Epoxide/CO_2 ROCOP Propagation Cycle and Cyclic Carbonate Formation by (b) Carbonate Backbiting and (c) Alkoxide Backbiting during CHO/CO_2 ROCOP

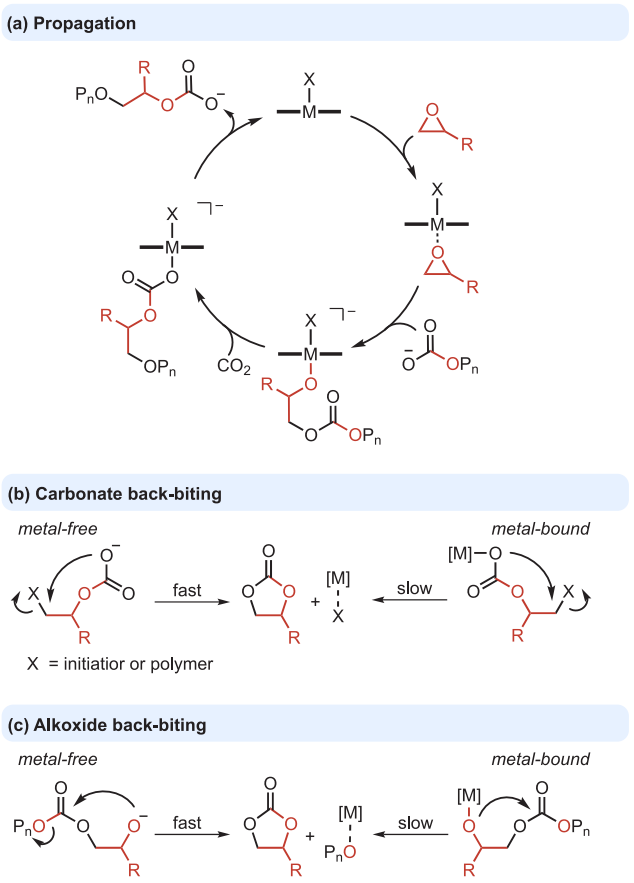

whereby the cocatalyst is covalently tethered to the Lewis acid to limit dissociation of carboxylate and alkoxide chain ends and suppress cyclic carbonate formation.

Darensbourg and Yeung investigated the thermodynamic and kinetic factors governing the coupling of common epoxides and CO_2 to give polycarbonates and cyclic carbonates.[95] Calculated enthalpies of formation indicated that polycarbonate formation was more exothermic (ΔH = −21 to −23 kcal/mol), whereas formation of the corresponding cyclic carbonates was less exothermic (ΔH = −8 to −18 kcal/mol). However, for most epoxides, cyclic carbonate formation is more exergonic than polycarbonate production due to the increase in entropy resulting from backbiting and expulsion of a small molecule. Consequently, cyclic carbonate is the thermodynamically favored epoxide/CO_2 coupling product, and exclusive polycarbonate formation during ROCOP is achieved through kinetic control over ring-opening and backbiting reactions.

4.2. Effect of Epoxide Structure on Cyclic Carbonate Formation. The epoxide structure significantly affects the thermodynamics and kinetics of polycarbonate versus cyclic carbonate formation during epoxide/CO_2 ROCOP. For example, ROCOP of CHO/CO_2 using either binary or multifunctional catalysts is highly selective for PCHC, whereas ROCOP of terminal epoxides such as PO is prone to cyclic carbonate formation when using binary catalysts. However, multifunctional catalysts have demonstrated significantly enhanced polymer selectivity in epoxide/CO_2 copolymerization when using terminal or alicyclic epoxides.

Nozaki and co-workers effectively mitigated cyclic carbonate formation during the ROCOP of terminal epoxides and CO_2 by employing a multifunctional bispiperidinium (salcy)CoOAc complex (**cat31**).[46] In particular, **cat31**'s pendant protonated piperidinium groups controlled the nucleophilicity of the growing chain ends to effectively suppress backbiting and therefore reduce cyclic carbonate formation (Scheme 7). PO/

Scheme 7. Protonated Bispiperidinium (salcy)CoOAc Complex cat31 Prevents Backbiting and Cyclic Carbonate Formation by Attenuating Propagating Chain-End Nucleophilicity

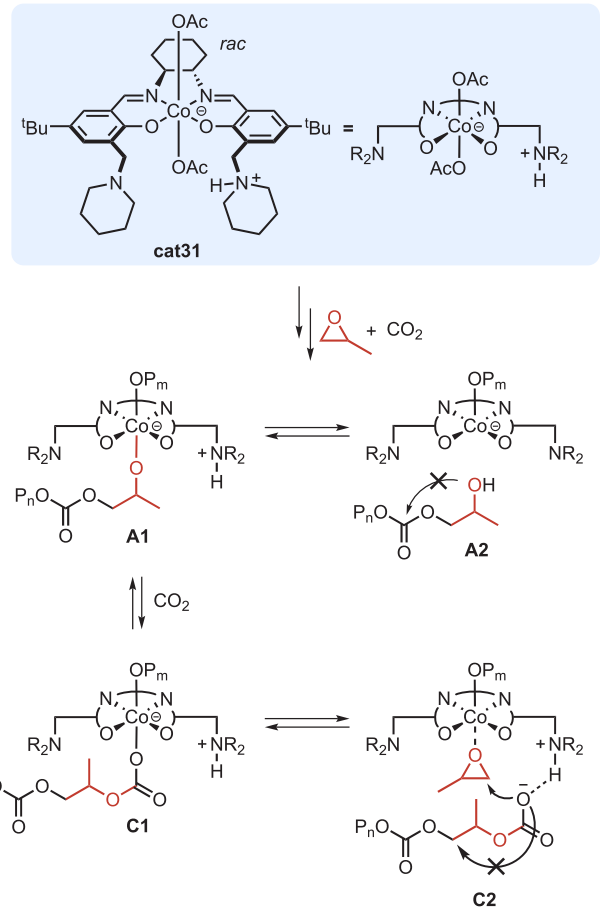

CO_2 ROCOP using **cat31** produced exclusively alternating poly(propylene carbonate) (PPC) in 77% yield with TOF = 127 h^{-1} ([**cat31**]$_0$:PO]$_0$ = 1:2000, 1.4 MPa CO_2, T = 25 °C). Meanwhile, copolymerization of PO/CO_2 (6000 equiv PO) under the same conditions using the analogous binary catalyst system (salcy)CoCl/[PPN]$OBzF_5$/*N*-methylpiperidinium acetate gave 34% PPC and 37% propylene carbonate (PC). This discrepancy demonstrates that covalent attachment of the protonated piperidinium cocatalyst is essential for suppressing backbiting reactions. The authors proposed that cyclic carbonate formation was subverted due to reversible protonation of growing chain ends (Scheme 7). Following reaction of an anionic chain end with either epoxide or CO_2, the resulting metal-bound alkoxide **A1** or carbonate **C1** is protonated by the pendant piperidinium to produce the corresponding alcohol **A2** or carbonic acid **C2**, which are

insufficiently nucleophilic to backbite and form cyclic carbonate. Meanwhile, the protonated species **A2** and **C2** are still able to react with CO_2 and epoxide, respectively, to produce copolymer.

Wang and co-workers also maintained high selectivity for PPC during PO/CO_2 ROCOP by using a multifunctional (TPP)$CoNO_3$ catalyst with pendant ammonium cocatalysts.[67] PO/CO_2 ROCOP using **cat18** proceeded with >99% polymer selectivity at 25 and 50 °C, with TOFs of 120 h^{-1} and 495 h^{-1}, respectively ($[PO]_0$:[**cat18**]$_0$ = 1500:1, 4.0 MPa CO_2). The analogous binary system consisting of (TPP)CoCl/[PPN]Cl decreased polycarbonate selectivity to 82% at 50 °C, highlighting the importance of the tethered ammonium cocatalysts in suppressing cyclic carbonate formation at higher temperatures.[96]

Multifunctional catalysts containing Al Lewis acid centers often promote backbiting to cyclic carbonate in epoxide/CO_2 reactions; indeed, multifunctional Al complexes have been specifically optimized for the cyclic carbonate product.[97−100] Wang and co-workers developed a range of multifunctional (TPP)AlCl catalysts (**cat13**−**cat17**) that are selective for polycarbonate formation.[69] Increasing the length of the alkyl linker from n = 2 (**cat13**) to n = 6 (**cat17**) increased catalyst activity at 70 °C from 250 h^{-1} to 400 h^{-1} and PPC selectivity from 72% to 83%, respectively (Figure 10a).

Wang and co-workers also observed that catalytic efficiency and polymer selectivity depends upon the Lewis acidity of the metal center, which can be tuned by varying the substituents in the *meso*-ring position of the porphyrin ligand. While the *p*-bromo-substituted **cat20** exhibited reduced catalyst activity as compared to the unsubstituted **cat19** (TOF = 330 h^{-1} vs 400 h^{-1}), PPC selectivity increased from 87% to 93% at 70 °C (Figure 10b). Installing an electron-donating methoxy group (**cat21**) greatly enhanced catalytic activity (TOF = 340 h^{-1}), but polymer selectivity was unaffected (%PCC = 88%). The authors initially proposed that increasing the Lewis acidity of the metal center enhances interactions between the anionic chain end and aluminum center, disfavoring cyclic carbonate formation but reducing catalytic activity. Reducing the Lewis acidity of the metal center by introducing an electron-donating group therefore induces the opposite effect.

However, Wang and co-workers prepared a series of (TPP)$AlNO_3$ catalysts (n = 3) whose polymer selectivity, catalytic activity, and Lewis acidity contradicts the proposed relationship (Figure 10b).[68] Installing a moderately electron-donating ^{t}Bu group in the *para* position (**cat23**) resulted in a distinct increase in activity (TOF = 449 h^{-1}) compared to the unsubstituted **cat22** (TOF = 306 h^{-1}), in agreement with previous findings. However, polymer selectivity also increased from 87% to 92%. Interestingly, installing an electron-withdrawing C_6F_5 group in the *meso* position of the porphyrin framework (**cat24**) also induced an increase in catalytic activity (TOF = 392 h^{-1}, %PPC = 88%), inconsistent with previous findings. While electron-donating groups do seem to increase catalytic activity, there is no clear trend between Lewis acidity, polymer selectivity, and catalytic activity based on these (TPP)$AlNO_3$ catalysts.

Wang and co-workers developed a series of multifunctional (salen)CoCl complexes to examine the effect of varying Lewis base substituents on polymer selectivity in PO/CO_2 copolymerization.[101] Catalysts featuring a Lewis base constrained in a ring (**cat81**−**cat83**) maintained moderately high PPC selectivity (91−95%), whereas **cat84** featuring an acyclic

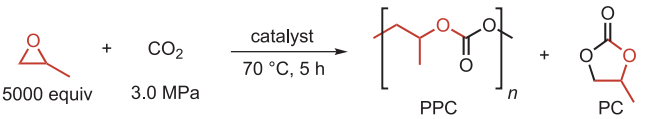

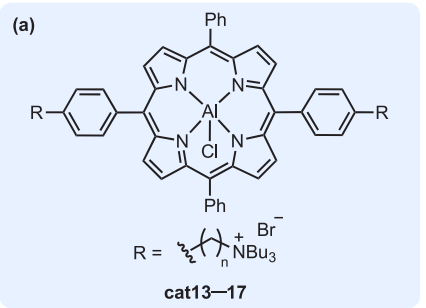

Linker length variation: effects on catalyst activity and selectivity

catalyst	n	TOF (h^{-1})	%PPC
cat13	2	250	72
cat14	3	330	75
cat15	4	360	82
cat16	5	380	82
cat17	6	400	83

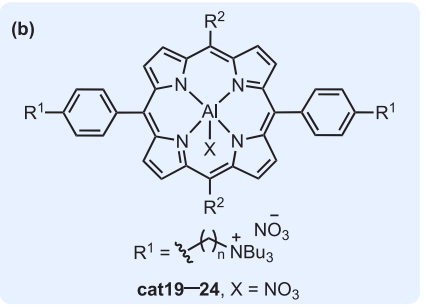

Substituent variation: effects on catalyst activity and selectivity

catalyst	n	R^2	TOF (h^{-1})	%PPC
cat19	6	Ph	290	87
cat20	6	*p*-BrPh	270	93
cat21	6	*p*-OMePh	340	88
cat22*	3	Ph	306	87
cat23*	3	*p*-^{t}BuPh	449	92
cat24*	3	C_6F_5	392	88

*Time = 2 h

Figure 10. Activity and selectivity of **cat13**−**cat17** and **cat19**−**cat24** in PO/CO_2 ROCOP.

tertiary amine exhibited diminished PPC selectivity (75%) (Figure 11). Catalysts featuring piperidine (**cat81**) or morpholine (**cat82**) pendant groups maintained activity (TOF = 35 h^{-1}) greater than that of pyrrolidine-functional **cat83** (TOF = 19 h^{-1}) or acyclic amine-functional **cat84** (TOF = 22 h^{-1}).

Alicyclic epoxides such as CHO generally are less prone to cyclic carbonate formation during epoxide/CO_2 ROCOP as compared to terminal epoxides such as PO. However, the propensity of CHO/CO_2 ROCOP to selectively produce PCHC does not translate to similar alicyclic epoxides such as cyclopentene oxide (CPO). Darensbourg and co-workers demonstrated that CHO/CO_2 ROCOP using a binary (salcy)CrCl/[PPN]N_3 catalyst system at 80 °C and 3.5 MPa CO_2 yielded exclusively PCHC (Figure 12a) whereas polymerization of CPO/CO_2 using (salcy)CrCl/[PPN]N_3 under the same conditions afforded >99% *cis*-cyclopentene carbonate

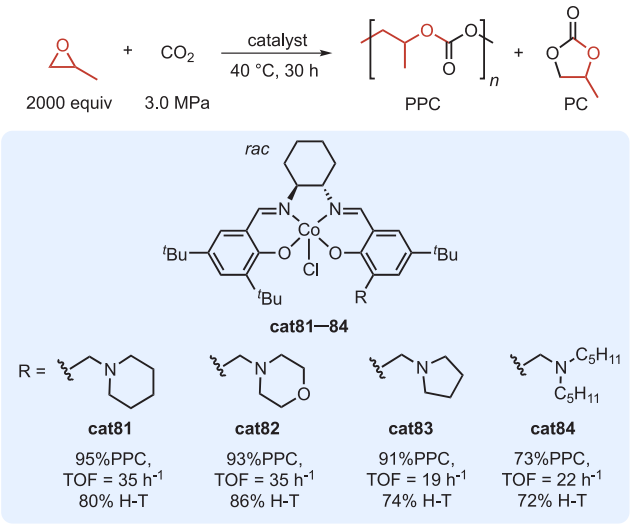

Figure 11. Epoxide/CO_2 ROCOP mediated by Lewis-base-functional (salcy)CoCl catalysts **cat81**−**cat84**.

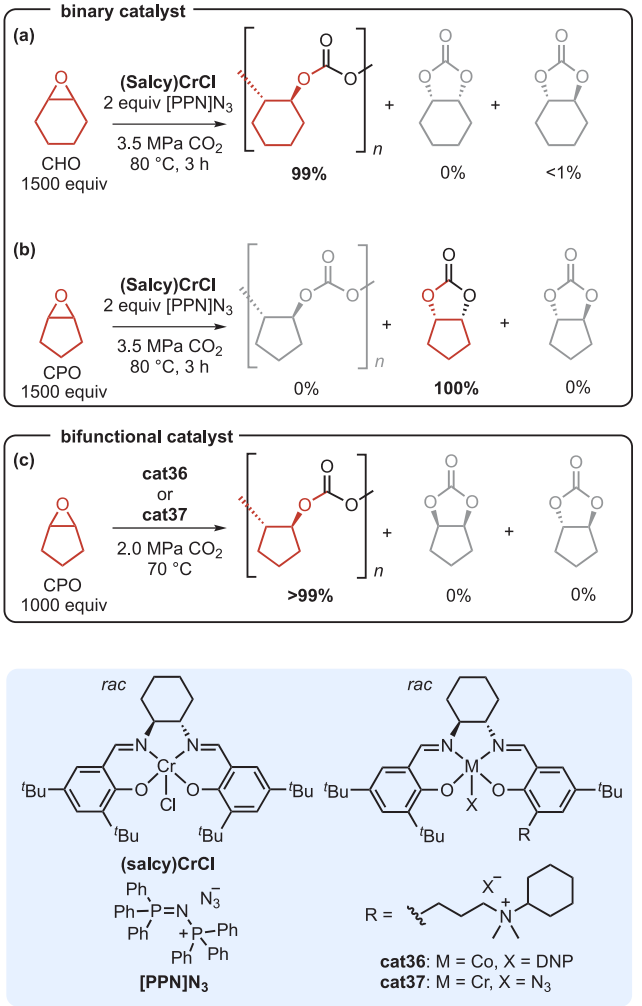

Figure 12. ROCOP of (a) CHO/CO_2 and (b) CPO/CO_2 using the binary catalyst system (salcy)CrCl/[PPN]N_3. (c) Use of multifunctional catalysts **cat36** and **cat37** at 70 °C produce exclusively PCPC during CPO/CO_2 ROCOP.

(*cis*-CPC) (Figure 12b).[61] It is noteworthy that *cis*-cyclohexene carbonate (*cis*-CHC) resulting from carbonate backbiting is almost never observed during CHO/CO_2 ROCOP. This absence is largely attributed to the additional energetic barrier associated with the necessary endergonic chair-to-boat conformational change (ΔG = 4.7 kcal/mol) required prior to cyclization, which has an additional energy barrier of $\Delta G^{\ddagger}$ = 21.1 kcal/mol (Scheme 8a). Meanwhile, alkoxide backbiting to

Scheme 8. Cyclic Carbonate Formation during CHO/CO_2 ROCOP

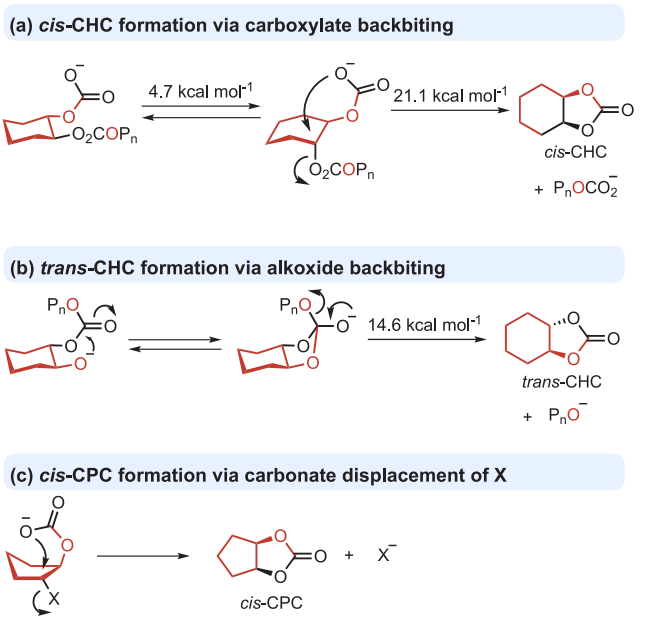

form *trans*-cyclohexene carbonate (*trans*-CHC) is only observed under CO_2-starved conditions where most chain ends are alkoxides (Scheme 8b). Darensbourg calculated the energy barrier of unbound alkoxide backbiting during CHO/CO_2 ROCOP to be 14.6 kcal/mol, which is approximately 3 kcal/mol higher than the energy barrier for unbound alkoxide backbiting of aliphatic epoxides. This difference further increases the favorability of PCHC formation over CHC as compared to other aliphatic epoxides.

To improve the polycarbonate selectivity of CPO/CO_2 ROCOP, Darensbourg and co-workers employed multifunctional (salcy)CoDNP **cat36** with a pendant dimethylcyclohexylammonium cocatalyst, affording >99% PCPC and moderate activities (TOF = 57 h^{-1}) (Figure 12c).[61] The authors proposed that the covalently linked piperidinium cocatalyst maintains proximity between the propagating chain ends and Lewis acid, thereby reducing the activation energy of epoxide ring-opening by carbonate chain ends. Computational studies by Lu and co-workers confirmed that multifunctional catalysts lower the activation energy of rate-limiting epoxide ring-opening relative to backbiting (vide supra). Despite high activity and selectivity toward ROCOP of CPO/CO_2, multifunctional Co(III) complex **cat36** is prone to reduction to the inactive Co(II) complex at higher temperatures, as evidenced by decreased catalyst activity when increasing the temperature from 70 °C (TOF = 57 h^{-1}) to 100 °C (TOF = 22 h^{-1}). However, multifunctional (salcy)CrN_3 catalyst **cat37** was thermally stable with good activities at higher temperatures

(TOF = 50 h^{-1}, 100 °C), albeit with slightly reduced PCPC selectivity (94%).

Poly(indene carbonate) (PIC) is of interest as a high-T_g alternative to bisphenol A-based polycarbonate (T_g = 154 °C) due to its rigid semiaromatic bicyclic structure. In 2011, Darensbourg and co-workers first reported the copolymerization of indene oxide (IO) and CO_2 using a binary (salcy)CoDNP/[PPN]DNP catalyst system, affording PIC with T_g values up to 138 °C.[102] Reaction temperatures as low as 0 °C were required to minimize cyclic carbonate formation using the binary catalyst system, but low catalyst activities (TOF = 1.7 h^{-1}) and poor selectivity for PIC (64%) were observed. Inspired by the high selectivity of multifunctional **cat36** toward polycarbonate formation during ROCOP of CPO/CO_2, Darensbourg and co-workers employed quaternary ammonium-tethered (salcy)Co(III) catalysts toward the ROCOP of IO/CO_2.[64] Multifunctional catalysts **cat35** and **cat39** (Figure 13a) exhibited high selectivity toward PIC

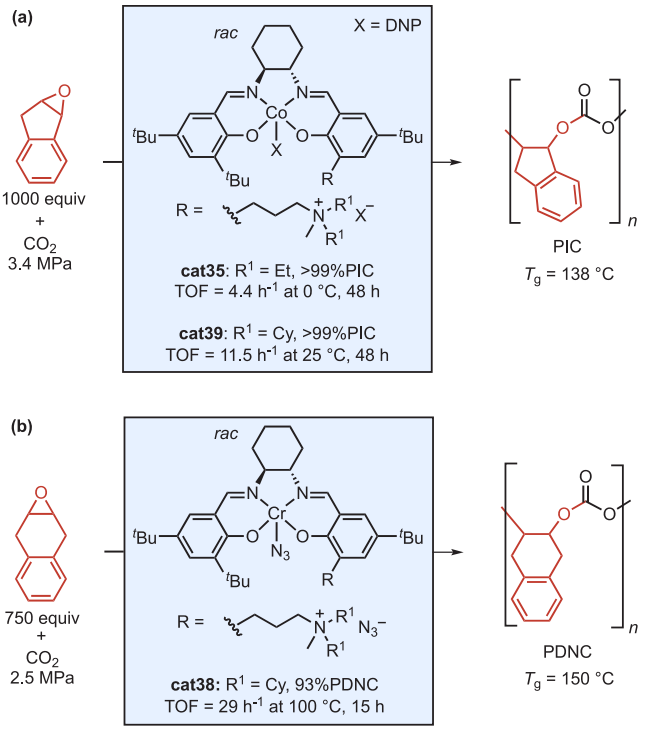

Figure 13. ROCOP of (a) indene oxide and (b) 1,4-dihydronaphthalene oxide using multifunctional catalysts.

(>99%) but exhibited low catalyst activities of TOF = 4.4 h^{-1} and 11.5 h^{-1} at 0 and 25 °C, respectively. ROCOP of IO/CO_2 at 40 °C using **cat39** produced exclusively *cis*-indene carbonate in 4.5% yield, indicating that lower reaction temperatures are required to produce PIC with high selectivity using this catalyst system.

Poly(1,4-dihydronaphthalene carbonate) (PDNC) is also a promising candidate as a high-T_g polycarbonate. Prior efforts to synthesize PDNC by ROCOP using a binary (salcy)CrCl/*N*-methylimidazole catalyst system yielded predominately *cis*-1,4-dihydronaphthalene carbonate (*cis*-DNC).[103] The propensity of 1,4-dihydronaphthalene oxide (DNO) and CO_2 coupling to produce *cis*-DNC is likely due to the boatlike conformation of dihydronaphthalenes imposed by the fused benzene ring, which favors intramolecular carbonate attack like that observed during CPO/CO_2 ROCOP (vide supra). More recently, Darensbourg and co-workers employed multifunctional (salcy)MX (M = Cr, Co) catalysts with pendant quaternary ammonium cocatalysts for the ROCOP of DNO/CO_2 (Figure 13b).[104] Multifunctional (salcy)CrN_3 catalyst **cat38** exhibited relatively high selectivity for polycarbonate (93%) and moderate activity (TOF = 29 h^{-1}) for the ROCOP of DNO/CO_2 ($[DNO]_0$:$[Cr]_0$ = 750:1, 2.5 MPa CO_2, T = 100 °C). Meanwhile, the binary (salcy)CrX/cocatalyst systems investigated in this work gave poor selectivity for polycarbonate with low activities. For example, the binary (salcy)-CrN_3/$[Bu_4N]N_3$ catalyst system comparable to **cat38** resulted in low polycarbonate selectivity (67% PDNC) and low activity of TOF = 19 h^{-1} (2.5 MPa CO_2 at 70 °C). The improved activity and selectivity toward ROCOP of DNO/CO_2 exhibited by **cat38** likely stems from the tethered onium cocatalyst that maintains close proximity of the dissociated carbonate chain ends to the Lewis acid center, increasing the rate of epoxide ring-opening relative to the rate of backbiting. **cat38**-catalyzed ROCOP of DNO/CO_2 yielded PDNC of M_n = 6.7 kDa, and T_g = 136 °C. However, higher molecular weights could not be achieved by increasing $[DNO]_0$:$[Cr]_0$. Surprisingly, the (salcy)CoX (X = DNP, N_3, Cl, or O_2CCF_3) analogues of **cat38** were inactive toward the coupling of DNO and CO_2 to either polycarbonate or cyclic carbonate over a range of temperatures (T = 0–70 °C), monomer concentrations (neat or in solvent), and reaction times (up to 5 days).

Darensbourg and co-workers also examined the copolymerization of *cis*- or *trans*-2-butene oxide (*cis*- or *trans*-2BO) and CO_2 as a route to poly(*trans*-2-butene carbonate) (P*t*2BC), which has a T_g that is nearly 60 °C higher than that of poly(1-butene carbonate) (T_g = 9 °C). Only *cis*-2BO was active toward copolymerization using a range of binary and multifunctional Co(III) and Cr(III) catalysts.[62] Copolymerization of *cis*-2BO with CO_2 using the binary systems (salcy)-CoDNP/[PPN]DNP or (salcy)CrN_3/2 equiv $[PPN]N_3$ at 40 °C afforded P*t*2BC with poor polymer selectivities of 75% and 30%, respectively (Figure 14). Furthermore, increasing the reaction temperature to 70 °C produced exclusively cyclic carbonate using these catalysts. By contrast, multifunctional catalysts **cat38** and **cat39** possessing pendant ammonium cocatalysts yielded P*t*2BC with higher polymer selectivity, affording 79% and >99% P*t*2BC, respectively. Increasing the polymerization temperature decreased polymer selectivity with **cat39**, producing P*t*2BC with 65% selectivity at 70 °C. Interestingly, only *trans*-2-butene carbonate (*t*2BC) was observed during ROCOP of *cis*-2BO/CO_2 when employing **cat38** and **cat39**, suggesting that backbiting occurs exclusively via the alkoxide chain end (vida supra). By contrast, both *trans*- and *cis*-butene carbonate were observed in *cis*-2BO/CO_2 copolymerizations carried out using the binary catalysts (salcy)CoDNP/[PPN]DNP or (salcy)CrN_3/2 equiv [PPN]-N_3, indicating that both alkoxide and carboxylate backbiting mechanisms were operational. Darensbourg and co-workers also examined the copolymerization of isobutylene oxide (IBO) and CO_2 using the same binary and multifunctional Co(III) and Cr(III) catalyst systems. Neither of the multifunctional catalysts **cat39** and **cat38** produced poly(isobutylene carbonate) (PIBC) or isobutylene carbonate (IBC), whereas only IBC was generated using the binary catalysts (salcy)CoDNP/[PPN]DNP and (salcy)CrN_3/2 equiv $[PPN]N_3$. The authors suggested that the stricter spatial environment imposed by the pendant ammonium cocatalyst

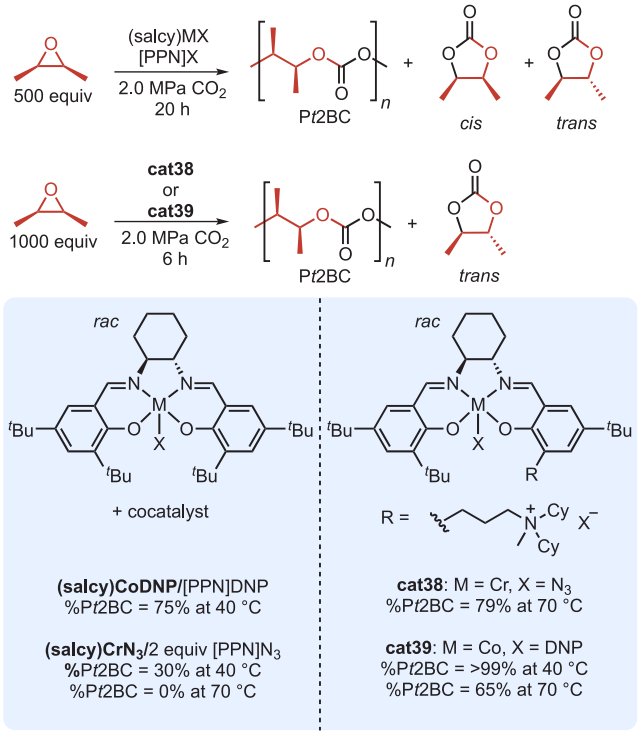

Figure 14. Activity and selectivity of binary and multifunctional Co or Cr catalysts during ROCOP of *cis*-BO and CO_2.

on the metal center of the multifunctional catalyst prevents ring-opening of the more sterically crowded IBO.

4.3. Cyclic Carbonate Formation during ROCOP of CO_2 and Electron-Deficient Epoxides. In contrast to electronically unbiased epoxides such as PO that undergo nucleophilic ring-opening at the less sterically hindered C_β-methylene, epoxides with pendent electron-withdrawing groups (EWGs) commonly ring-open at the more substituted C_α-methine due to its increased electrophilicity (Scheme 9).

Scheme 9. Influence of Electronic and Steric Constraints on the Regioselectivity of Epoxide Ring-Opening during Epoxide/CO_2 ROCOP

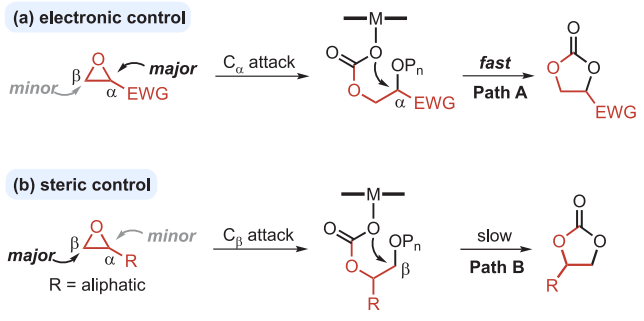

Consequently, cyclic carbonate formation occurs rapidly during ROCOP of CO_2 and electron-deficient epoxides such as epichlorohydrin (ECH) and styrene oxide (SO) due to favorable intramolecular attack by the carbonate anion at the electrophilic C_α-methine (Scheme 9, path A). Meanwhile, cyclic carbonate formation is suppressed during ROCOP of aliphatic monosubstituted epoxides/CO_2 due to slower carbonate backbiting at the less reactive C_β-methylene (Scheme 9, path B).

Darensbourg and co-workers measured the differences in the activation energy barriers (ΔE_a) of cyclic carbonate and polycarbonate formation for the ROCOP of ECH/CO_2 and PO/CO_2 using binary (salcy)CoDNP with either [PPN]DNP or MeTBD as a cocatalyst.[105] ΔE_a values for cyclic carbonate versus polycarbonate formation for ECH/CO_2 and PO/CO_2 coupling were 10.9 and 12.8 kcal/mol, respectively. Consequently, the rate of epichlorohydrin carbonate (ECHC) formation exceeds that of poly(epichlorohydrin carbonate) (PECHC) above 5 °C, whereas higher temperatures (>80 °C) are required for the rate of PC formation to surpass that of PPC. Indeed, ECH/CO_2 ROCOP catalyzed by (salcy)CoDNP using either [PPN]DNP or MeTBD cocatalysts resulted in low polycarbonate selectivity at 25 °C (10% PECHC for both cocatalysts) and only moderate selectivity at 0 °C (61% and 65% PECHC, respectively). To mitigate the kinetic favorability of ECHC formation during ECH/CO_2 ROCOP, Darensbourg and co-workers employed multifunctional (salcy)CoDNP complexes with either a pendant TBD (**cat75**) or quaternary ammonium (**cat35**) cocatalyst; the covalently tethered cocatalyst maintains proximity of the propagating chains to the Lewis acid, increasing the rate of epoxide ring-opening relative to backbiting. ROCOP of ECH/CO_2 at 0 °C using multifunctional catalysts **cat75** and **cat35** afforded PECHC with >99% selectivity and exhibited moderate activities (36 h^{-1} and 37 h^{-1}, respectively) (Figure 15). A >99% selectivity for

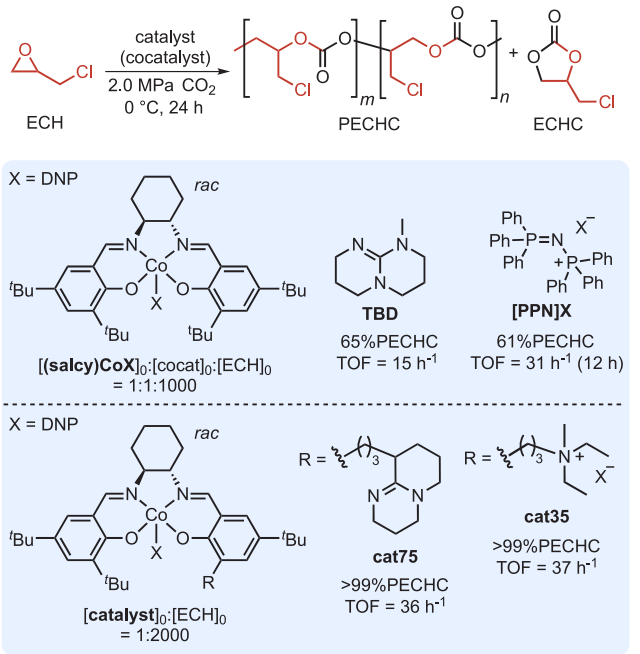

Figure 15. ECH/CO_2 ROCOP using binary and multifunctional (salcy)CoDNP catalyst systems.

polycarbonate was only maintained at low temperatures; copolymerization at ambient temperatures resulted in diminished polymer selectivity using **cat75** (72%PECHC) and **cat35** (75%PECHC).

Darensbourg and co-workers investigated the effect of binary and multifunctional catalysts on styrene carbonate (SC) formation during styrene oxide SO/CO_2 ROCOP using (salcy)CoDNP/[PPN]DNP and **cat75** catalyst systems (Figure 16).[106] (Salcy)CoDNP/[PPN]DNP afforded poly(styrene carbonate) (PSC) with moderate selectivity (91%)

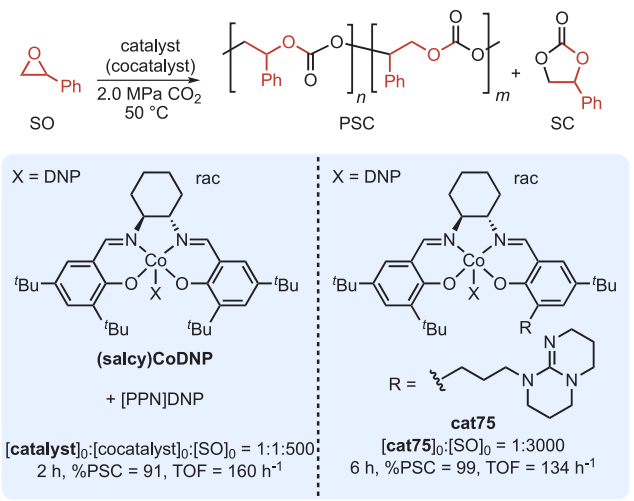

Figure 16. Influence of binary ((salcy)CoDNP/[PPN]DNP) and multifunctional (**cat75**) catalyst systems on PSC and SC formation during SO/CO_2 ROCOP.

whereas **cat75**-catalyzed ROCOP of SO/CO_2 produced exclusively PSC (>99%) under the same conditions. ^{13}C NMR analysis of PSC produced using **cat75** revealed a head-to-tail content of 51%, indicating near equal ring-opening of SO at the C_α-methine and C_β-methylene carbons. By contrast, using binary (salcy)CoDNP/[PPN]DNP in the copolymerization of (*S*)-SO yielded head-to-tail content of 82%. As noted previously, nucleophilic ring-opening at the more substituted C_α-methine favors intramolecular carbonate attack and concomitant cyclic carbonate formation.

4.4. Effect of Initiating Species on Cyclic Carbonate Formation. The catalyst- and cocatalyst-derived initiating species (X) can significantly affect cyclic carbonate formation during epoxide/CO_2 ROCOP. Following initiation by ring-opening of epoxide by X and subsequent CO_2 insertion, the resulting carbonate anion can backbite to produce cyclic carbonate and regenerate the initiating species, X (Scheme 10, path A). Decreasing the leaving group ability of X and increasing the rate of epoxide ring-opening relative to backbiting improves selectivity for polycarbonate.[60] Subsequent enchainment of epoxide and CO_2 following initiation prevents backbiting at the C−X α-terminus due to the less favorable macrocyclic transition state required for intramolecular nucleophilic displacement of X (Scheme 10, path B). Multifunctional catalysts wherein the cocatalyst is covalently attached to the Lewis acid increase the rate of epoxide ring-opening (vide supra) and therefore suppress the formation of cyclic carbonate by displacement of the initiating species X.

Scheme 10. (A) Cyclic Carbonate Formation by Intramolecular Displacement of the Initiating Species X by the Carbonate Anion. (B) Insertion of Multiple Monomers Units Prevents Backbiting at the C−X α-Terminus

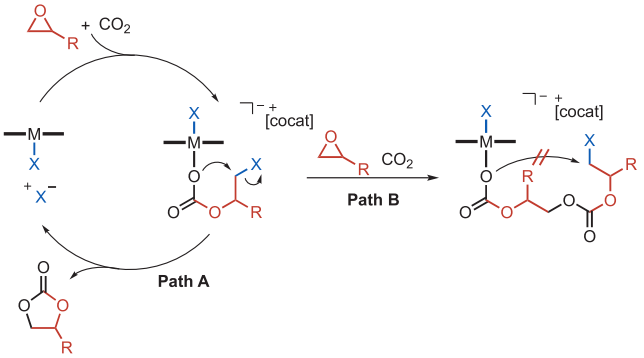

Nozaki, Ema, and Hasegawa prepared Mg and Zn multifunctional porphyrin catalysts whose polycarbonate selectivity was influenced by the initiator, X. **cat27** and **cat29** featuring Cl initiators maintained moderate catalytic activity (TOF = 27 h^{-1} and 48 h^{-1}, respectively) and limited polymer selectivity (52%PCHC and 63%PCHC, respectively) in CHO/CO_2 ROCOP (Figure 17).[70] During ROCOP of CO_2 and terminal epoxides, **cat28** and **cat30** featuring Br initiators produced exclusively cyclic carbonates.[107,108] DFT calculations of PO/CO_2 coupling indicated that backbiting to form cyclic carbonate is more energetically favorable with a Br anion: an E_a of 17.1 kcal/mol for ring-closing to form cyclic carbonate was calculated for a simplified analogue of **cat28** (X = Br), whereas a higher E_a of 18.0 kcal/mol was calculated for a simplified analogue of **cat27** (X = Cl).[109]

Wang and co-workers also explored the effect of initiator species on polymer selectivity using a range of (salen)CoX multifunctional complexes with two tethered *N*-morpholino Lewis bases.[110] Multifunctional catalysts **cat95** and **cat98** demonstrated very low activity due to the non- or poorly nucleophilic initiating X-groups (Figure 18). Catalysts prepared with more nucleophilic X-groups Cl (**cat94**), NO_3 (**cat96**), $O(C{=}O)CF_3$ (**cat97**), and N_3 (**cat99**) produced a range of polymer selectivities, although no trend between anion and selectivity was established.

4.5. Epoxide/COS ROCOP. ROCOP of epoxides and carbonyl sulfide (COS) is a viable approach to synthesize poly(thiocarbonate)s, which are of interest as high T_g and T_m materials with increased hydrolytic ability and biodegradability. Epoxide/COS ROCOP occurs analogously to epoxide/CO_2 copolymerization: an initiator ring-opens epoxide to produce a metal-bound alkoxide, which undergoes COS insertion to form polymer linkage **L1** or cyclic carbonate **C1** (Scheme 11).[15] Epoxide/COS ROCOP shares similar challenges to those faced by analogous epoxide/CO_2 copolymerization, including regioselectivity and polycarbonate versus cyclic carbonate selectivity. Additionally, the asymmetric COS structure introduces the possibility of the oxygen−sulfur exchange reaction (O/S E-R) wherein epoxide and COS coupling can generate the corresponding thiirane and CO_2 (Scheme 11). Epoxide, COS, thiirane, and CO_2 may all serve as comonomers for copolymerization, enabling the formation of (di)-thiocarbonate backbone linkages and cyclic (di)thiocarbonates. Furthermore, the asymmetric nature of COS introduces additional regiochemical complexity: either the oxygen or sulfur atom can coordinate to the metal center, leading to the formation of backbone linkages **L1** and **L4** and thiocarbonates **C1** and **C4**, respectively. Because polymer properties such as crystallinity are closely tied to monomer sequence and regularity, it is desirable to develop ROCOP catalysts that suppress O/S E-R and maintain regioselectivity such that only a single backbone linkage is formed.

Lu and co-workers demonstrated that multifunctional salcy (M = Co, Cr) catalysts with a pendant TBD unit are suitable for epoxide/COS ROCOP, with the identity of the metal center being key for the suppression of side reactions.[93] ROCOP of PO/COS using multifunctional **cat76** occurs with

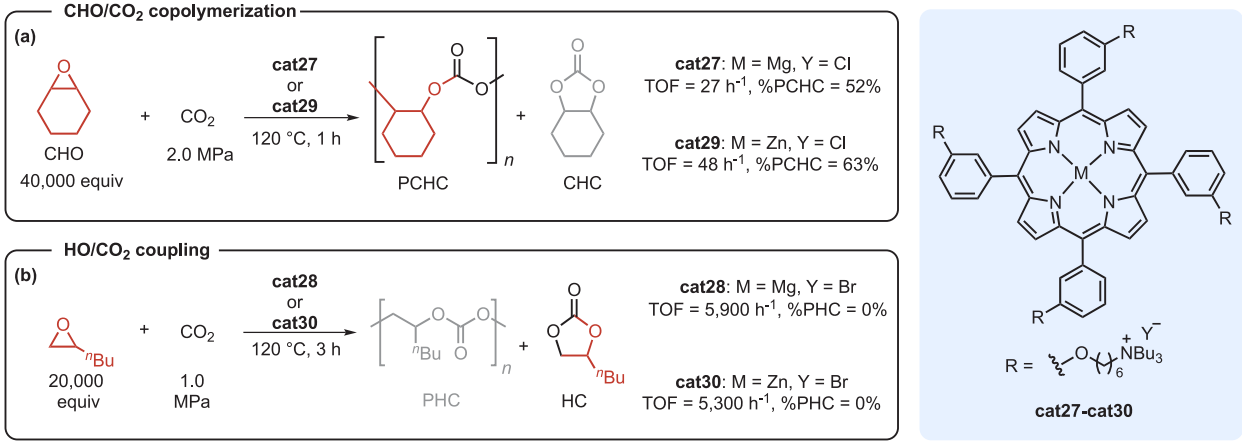

Figure 17. Multifunctional Mg and Zn catalysts used in (a) CHO/CO_2 copolymerization and (b) HO/CO_2 coupling.

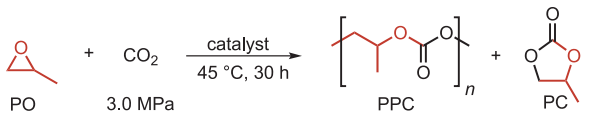

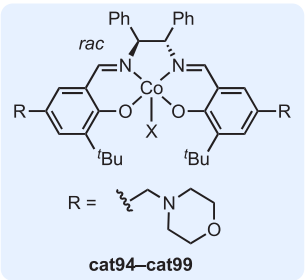

cat	X	%PPC	TOF (h^{-1})
cat94	Cl	97	35
cat95	Br	14	1
cat96	NO_3	92	48
cat97	$O(C{=}O)CF_3$	76	35
cat98	BF_4	89	6
cat99	N_3	58	31

$[cat]_0:[PO]_0 = 1:2000$

Figure 18. Decreasing leaving group ability of X increases selectivity for PPC.

low selectivity for poly(propylene monothiocarbonate) (PPMTC) (60%) and moderate catalytic activity of TOF = 103 h^{-1} at 80 °C ($[\mathbf{cat76}]_0:[PO]_0:[COS]_0$ = 1:10 000:20 000) (Figure 19). However, using the Cr analogue (**cat77**) affords perfectly alternating PPMT with high regioregularity, high copolymer selectivity >99%, and substantially increased catalyst activity of TOF = 29 300 h^{-1} at 80 °C ($[\mathbf{cat77}]_0:[PO]_0:[COS]_0$ = 1:100 000:200 000). Furthermore, O/S E-R was not observed. The analogous binary (salcy)$CrNO_3$/MeTBD catalyst suppressed O/S E-R at room temperature, whereas using [PPN]Cl as the cocatalyst at 60 °C resulted in increased O/S E-R and cyclic thiocarbonate formation.[111] However, the (salcy)$CrNO_3$/MeTBD system was not investigated at higher temperatures. The authors rationalized that the increase in O/S E-R when using [PPN]Cl as the cocatalyst was due to Cr−OH formation at elevated temperatures. By contrast, multifunctional **cat77** suppresses O/S E-R completely, even at higher temperatures.

Lu and co-workers also applied **cat77** to epoxide/COS ROCOP using an expanded epoxide scope (Figure 19). Monosubstituted epoxides including butene oxide (BO), hexene oxide (HO), benzyl glycidyl ether (BnGE), and phenyl glycidyl ether (PGE) were copolymerized with COS with over 99% polymer selectivity and TOF values ranging from 21 500 to 53 900 h^{-1} at 80 °C ($[\mathbf{cat77}]_0:[epoxide]_0:[COS]_0$ = 1:50 000:100 000). All copolymerizations afforded perfectly alternating poly(monothiocarbonate) with M_n values exceeding 100 kDa and dispersities less than 1.4. However, **cat77** was much less active toward copolymerization of 2,3-disubstituted epoxides CHO and CPO with COS, achieving TOF values of 260 h^{-1} and 1360 h^{-1}, respectively.

Scheme 11. Possible Backbone Linkages and Cyclic Carbonate Structures Due to Oxygen−Sulfur Exchange during Epoxide/COS ROCOP

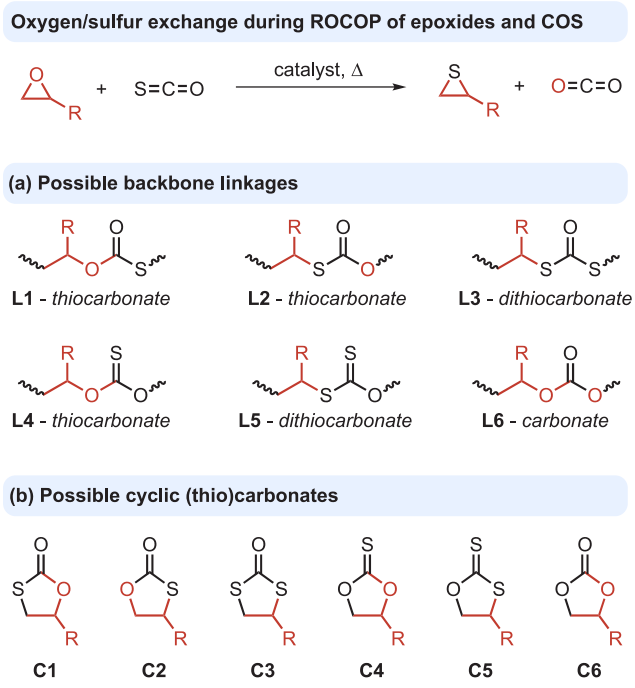

Ren, Lu, and co-workers explored the effect of initiating species on cyclic (thio)carbonate formation during epoxide/COS ROCOP using TBD-tethered (salan)FeX catalysts (Figure 20).[92] ROCOP of PO/COS at 80 °C using **cat79** (X = Cl) resulted in only 67% polythiocarbonate. By contrast, under the same conditions, high selectivity for PPMTC (>99%) was achieved with **cat80** (X = NO_3), owing to the poorer leaving group ability of NO_3 as compared to Cl. Notably, **cat80**-catalyzed copolymerization of COS with SO, CPO, or ECH resulted in high (>99%) poly(monothiocarbonate) selectivity and no O/S E-R.

ROCOP of COS with electronically biased epoxides such as ECH is particularly challenging due to the increased rate of

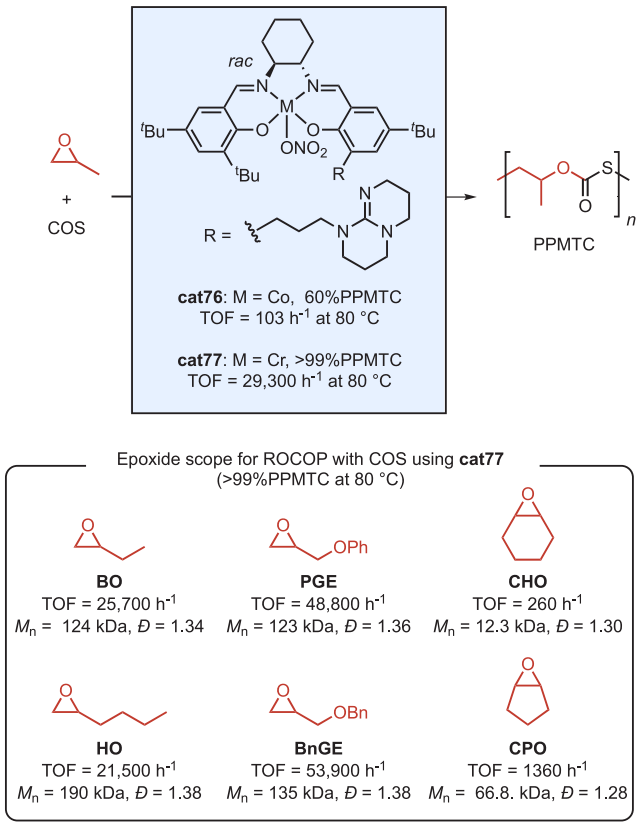

Figure 19. Scope and activity of **cat76** and **cat77** in epoxide/COS ROCOP.

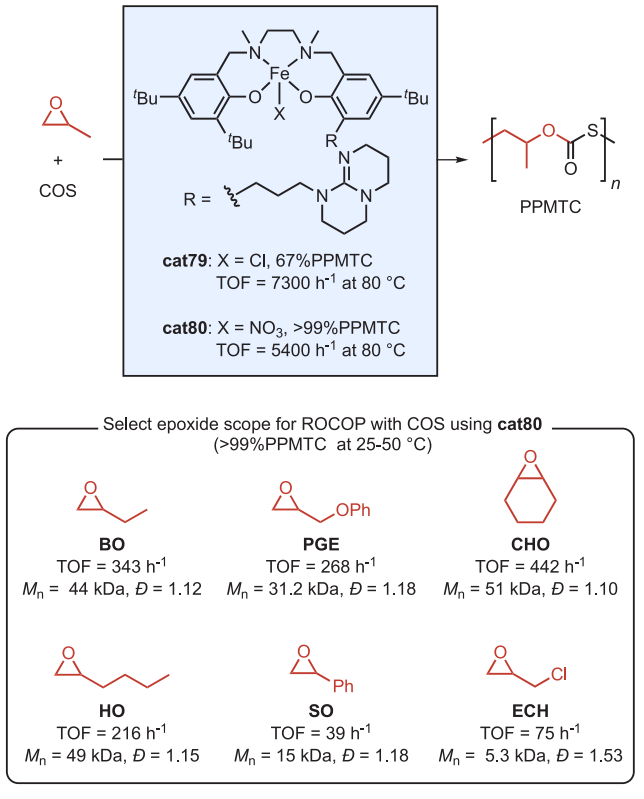

Figure 20. Scope and activity of **cat79** and **cat80** in epoxide/COS ROCOP.

(thio)carbonate backbiting at the more electrophilic C_α position as described previously for ECH/CO_2 ROCOP (Scheme 9). Additionally, the increased nucleophilicity of the thiocarbonate anion enables epoxide ring-opening at both the C_α and C_β positions of ECH, further reducing regioselectivity. Chain transfer to ECH can also occur when the more nucleophilic thiocarbonate chain end reacts at the pendant CH_2Cl position of ECH by nucleophilic substitution, leading to epoxy-functional chain ends and decreased molecular weight control (Scheme 12, vide infra). Therefore, multifunctional

Scheme 12. Proposed ECH/COS ROCOP Mechanisms Using cat74

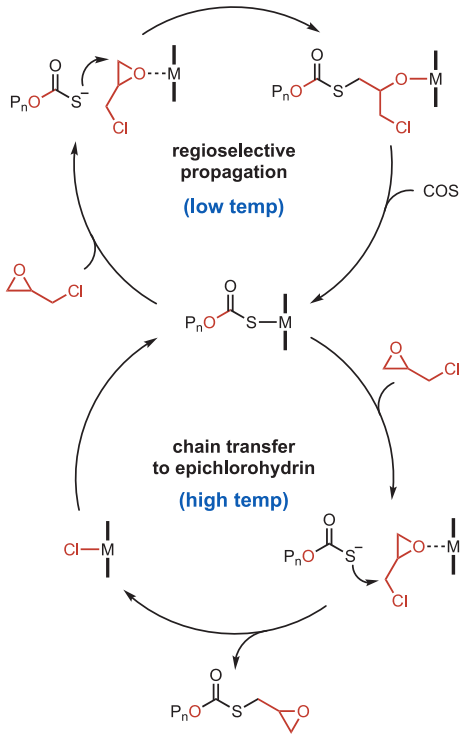

catalysts for controlled copolymerization of COS and epichlorohydrin must eliminate O/S E−R, prevent cyclic thiocarbonate formation, and maintain regioselectivity.

Lu and co-workers employed chiral **cat74** (*R*,*R*) for the ROCOP of (*S*)-ECH/COS at 25 °C to produce perfectly alternating poly((*S*)-epichlorohydrin monothiocarbonate) (PECHTC) with 98% polymer selectivity and regioselective ring-opening at the less-hindered C_β position of ECH (Figure 21).[112] No O/S E-R was observed. However, the low molecular weight and high dispersity (M_n = 810 Da, $Đ$ = 1.87) of the resulting copolymer indicated that chain transfer to ECH was operational during polymerization. Lowering the reaction temperature and increasing the catalyst loading ($[COS]_0$:$[(S)\text{-ECH}]_0$:$[\textbf{cat74}]_0$ = 1500:1000:1) increased copolymer molecular weight and decreased dispersity: at −10 °C and −25 °C, the copolymerization of COS and (*S*)-ECH afforded 1.5 kDa ($Đ$ = 1.51, >99% PECHTC) and a 3.1 kDa ($Đ$ = 1.37, >99% PECHTC) copolymer, respectively.

ESI-TOF MS analysis of PECHTC produced using **cat74** revealed that the polymer chain ends comprised thioglycidyl ether units, indicating that chain transfer to ECH was occurring during polymerization. The authors proposed two temperature-dependent mechanisms to explain the formation

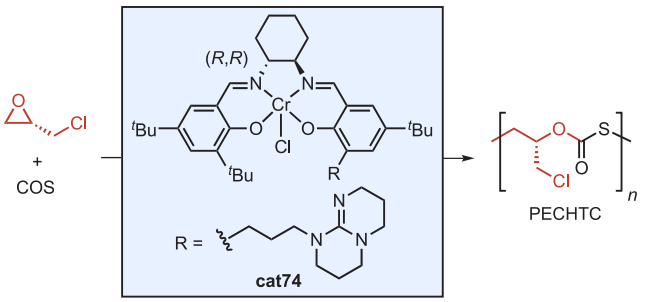

temperature	% conv.	M_n (Da)	$Đ$
25 °C	78	810	1.87
0 °C	63	1170	1.63
-10 °C	55	1470	1.51
-25 °C	45	3130	1.37

M_n decreases with increasing temperature due to increased chain transfer

Figure 21. Temperature-dependent activity of **cat74** in ECH/COS ROCOP.

of epoxide end groups during ECH/COS ROCOP. At lower temperatures, thiocarbonate chain ends ring-open ECH at the methylene carbon followed by rapid COS insertion and subsequent propagation (Scheme 12). However, higher temperatures increase the rate of competitive nucleophilic substitution at the methylene chloride position of ECH by thiocarbonate chain ends, generating the corresponding thioglycidyl ether chain end and regenerating **cat74**, which can reinitiate polymerization. Accordingly, molecular weight increased, and dispersity decreased as the polymerization temperature was reduced from 25 °C to −25 °C.

4.6. Transesterification and Epimerization. ROCOP of epoxides and cyclic anhydrides performed using excess epoxide is prone to transesterification and epimerization due to persistent alkoxide chain ends that form after reaching full conversion of cyclic anhydride (Scheme 13). Such side reactions lead to undesirable changes in polyester thermomechanical properties, and consequently polymerizations must be stopped prior to full conversion for many binary catalyst systems.[113]

Coates and co-workers developed a multifunctional (salph)AlCl catalyst **cat43** with pendant tris(dialkylamino)cyclopropenium chloride ([CyPr]Cl) cocatalyst that suppresses both transesterification and epimerization up to 24 h beyond full cyclic anhydride conversion for the ROCOP of PO and CPMA (Figure 22). The authors showed that the analogous binary (salph)AlCl/[CyPr]Cl catalyst system also prevented polyester backbone degradation and rationalized that the weakly interacting TDAC counterion promotes formation of the less reactive hexacoordinate aluminate species (Scheme 13). By comparison, using (salph)AlCl/[PPN]Cl resulted in rapid transesterification and epimerization following complete cyclic anhydride consumption under the same conditions. In further support of the hexacoordinate hypothesis, Coates and co-workers showed that electron-withdrawing *para*-substituents on the salicylidene moiety of (salph)AlCl catalysts increase Lewis acidity and suppress polyester backbone degradation by favoring the hexacoordinate aluminate species.[113] The multifunctional aminocyclopropenium catalyst suppressed side reactions even at low catalyst

Scheme 13. Transesterification and Epimerization Side Reactions Due to Formation of Bisalkoxide Intermediate in Epoxide/Anhydride ROCOP

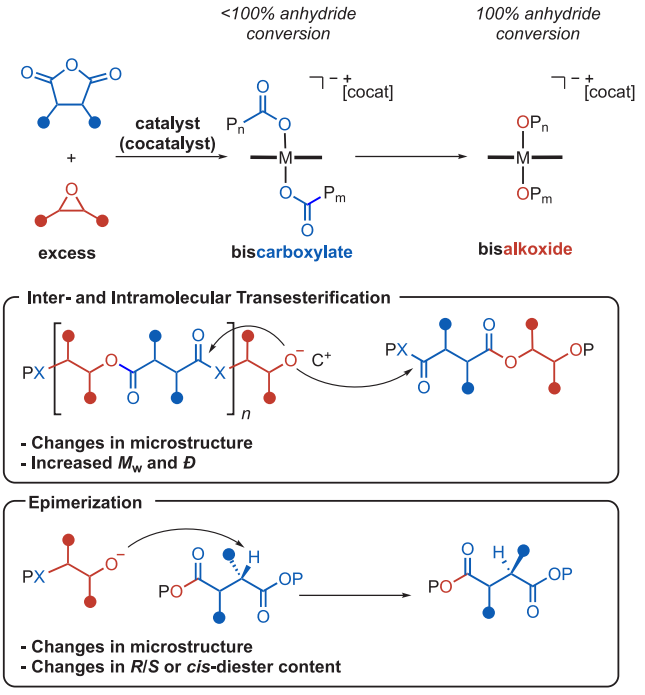

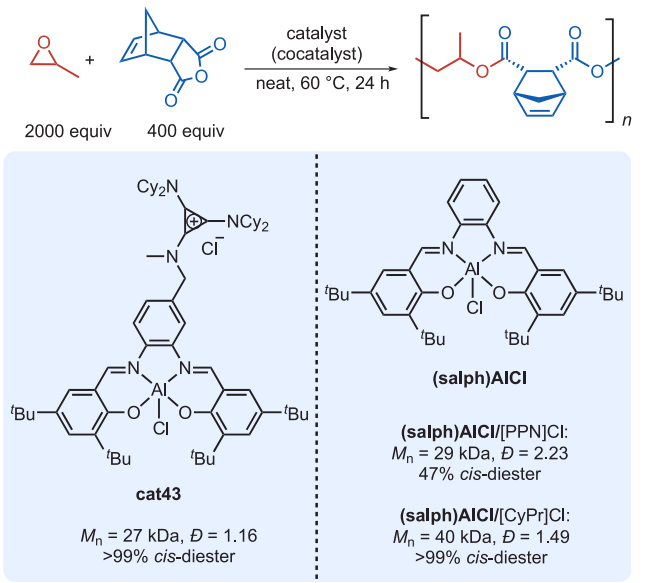

Figure 22. Suppression of side reactions in PO/CPMA ROCOP using **cat43**.

loadings, without loss in catalyst activity (TOF = 90 h^{-1} at 0.025 mol % **cat43**). Under the same conditions, the binary (salph)AlCl with either [PPN]Cl or [TDAC]Cl failed to maintain good catalytic activity (TOF = 15 h^{-1} and 19 h^{-1}, respectively).

Copolymerization of epoxides and thioanhydrides is particularly challenging due to considerable transesterification prior to full thioanhydride conversion owing to the increased reactivity of thioester linkages as compared to esters. To address this issue, Lu, Ren, and co-workers employed multifunctional **cat78** with a tethered TBD cocatalyst to the

ROCOP of PO and phthalic thioanhydride (PTA) ([**cat78**]$_0$:[PTA]$_0$:[PO]$_0$ 1:250:1000, T = 25 °C) to produce a perfectly alternating poly(thioester) (TOF = 113 h^{-1}, M_n = 15.9 kDa, $Đ$ = 1.2).[114] ^{13}C NMR analysis of the copolymer confirmed the absence of transesterification for up to 20 h. By contrast, using the binary (salcy)CrCl/[PPN]Cl system ([[(salcy)CrCl]$_0$:[[PPN]Cl]$_0$:[PTA]$_0$:[PO]$_0$ = 1:1:250:1000, T = 25 °C) produced copolymer with higher dispersities ($Đ$ = 1.43) indicative of transesterification, even though polymerization was stopped at 77% conversion.[115] However, suppression of transesterification by **cat78** is only maintained at room temperature. Performing the copolymerization of PO/PTA at 70 °C increased catalytic activity (TOF = 567 h^{-1}) but also increased transesterification to 27%. **cat78** was also able to copolymerize COS with a range of epoxides at low catalyst loadings, maintaining a perfectly alternating polymer structure and achieving molecular weights exceeding 100 kDa (Figure 23).

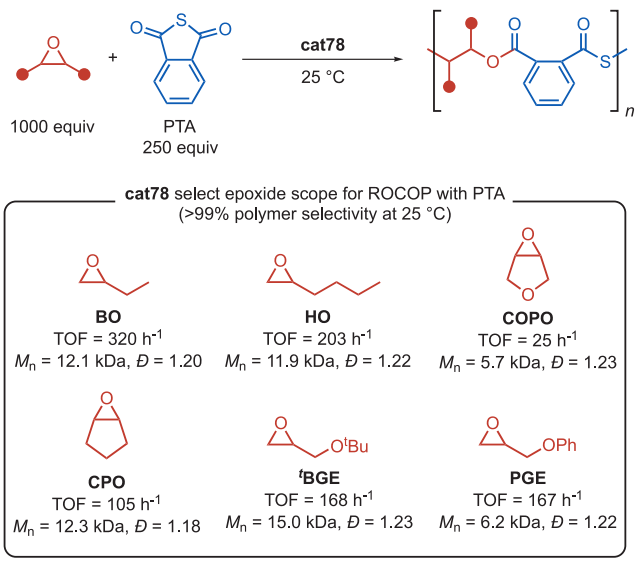

Figure 23. Epoxide/PTA ROCOP using **cat78**.

The authors proposed the improved polymerization control imparted by **cat78** is due to an intermolecular monomer enchainment mechanism involving the tethered TBD cocatalyst (Scheme 14). From the Cr(III) alkoxide intermediate, the pendant TBD unit preferentially ring-opens PTA to produce the corresponding thiocarboxylate−TBD adduct which then coordinates to the metal center, inducing dissociation of the alkoxide chain end. Gibbs free-energy profiles calculated by DFT suggest that the dissociated alkoxide chain end is most energetically favored to attack the thiocarboxylate−TBD adduct, producing a new thioester linkage and regenerating the pendent TBD cocatalyst. Thus, the TBD tether in the presence of the thioanhydride enforces proximity between the resulting thiocarboxylate and the alkoxide chain ends to discourage transesterification.

5. MULTIFUNCTIONAL ORGANOCATALYSTS FOR ROCOP

While metal-based multifunctional catalysts have demonstrated excellent catalytic performance, there is growing concern over their cost, synthetic complexity, and toxicity, especially as metal residues may remain in the resulting polymers.[116,117]

Scheme 14. Proposed PO/PTA ROCOP Mechanism Using cat78

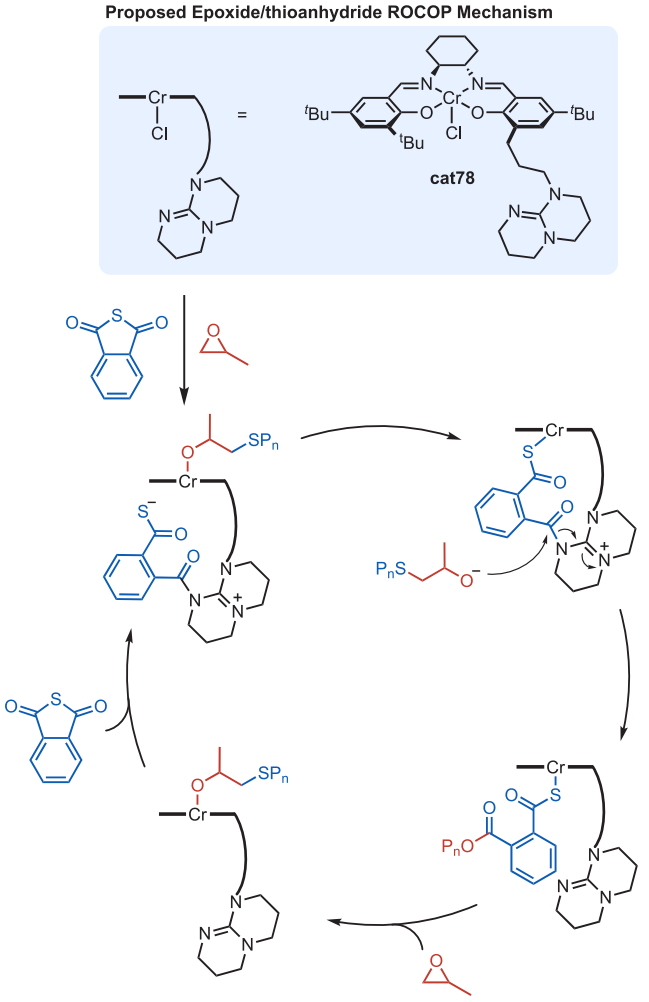

Recent interest in more sustainable alternatives to traditional metal-based ROCOP catalysts has led to the development of metal-free multifunctional organoborane catalysts.

Wu and co-workers developed a series of organocatalysts featuring a 9-borabicyclo[3.3.1]nonane (9-BBN) Lewis acid tethered to a tetraalkylammonium cocatalyst (**cat53**−**cat60**, Figure 24).[76] The authors studied the effects of alkyl linker length and ammonium counterion (Cl, Br, or I) on catalyst activity and polycarbonate selectivity during CHO/CO_2 ROCOP. A >99% selectivity for PCHC was observed for each of the multifunctional borane catalyst derivatives, with catalyst activities ranging from TOF = 117 h^{-1} (**cat53**, n = 1, X = Br, R = Et) to TOF = 517 h^{-1} (**cat56**, n = 3, X = Br, R = Et). While **cat53** only required the use of 1 equiv of boron to maintain high activity, CHO/CO_2 ROCOP using the corresponding binary system consisting of 2 equiv of hexyl-9-BBN and 1 equiv of BTEAB maintained lower activity (TOF = 330 h^{-1}) at 80 °C (Figure 24).

Similarly, a range of tetraalkylammonium-tethered 9-BBN catalysts with varying alkyl linker lengths and ammonium counterions were investigated for CHO/PA ROCOP (**cat61**−**cat67**, Figure 25).[118] The lowest catalyst activities were observed for catalysts **cat61** (X = Cl) and **cat62** (X = Br) which possess the shortest alkyl spacer length studied (n = 1). Meanwhile, the highest activity was achieved when n = 3, with

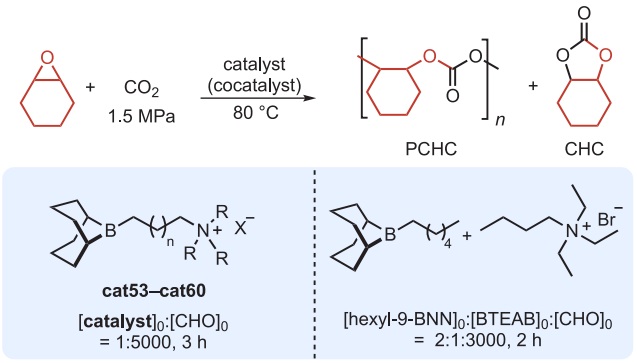

catalyst	n	X	R	TOF (h^{-1})
cat53	1	Br	Et	117
cat54	2	Br	Et	433
cat55	3	Cl	Et	367
cat56	3	Br	Et	517
cat57	3	Br	Bu	483
cat58	3	I	Et	317
cat59	4	Br	Et	417
cat60	5	Br	Et	433
hexyl-9-BNN/BTEAB	-	-	-	330

Figure 24. Activity and selectivity of **cat53–cat60** in CHO/CO_2 ROCOP.

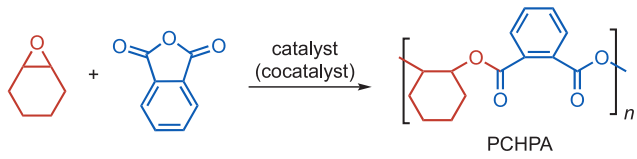

catalyst	n	X	TOF (h^{-1})
cat61	1	Br	45
cat62	1	Cl	84
cat63	2	Br	114
cat64	3	Cl	258
cat65	3	Br	219
cat66	3	I	168
cat67	4	Br	147
Et_3B/[PPN]Cl	-	-	33

Figure 25. Activity and selectivity of **cat61–cat67** in CHO/PA ROCOP.

cat64 (X = Cl) and **cat65** (X = Br) exhibiting TOF values of 258 h^{-1} and 219 h^{-1}, respectively. A similar effect of alkyl linker length on catalyst activity was also observed in CHO/CO_2 ROCOP mediated by multifunctional borane catalysts whereby the lowest and highest catalyst activities were obtained when the linker lengths were n = 1 and n = 3, respectively (vide supra). Although an exact binary analogue was not reported in this work, CHO/PA ROCOP using Et_3B/[PPN]Cl binary system at 100 °C exhibits diminished catalytic activity ($[Et_3B]_0$:$[[PPN]Cl]_0$:$[PA]_0$:$[PO]_0$ 2:1:200:200, 6 h, (TOF = 33 h^{-1}) (Figure 25).[119]

For the copolymerization of epoxides and CO_2, Liu and co-workers developed multifunctional boron catalysts featuring six boron units tethered to two ammonium cations via an aromatic backbone.[120] In reactions with PO, **cat68–cat70** maintained moderate catalytic activity and >99% polymer selectivity at room temperature but exhibited varying amounts of polyether formation depending on the geometry of the aromatic linker. *Para*-substituted **cat68** produced 88% carbonate linkages, *meta*-substituted **cat69** produced 83% carbonate linkages, and *ortho*-substituted **cat70** produced 55% carbonate linkages (Figure 26). The authors suggested that decreasing the

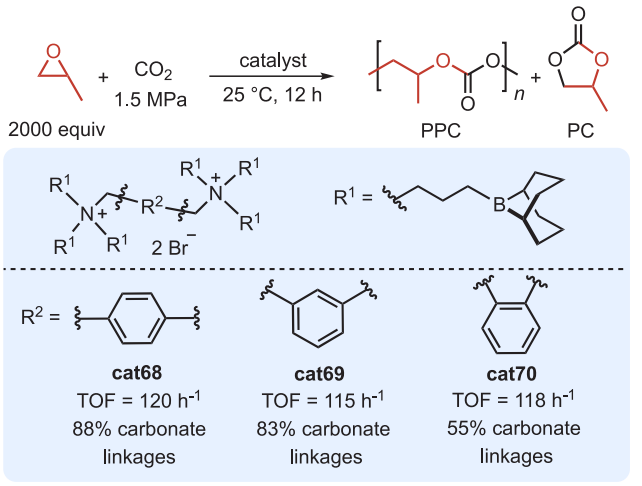

Figure 26. Activity and selectivity of **cat68–cat70** in CHO/CO_2 ROCOP.

distance between boron centers could promote epoxide homopolymerization by a dinuclear mechanism and therefore decrease carbonate linkage content. Notably, **cat68** was also active for ECH/CO_2 copolymerization: perfectly alternating PECH was produced with no observed epoxide homopolymerization or cyclic carbonate formation with a TOF of 39 h^{-1} ([**cat68**]$_0$:[ECH]$_0$ 1:500, 1.5 MPa CO_2, T = 40 °C).

Wu and co-workers developed a multifunctional organoboron catalyst **cat71** comprising four boron centers tethered to a common ammonium cocatalyst for the ROCOP of ECH/CO_2 that produced PECHC with high selectivity (>99%) and no polyether formation at temperatures up to 40 °C (Figure 27).[121] As previously discussed, ECH's heightened electrophilicity facilitates cyclic carbonate formation via backbiting at the more electrophilic C_a-methine. The energy difference between cyclic carbonate and polycarbonate formation for ECH/CO_2 coupling using **cat71** was 14.5 kcal/mol—significantly higher than the ΔE_a = 10.9 kcal/mol using binary

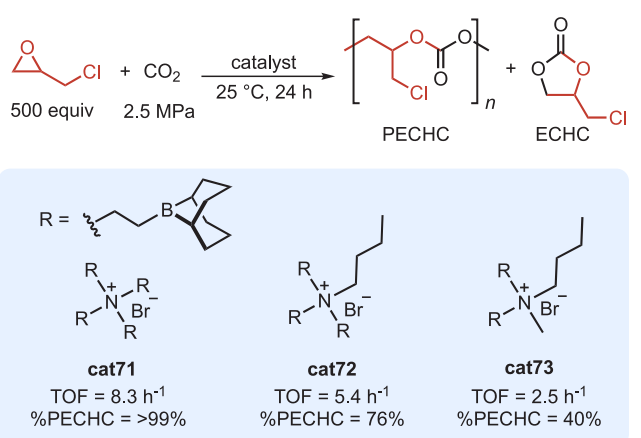

Figure 27. Activity and selectivity of **cat71–cat73** in ECH/CO_2 ROCOP.

salcy(Co)DNP/[PPN]DNP for ECH/CO_2 coupling (vide supra).[105] Increased kinetic favorability of ECHC formation at higher temperatures reduced polycarbonate selectivity to 90% at 60 °C. The authors attributed the high selectivity for PECHC afforded by **cat71** to the proximity of the boron centers that is maintained by the tetranuclear catalyst design. X-ray crystallographic analysis confirmed that tetranuclear **cat71** maintains an average boron−boron bond distance of 7.5 Å whereas trinuclear **cat72** and dinuclear **cat73** have increased boron−boron bond distances of 8.4 and 8.8 Å, respectively. Indeed, **cat72** and **cat73** produce reduced TOF (5.4 h^{-1} and 2.5 h^{-1}, respectively) and polycarbonate selectivity (76% and 40%, respectively).

6. USE OF CHAIN TRANSFER AND STEREOCONTROL TO ACCESS ADVANCED POLYMER ARCHITECTURES

Applying multifunctional catalysts to a wide range of monomers in epoxide copolymerization has enabled the synthesis of well-defined polycarbonates and polyesters with tunable molecular weights, dispersities, and regio- and stereochemistry. We will discuss two routes by which multifunctional catalysts can be used to access advanced polymer architectures and microstructures: in tandem with chain transfer agents to access multiblock polymers or via stereocontrolled polymerization to produce enantiomerically enriched polymers.

6.1. Mechanistic Considerations of Chain Transfer and Multifunctional Catalysts. Inoue and co-workers were the first to observe that the introduction of protic species during ROCOP causes reversible and rapid equilibration between protic species and alkoxide chain ends while maintaining uniform chain growth.[122] In particular, each equivalent of a chain transfer agent generates a dormant chain end and a new catalyst−alkoxide species, providing a controllable method to increase the number of polymer chains per catalyst (Scheme 15). Polymer molecular weights can

Scheme 15. Generalized Overview of Chain Transfer in Epoxide ROCOP

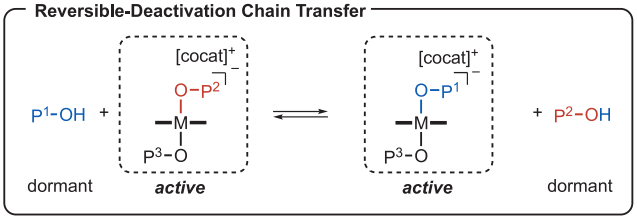

therefore be tuned by varying both the equivalents of catalyst-derived initiator and added chain transfer agent (CTA). In addition to reducing the amount of catalyst needed and affording excellent molecular weight control, the introduction of chain transfer agents enables control over end group identity, providing a route toward functionalizable polymers or advanced polymer architectures.

While many binary catalyst systems can be used in conjunction with protic CTAs, their vulnerability to dilution effects prohibits the formation of high-molecular weight polymers with the use of a CTA. Because multifunctional catalysts maintain better catalytic activity at low catalyst loading as compared to their binary analogues, pairing multifunctional catalysts with CTAs provides a means to access targeted molecular weight polymers with specific end group functionalities.

Coates and co-workers compared the behavior of multifunctional aminocyclopropenium **cat43** to the corresponding binary (salph)AlCl/[CyPr]Cl system in the presence of protic CTAs.[56b] In the copolymerization of PO and CPMA at 60 °C, **cat43** maintains a TOF of 82 h^{-1} without added CTA, and addition of 10 or 50 equiv of 1-adamantanecarboxylic acid ($AdCO_2H$) CTA had minimal effect on activity (TOF = 86 h^{-1}, and 70 h^{-1}, respectively). Using the analogous binary (salph)AlCl/[CyPr]Cl system, catalyst activities decreased from 49 h^{-1} (no CTA) to TOF = 29 h^{-1} and 12 h^{-1} with the addition of 1 or 50 equiv of $AdCO_2H$, respectively. Similarly, low TOF values of 17 h^{-1} and 9 h^{-1} were observed when using [PPN]Cl as the cocatalyst in the presence of 10 or 50 equiv of $AdCO_2H$, respectively. This result demonstrates that the lack of a covalent tether between the catalyst and cocatalyst, not the cocatalyst identity, is responsible for the reduced activity of the binary systems in the presence of CTA. A range of CTAs comprising alcohol, thiol, amine, and carboxylic functional groups functioned as efficient CTAs for epoxide/cyclic anhydride ROCOP (Figure 28). Multifunctional **cat43** maintained high activity (TOF = 86 h^{-1}) at low loadings in the presence of protic CTA, a feat unattainable in the corresponding binary system. On the basis of Lineweaver−Burk plots that suggest copolymerization mediated by **cat43** is not inhibited significantly by binding of alcohol chain ends, Coates and co-workers suggested that tethering the aminocyclopropenium to the Al salph favors a hexacoordinate complex in which two chain ends remain coordinated to the metal center, therefore inhibiting competitive binding. Without the proximity enforced by a tethered cocatalyst, the hexacoordinate complex is not as readily maintained in the binary system, allowing competitive binding between alcohol chain ends and the metal center to occur more readily.

For early versions of Lee's tetrafunctional (salcy)Co catalyst, CTA compatibility depended not only on catalyst structure but on initiator identity.[66] During the copolymerization of PO/CO_2, **cat5** exhibits a long induction period of 260 min. Lee and co-workers hypothesized that the presence of water slows the rate of initiation by coordinating to DNP; indeed, when over 20 equiv of either water or methanol was added, initiation no longer occurred (Figure 29). Substituting two loosely bound DNP homoconjugates enhanced catalytic activity (TOF = 15 000 h^{-1}) and eliminated the previously observed induction period, as the DNP homoconjugates are less hygroscopic and prevent coordination to water. Similarly, **cat6** (X = NO_3) was used in conjunction with multifunctional CTAs, including tri- and tetracarboxylic acids, to produce narrow-dispersity polymers with only a slight reduction in TOF (8100−11 500 h^{-1}). Installing specific multifunctional alcohols and carboxylic acids as polymer end groups allowed Lee and colleagues to repolymerize to form nonlinear polymer architectures. Notably, utilizing **cat6** allowed Lee and co-workers to maintain the same catalytic efficiency with up to 200 equiv of adipic acid added as a CTA (TOF = 14 500−15 700 h^{-1}).[123]

Interestingly, Darensbourg and co-workers' (salcy)Co catalyst comprising an amino tether and DNP^{-1} counteranion (**cat40**) is only active for CO_2/*tert*-butyl 3,4-epoxybutanoate (^{t}BuEB) copolymerization in the presence of water.[124] While no copolymerization of ^{t}BuEB occurred in the absence of water, **cat40** exhibited a TOF of 62.5 h^{-1} when trace water was

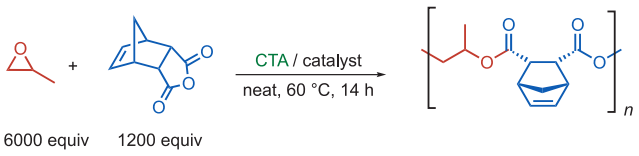

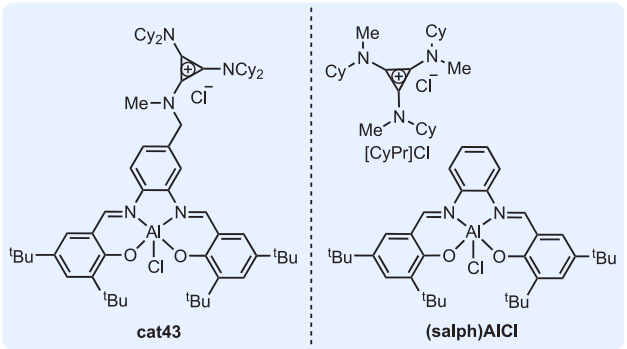

catalyst	cocatalyst	$AdCO_2H$ (equiv)	conv (%)	TOF (h^{-1})
cat43	-	0	96	82
cat43	-	1	98	84
cat43	-	10	>99	86
cat43	-	50	82	77
(salph)AlCl	[CyPr]Cl	0	57	49
(salph)AlCl	[CyPr]Cl	1	34	29
(salph)AlCl	[CyPr]Cl	10	21	18
(salph)AlCl	[CyPr]Cl	50	14	12

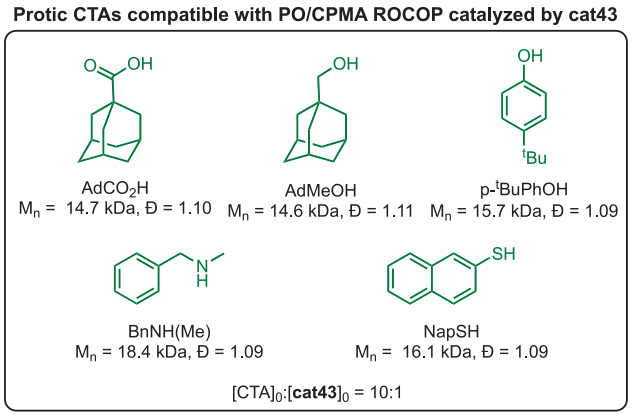

Figure 28. PO/CPMA ROCOP using **cat43** in conjunction with chain transfer agents.

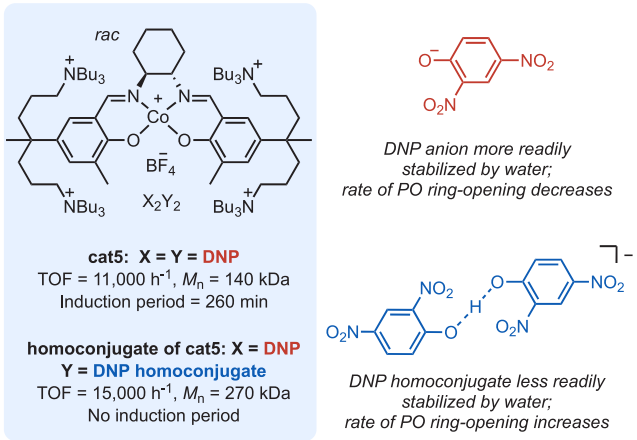

Figure 29. CTA compatibility of **cat5** in PO/CO_2 copolymerization.

introduced in the polymerization system, allowing the formation of fully regioregular poly(*tert*-butyl 3,4-epoxybutanoate) (P^tBuEB) with 100% H-T linkages (Figure 30). The

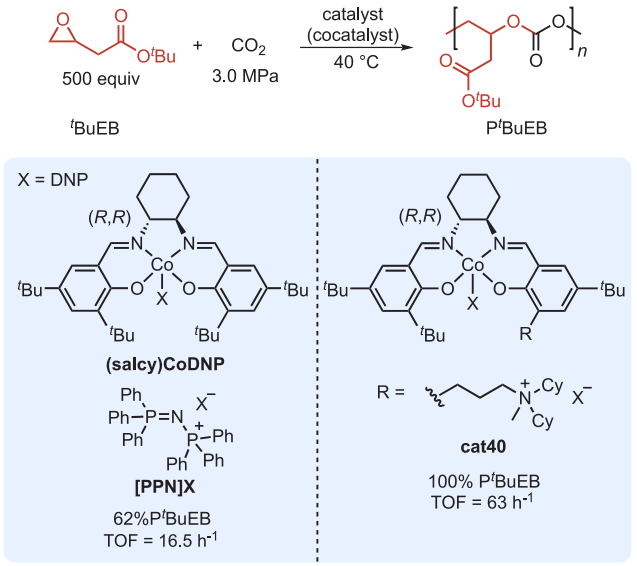

Figure 30. $^tBuEB/CO_2$ ROCOP using **cat40** in the presence of water.

authors rationalized that polymerization in this catalytic system is only initiated by weakly basic nucleophiles, such as those generated from chain transfer or hydrolysis reactions. Synthesis of poly(methyl 3,4-epoxybutanoate) under the same conditions did not afford the same regioselectivity (91.8% head-to-tail linkages), suggesting that the steric influence of the epoxide substituent (^{t}Bu versus Me) is largely responsible for the site of ring-opening.

6.2. Terpolymerizations. In an early example of a ring-opening terpolymerization, Nozaki and co-workers employed **cat31** to copolymerize two epoxide comonomers with CO_2.[46] Bimodal GPC traces due to trace water was indicative of the living nature of the copolymerization in the presence of protic species. Indeed, the addition of 2 equiv of methanol relative to **cat31** in PO/CO_2 copolymerization produced a 5.1 kDa copolymer with low dispersity ($Đ$ = 1.06) and methoxy initiating groups. Given the living chain end retention afforded by **cat31** in the presence of protic species, the authors copolymerized PO/CO_2 to high conversion to form a PPC block which was then chain-extended with hexene oxide (HO) and CO_2 to produce the corresponding PPC-*b*-PHC diblock copolymer (PHC = poly(hexene carbonate)). A clear shift of the GPC trace of the initial PPC block to lower elution volume following chain extension with HO/CO_2 corroborated that **cat31** maintained active chain ends following full consumption of PO. Unlike previous systems which required tapering between blocks to avoid backbiting, this multifunctional catalyst enabled the synthesis of PPC-*b*-PHC in a one-pot process via sequential monomer addition.

Applying a similar sequential addition approach, Ren and co-workers synthesized ABA triblock terpolymers from EO, PO, and COS using **cat77** (Scheme 16).[125] The alternating copolymerization of EO and COS produced copolymers with M_n values up to 193 kDa and T_m values between 125−128 °C. The authors sought to prepare thermoplastic elastomers using the semicrystalline poly(ethylene monothiocarbonate) (PEMTC) as the hard block segments. Using ethylene glycol

Scheme 16. (A) Synthesis of Polycarbonate and (B) Polymonothiocarbonate Multiblock Copolymers

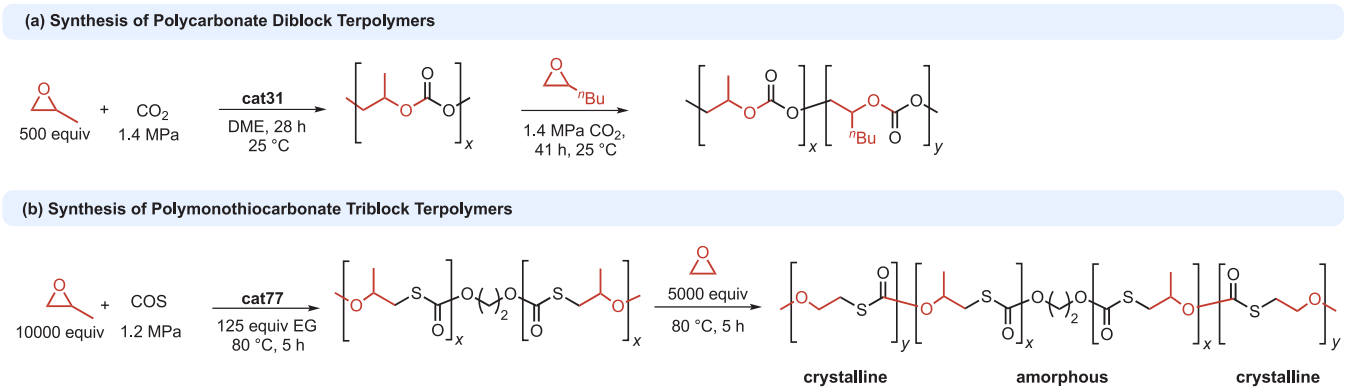

(EG) as a difunctional chain transfer agent, PO/COS ROCOP produced a hydroxy-telechelic soft block (M_n = 9.0 kDa, $Đ$ = 1.19) that was subsequently chain extended with EO/COS to install the outer hard block segments. Successful chain extension was evidenced by a shift in the GPC trace to lower elution volumes (M_n = 13.3 kDa, $Đ$ = 1.18) following formation of the PEMTC block. ^{1}H NMR spectroscopy revealed that the ABA triblock possessed 30% EO/COS content in the outer blocks and 70% PO/COS in the central segment. The triblock terpolymer demonstrated a maximum tensile strength of 11.2 MPa with a strain failure of 575% and high elastic recovery (~90%) over multiple loading and unloading cycles. An EO/COS copolymer possessing similar M_n exhibited a tensile strength of only 1.6 MPa and a strain to failure greater than 1000%. These results demonstrate that epoxide comonomer identity and block architecture provide a means of tuning poly(monothiocarbonate) tensile properties.

As an alternative to sequentially copolymerizing different epoxide comonomers into distinct blocks, Lee and co-workers evaluated the reactivity ratios of PO and BO, hexene oxide (HO), or CHO comonomers in one-pot terpolymerizations with CO_2 catalyzed by an imine-uncoordinated (salcy)Co complex bearing four quaternary ammonium salts (**cat5**) (Chart 3).[126] In all terpolymerizations, **cat5** was highly selective for alternating ROCOP, and no ether linkages were observed (Figure 31). The Fineman–Ross method was used to

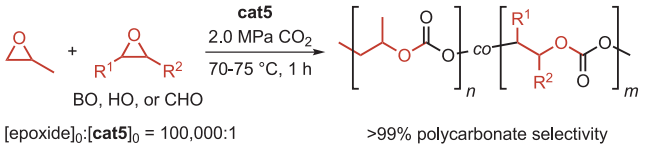

Figure 31. One-pot terpolymerizations PO/epoxide and CO_2 using **cat5**.

measure the reactivity ratios of forming PO–CO_2 and coepoxide–CO_2 repeat units. Terpolymerization of PO, CHO, and CO_2 afforded reactivity ratios of 1.7 (r_{PO}) and 0.37 (r_{CHO}), indicating that both PO–CO_2 and CHO–CO_2 chain ends preferentially ring-open PO over CHO. Terpolymerizations of PO and HO demonstrated Fineman–Ross reactivity ratios approaching statistical epoxide incorporation (r_{PO} = 1.9, r_{HO} = 0.46, $r_{PO} \times r_{HO}$ = 0.87), but increasing HO loading substantially decreased reaction rates (TOF = 8600 h^{-1} at 0.20 f_{HO} versus 4900 h^{-1} at 1.00 f_{HO}). Terpolymerizations of the more similar comonomers PO and BO exhibited similar reaction rates at various feed ratios (TOF = 9500 h^{-1} at 0.20 f_{BO} versus 10300 h^{-1} at 1.00 f_{BO}). The terpolymer T_g and T_d values exhibited positive correlations with the mole fraction of CHO incorporated (F_{CHO}). In contrast to the rigidity imparted by CHO, polycarbonates incorporating higher mole fractions of structural isomer HO had lower T_g values. As observed for HO, polymerizations of PO and BO approached ideal behavior (r_{PO} = 1.4, r_{BO} = 0.58, $r_{PO} \times r_{BO}$ = 0.81), and polycarbonates comprising higher mole fractions of BO exhibited lower T_g values. Varying the epoxide comonomer identity and mole fraction in terpolymerizations with PO and CO_2 afforded tunable T_g values from 0 °C to 100 °C and improved thermal stability. Reactions in the presence of styrene oxide, isobutylene oxide, and glycidyl ethers produced exclusively PO/CO_2 copolymers, further underscoring the importance of epoxide comonomer reactivity ratios in determining terpolymer microstructure.

Lu and co-workers sought to tune the T_g of polycarbonate terpolymers by varying the incorporation of PO and CHO comonomers.[55] As previously discussed, Lee and co-workers observed that PO/CHO/CO_2 copolymerizations catalyzed by an imine-uncoordinated Co complex preferentially incorporate PO over CHO early in the polymerization.[126] Indeed, Lu and co-workers observed that multifunctional (salcy)CoDNP complex **cat35** with one tethered quaternary ammonium cocatalyst was highly active for PO/CO_2 copolymerizations (TOF = 5160 h^{-1}, 2.5 MPa CO_2, T = 90 °C), nearly double the activity observed for CHO/CO_2 copolymerization (TOF = 3020 h^{-1}, 2.5 MPa CO_2, T = 90 °C). Surprisingly, the two epoxide comonomers were incorporated at similar rates when a 50:50 PO:CHO mixture was used: from 5–45% conversion, the terpolymers comprised ~52:48 PO:CHO with an intermediate TOF of 3590 h^{-1}, suggesting that CHO inhibits the reactivity of PO. The similar rates of incorporation of PO and CHO produced a random terpolymer in a one-pot reaction (Figure 32a). Adjusting the mole fractions in the monomer feed produced proportionate changes in terpolymer epoxide content and corresponding changes to the T_g values. Although CHO and PO exhibited similar reactivities in terpolymerizations with CO_2, other aliphatic epoxides were incorporated at different rates: EO was the most reactive, while epoxides with longer aliphatic substituents incorporated more slowly than CHO. These results demonstrate that comonomer reactivity ratios are determined both by substrate bias and catalyst design.

To introduce a reactive olefin unit pendant to the polycarbonate backbone, Duan and co-workers used a

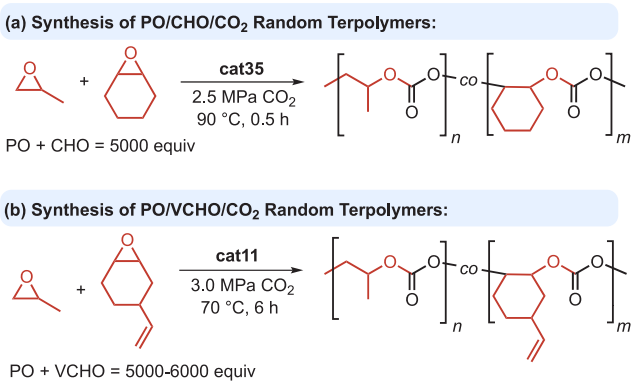

Figure 32. Synthesis of random terpolymers using multifunctional catalysts.

(salcy)$CoNO_3$ complex bearing two quaternary ammonium cocatalysts to catalyze the terpolymerization of PO, 4-vinyl cyclohexene oxide (VCHO), and CO_2 (Figure 32b).[127] In the absence of PO, mixtures of VCHO/CO_2 and **cat11** produced neither copolymer nor cyclic carbonate, but addition of trace PO promoted alternating enchainment. Holding the total epoxide concentration constant, Duan and co-workers observed that increasing the VCHO:PO ratio from 2:8 to 5:5 significantly decreased reaction rate (TOF = 668 h^{-1} to 97 h^{-1}, respectively, $[Co]_0$:$[epoxide]_0$ = 1:5000−6000). Nonetheless, terpolymerizations of VCHO, PO, and CO_2 proceeded to high conversion without ether linkages. The resulting polycarbonates exhibited a single T_g value that increased linearly on VCHO incorporation. To further modulate the thermal properties of the terpolymers, the authors reacted the vinyl groups with *m*-chloroperoxybenzoic acid to install pendant epoxide units. A second post-polymerization modification converted the newly installed epoxides into cyclic carbonate side chains. Each functionalization step increased the bulk of the pendant unit and produced a corresponding increase in the T_g values of the vinyl-, epoxy-, and cyclic carbonate-functionalized terpolymers. By tuning the PO:VCHO ratio and installing different side-chain units, Duan and co-workers were able to access polycarbonate terpolymers with a wide range of T_g values up to 196 °C.

Multifunctional catalysts have also been used to perform terpolymerizations of epoxides, CO_2, and cyclic anhydrides. Liu and co-workers employed a multifunctional **cat11** for terpolymerizations of PO, CO_2, and carbic anhydride (CPMA) (Figure 33a).[128] The catalyst rapidly polymerized PO, CO_2, and CPMA at low catalyst loadings ($[Co]_0$:$[PO]_0$ = 1:16000, TOF = ∼1000 h^{-1}, 3.0 MPa CO_2, T = 60 °C). CPMA was preferentially incorporated over CO_2 and was fully consumed in the first 4 h of the 8-h polymerization. The DSC thermograms of the poly(ester-*block*-carbonate)s revealed two distinct thermal transitions associated with the glass transitions of the polyester (T_g = 62−67 °C) and polycarbonate blocks (T_g = 39−42 °C). Similarly, thermogravimetric analysis (TGA) revealed a two-step degradation process in which the polycarbonate segment degrades at a temperature lower than that for the polyester segment. These results further corroborate that the microstructure is blocky rather than random. The authors next evaluated the effect of the tricyclic anhydride conformation (*endo* versus *exo*): at full conversion of the tricyclic anhydride, terpolymerizations with *exo*-CPMA reached higher conversions (51%) than those

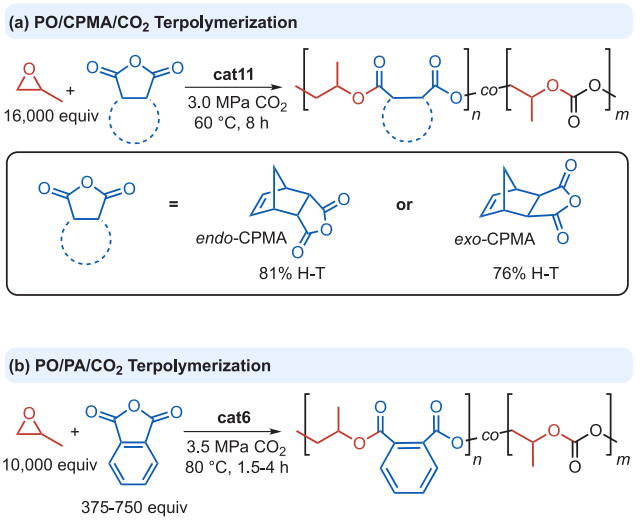

Figure 33. Synthesis of poly(ester-*co*-carbonate)s promoted by multifunctional catalysts.

employing *endo*-CPMA (29%) under identical conditions ($[cat]_0$:$[PO]_0$[CPMA]$_0$ = 1:16 000:1000, 3.0 MPa CO_2, T = 60 °C, 8.0 h). The authors proposed that the *exo*-CPMA isomer reacts more readily than the more sterically encumbered *endo* isomer. Moreover, polymerizations incorporating the *endo* isomer also produced more propylene carbonate byproduct relative to those incorporating the *exo* isomer. However, terpolymerizations with *exo*-CPMA were also subject to more frequent regioerrors (75% head-to-tail linkages) relative to those using the *endo*-isomer (81% head-to-tail linkages).

Lee and co-workers applied a multifunctional (salcy)CoX complex bearing quaternary ammonium salts to terpolymerizations of PO, CO_2, and PA (Figure 33b).[129] **cat6**-catalyzed terpolymerizations achieved TOFs (12 000 h^{-1}) intermediate between those of PO/PA copolymerization (∼1500 h^{-1}) and PO/CO_2 copolymerization (16 000 h^{-1}), even in the presence of up to 60 equiv of ethanol as a CTA. Although the rate of PO/PA copolymerization is slower, the authors observed that cyclic anhydride is preferentially consumed in the first 4 h prior to incorporation of CO_2, as was observed by Liu and co-workers.[128] This counterintuitive result arises from distinct rate-limiting and selectivity determining steps: phthalic anhydride ring-opening is faster than CO_2 insertion, but benzoate chain ends perform rate-limiting epoxide ring-opening more slowly than do carbonate chain ends.[130] Interestingly, introduction of ethanol CTA increased the rate of PA incorporation and subsequently tuned the T_g of the resulting terpolymers. Without added ethanol, PA conversion reached 38% in 1.5 h and the resulting terpolymer had a f_{PA} = 0.12; the introduction of 60 equiv of ethanol increased conversion of PA to 50% and had a f_{PA} = 0.18. The authors rationalized that the increased rate of PA consumption is due to an additional ring-opening of anhydride in which the OH terminus can directly react with PA without the aid of **cat6**. Although PA is preferentially incorporated early in the reaction, DSC thermograms of the terpolymers revealed a single T_g value 39−48 °C, suggesting a gradient poly(ester-*co*-carbonate) structure, rather than distinct polyester and polycarbonate blocks. Polymers with a high degree of PA incorporation (f_{PA} = 0.23) exhibited rigidity (T_g = 48 °C)

higher than that of copolymers with less PA incorporation (f_{PA} = 0.10, T_g = 38 °C). Furthermore, Lee and co-workers observed negligible cyclic carbonate formation even in the presence of significant amounts of cyclic anhydride. It is unclear whether these differences from the previously discussed CPMA/PO/CO_2 terpolymerization arise from the more active catalyst or the PA comonomer.

Thus far, the discussion has focused on terpolymerizations in which a multifunctional catalyst has been used to enchain multiple comonomers in a one-pot mixture or via polymerization of comonomers through sequential monomer addition in the presence of a difunctional CTA. Alternative approaches to terpolymer synthesis include chain extension of a telechelic "macro CTA", chain shuttling between different catalyst complexes, or orthogonal polymerizations from a two-site catalyst. These approaches require that both catalysts are highly selective for their respective polymerizations and are compatible with both the monomer mixture and polymer products.

Lu, Darensbourg, and co-workers performed a tandem terpolymerization in which a multifunctional Co complex and 1,8-diazabicyclo[5.4.0]undec-7-ene (DBU) organocatalyst were applied in two sequential steps (Figure 34).[131] **cat35**

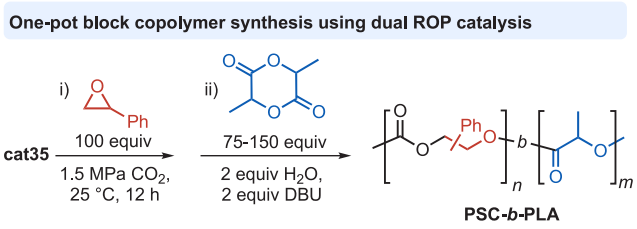

Figure 34. Synthesis of poly(styrene carbonate-*block*-lactide) catalyzed by a multifunctional complex and DBU organocatalyst.

was employed to first catalyze SO/CO_2 ROCOP, affording a monomodal molecular weight distribution comprising chains initiated solely by DNP anions. The authors rationalized that while trace water does generate a Co−OH complex from adventitious chain transfer, this complex is not nucleophilic enough to react with the electron-rich SO. Upon reaching high conversion of SO, the CO_2 was vented and the polymerization quenched with water (2 equiv per catalyst) to produce hydroxy-terminated chain ends. The resulting poly(styrene carbonate) macro CTA readily initiates ROP of lactide in the presence of catalytic DBU. In the absence of lactide, DBU rapidly depolymerizes poly(styrene carbonate), though facile ring-opening of the strained monomer suppresses this degradation pathway. The GPC chromatogram of the resulting block copolymer revealed a shift to higher molecular weight with preserved monomodality and low dispersity, suggesting uniform chain extension. Varying the SO and lactide loadings permitted facile tuning of molecular weights and block composition. Although sequential addition of the lactide monomer after full SO conversion ensures clean block formation, the DSC thermograms exhibited a single glass transition, suggesting that the polycarbonate and polyester segments are readily miscible. In a follow-up report, Darensbourg and co-workers employed water as a chain transfer agent with a binary (salcy)CoTFA/[PPN]TFA (TFA = trifluoroacetate) catalyst system to obtain hydroxytelechelic poly(propylene carbonate) for subsequent DBU-catalyzed chain extension with lactide to afford ABA triblock terpolymers.[132]

To synthesize poly(carbonate-*co*-ether)s, Lee and co-workers used alcohols to promote chain shuttling between two catalysts (Figure 35): **cat6** salts exclusively catalyze alternating

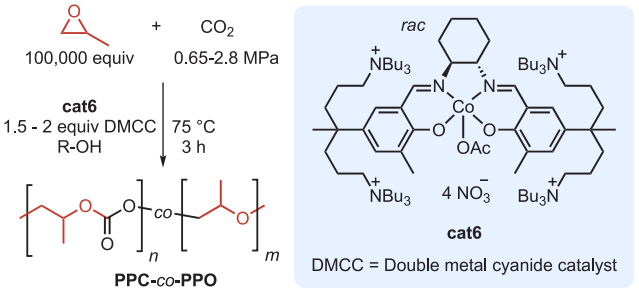

Figure 35. Chain shuttling between multifunctional **cat6** and double metal cyanide catalyst affords poly(propylene carbonate-*co*-propylene oxide) copolymers.

ROCOP of epoxide/CO_2 (>99% carbonate linkages), while a double metal cyanide catalyst (DMCC) preferentially homopolymerizes epoxide (89% ether linkages).[133] Some optimization was required to obtain conditions favoring dual catalysis: at low CO_2 pressures, polymerization by the DMCC dominated, whereas higher CO_2 pressures increased the rate of **cat6**-catalyzed epoxide/CO_2 ROCOP. The chain-shuttling dual catalysis strategy afforded poly(carbonate-*co*-ether)s with molecular weights up to 68 kDa and high dispersities (2.1−6.2). ^{1}H NMR spectroscopy corroborated the formation of poly(carbonate-*co*-ether)s rather than discrete polyether and polycarbonate homopolymers. The poly(carbonate-*co*-ether)s exhibited a single T_g value, while polycarbonate/polyether blends revealed two T_g values. Tuning the CO_2 pressure and catalyst ratio provided a means of controlling carbonate content (f_{CO2} = 0.20−0.67) and consequently T_g (−63 to 21 °C).

While one-pot terpolymerizations of epoxides, CO_2, cyclic anhydrides, and cyclic esters have employed multifunctional ROCOP catalysts bearing covalently tethered cocatalysts, efforts to expand the comonomer scope have inspired further catalyst design. Rather than incorporating secondary functionality to improve the rate-limiting ring-opening step, these multifunctional catalysts comprise two orthogonal polymerization sites for one-pot block copolymer synthesis.

Unlike (salen)MX_n complexes, β-diiminate zinc (BDI-Zn) catalysts do not typically require exogenous cocatalyst for epoxide/CO_2 ROCOP. Wu and co-workers synthesized a BDI-Zn catalyst with a bound carboxylate-functional trithiocarbonate (TTC) CTA capable of initiating epoxide/CO_2 ROCOP and mediating reversible addition−fragmentation chain transfer (RAFT) polymerization (Figure 36a).[134] This strategy of using a multifunctional initiator improved upon prevalent chain transfer approaches, which produce mixtures of CTA- and catalyst-derived chains. The presence of trithiocarbonate chain ends was corroborated by matrix-assisted laser desorption ionization−time-of-flight (MALDI-TOF) mass spectrometry, and ^{1}H NMR spectroscopy. To perform the ROCOP and RAFT polymerizations in a one-pot procedure, ROCOP of CHO and CO_2 was carried to full conversion of CHO followed by venting the excess CO_2. Azobisisobutyronitrile (AIBN) radical initiator and *N*-isopropylacrylamide

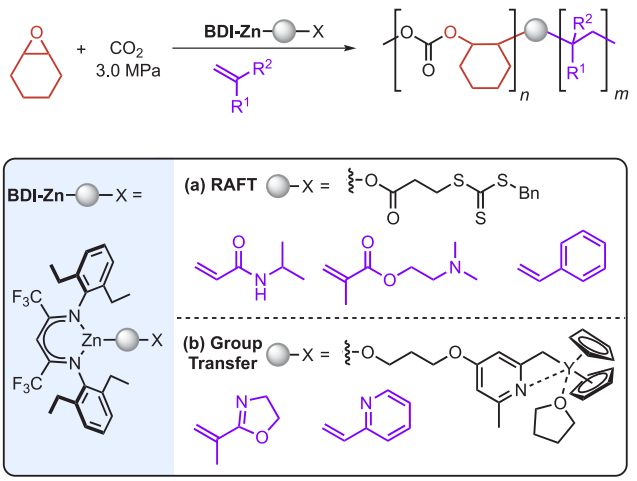

Figure 36. A heterobifunctional BDI-Zn/RAFT agent complex promotes sequential ROCOP and (a) RAFT polymerization or (b) group transfer polymerization steps to afford block copolymers.

(NIPAM) monomer were then added directly to the autoclave. The GPC chromatogram of the isolated block copolymers revealed a uniform shift to lower elution volumes while preserving the low dispersity of the poly(cyclohexene carbonate) block. The poly(cyclohexene carbonate-*block*-PNIPAM) diblock terpolymers are amphiphilic and self-assemble into thermoresponsive micelles in water. To access diverse diblock terpolymer properties, Wu and co-workers extended this synthetic strategy to a variety of vinyl monomers, including 2-(dimethylamino)ethyl methacrylate and styrene.

Adapting this strategy to couple ROCOP and group transfer polymerizations (GTP), Rieger and co-workers developed a heterobifunctional catalyst comprising BDI-Zn center and yttrium metallocene connected by a bifunctional pyridyl-alkoxide initiator (Figure 36b).[135] The authors anticipated that the two metal centers would promote orthogonal reactivity with high chemoselectivity. Indeed, reaction mixtures of mismatched monomers and monometallic complexes (CHO/CO_2 with yttrium metallocene or 2-vinylpyridine (2VP) with BDI-Zn) produced neither polymer nor degradation by-products. Applying the monometallic yttrium complex to the GTP of 2VP in the presence of CHO/CO_2 produced slightly slower rates than GTP performed in the absence of CHO/CO_2, which the authors attributed to competitive CO_2 binding at the metal center. ^{1}H NMR spectroscopy revealed that the addition of CO_2 altered the coordination environment around the yttrium center in the mixed metal complex and promoted dissociation of the pyridyl linker. However, sequential polymerization of 2VP followed by ROCOP chain extension successfully produced terpolymers. To perform a simultaneous, one-pot terpolymerization, yttrium-tethered BDI-Zn, CHO, and 2VP were combined prior to charging the system with CO_2. The resulting diblock terpolymer exhibited a monomodal molecular weight distribution, moderately low dispersity (1.30), and intermediate T_g value between those of the constituent blocks. MALDI-TOF spectroscopic analysis of the poly(2-vinyl pyridine) (P2VP) homopolymer corroborates the pyridiol-alkoxide initiator as an end group, which then serves as the linker between the P2VP and PCHC blocks. Exchanging 2VP for 2-isopropenyl-2-oxazoline demonstrated that the bifunctional Zn/Y catalyst can be applied to terpolymerizations of other Michael-type monomers.

6.3. Cross-Linked Networks. Lee and co-workers used multifunctional **cat6** bearing four quaternary ammonium salts to catalyze the terpolymerization of vinylcyclohexene diepoxide (VCHDE), PO, and CO (Figure 37).[136] Incorporation of

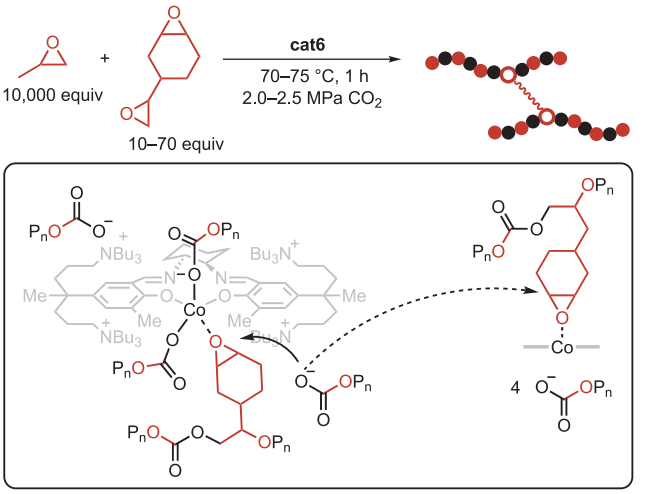

Figure 37. Multifunctional (salcy)CoX complex favors coupling of two to five polycarbonate chains rather than producing extensive cross-linked networks.

VCHDE into a growing chain affords a pendant epoxide unit, which may be ring-opened by a second growing chain to generate a cross-link. Long polymerization times (≥1.5 h) or ≥0.07 mol % diepoxide (1:70 [**cat6**]$_0$:[VCHDE]$_0$) followed by drying afforded a brittle powder whose insolubility confirmed successful cross-linking but precluded catalyst removal by filtration. Heating the catalyst-contaminated network to 150 °C promoted backbiting to cyclic carbonate, corroborating that catalyst removal is imperative to prevent polymer degradation. The authors therefore sought to synthesize lightly cross-linked, high molecular weight polycarbonate. Shortening the polymerization time (1.0 h) or decreasing the VCHDE loading to 0.01−0.06 mol % produced soluble materials. GPC analysis revealed bimodal distributions corresponding to linear and singly coupled chains, respectively; additionally, high molecular weight tails indicated the presence of lightly cross-linked chains. The authors proposed that the four tethered quaternary ammonium salts help to keep the five polymer chains associated with a single Co center. Diepoxide is therefore most likely to react with another chain associated with the same catalyst unit than with a chain coordinated to a distinct Co center (Figure 37). Consequently, the multifunctional catalyst structure favors two- to five-fold increases in molecular weight while simultaneously retarding formation of an infinite cross-linked network.

Coates, Hillmyer, and co-workers employed a multifunctional (salph)AlCl aminocyclopropenium complex **cat43** to synthesize polyester prepolymers via ROCOP for incorporation into covalent adaptive networks (CANs) (Scheme 17).[137] The **cat43**-mediated terpolymerization of vanillin glycidyl ether (VGE) with PO and PA afforded linear polyesters with gradient architectures, as VGE was preferentially incorporated early in the polymerization. Replacing PO with guaiacol glycidyl ether (GGE), which closely resembles VGE, as a comonomer produced statistical terpolymers with uniformly distributed VGE units. Reacting VGE's pendant

Scheme 17. Synthesis of Dynamic Imine-Linked Polyester CANs via ROCOP of PA, VGE, and PO and Subsequent Cross-Linking with 2,2′-(Ethylenedioxy)bis(ethylamine)

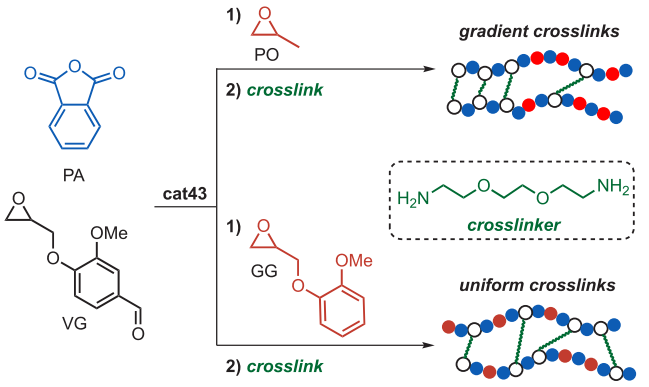

aldehyde units with a diamine cross-linked the gradient and statistical polyester prepolymers to form dynamic imine-linked networks. While the networks were insoluble in neutral solvents, addition of dilute acid promoted imine dissociation to afford polyester prepolymer, which could be recovered in >90% yield. The imine cross-linked polyester networks exhibited thermoset characteristics at ambient temperature, independent of cross-link density or distribution or comonomer composition. Furthermore, their elevated temperature thermomechanical behavior revealed the importance of cross-link distribution on material properties. Dynamic mechanical thermal analysis (DMTA) revealed that networks derived from prepolymers with statistical imine incorporation exhibited extended rubbery plateaus, while networks derived from prepolymers with gradient imine distribution revealed decreasing moduli due to plasticization by the lightly cross-linked chain ends. Both types of networks fully recovered their tensile strengths and cross-linking densities across multiple cycles of mechanical grinding and thermal reprocessing.

6.4. Stereocontrol. As stereoregular polymers frequently exhibit thermal and material properties superior to those of their atactic counterparts, stereocontrolled ROCOP is an important goal of multifunctional catalyst development. In ROCOP polyester synthesis, outer-sphere cyclic anhydride ring-opening precludes significant regio- or enantioselectivity beyond any inherent substrate bias. Efforts to control polyester and polycarbonate stereochemistry have therefore focused on the epoxide ring-opening step. As demonstrated in binary systems, chiral diamine backbones and bulky *o*-salicylidene substituents improve selective enchainment of a single epoxide enantiomer.[138] ROCOP typically proceeds via regioselective epoxide ring-opening at the less sterically hindered position to form head-to-tail linkages. For monosubstituted epoxides, ring-opening at the methylene is stereospecific, preserving the existing stereochemistry, while ring-opening at the chiral methine inverts the stereocenter (Scheme 18). In contrast to binary systems in which the catalyst and cocatalyst can reorient themselves, multifunctional catalysts impose additional geometric constraints; optimizing the relative positions of the chiral Lewis acid and cocatalyst is critical for enantio- and regioselective ROCOP.

Nozaki and co-workers demonstrated that installing a protic ammonium unit pendant to a (salcy)CoX complex improved selectivity for polycarbonate by preventing backbiting to cyclic carbonate even at high epoxide conversions (vide supra).[46]

Scheme 18. Effect of Epoxide Ring-Opening Regioselectivity on Possible Stereochemical Outcomes

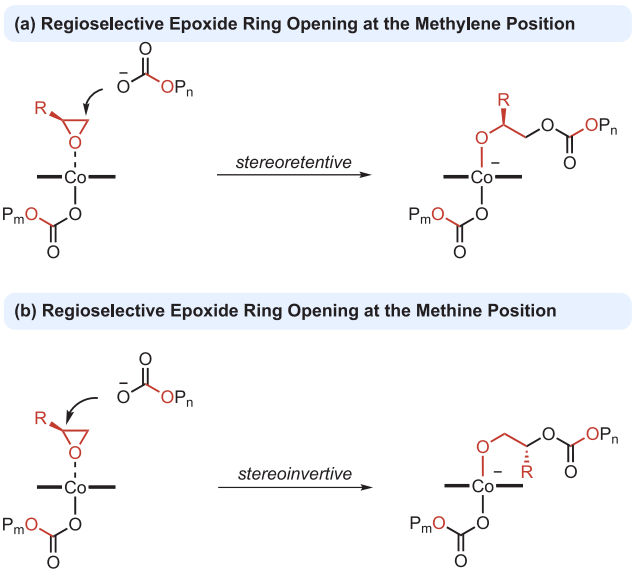

Other enantiopure (salcy)CoX complexes degrade the polycarbonate product after full consumption of the preferred epoxide enantiomer. However, the authors anticipated that the protic ammonium complexes would perform kinetic resolution ROCOP and then enchain the chirality mismatched epoxide, albeit at slower rates.[139] The resulting copolymers would exhibit a previously unreported stereogradient microstructure, comprising two isotactic blocks of opposite chirality with a tapered midsection (Figure 38). In reactions of PO with CO_2, the previously reported *o*-piperidinium complex **cat32** with

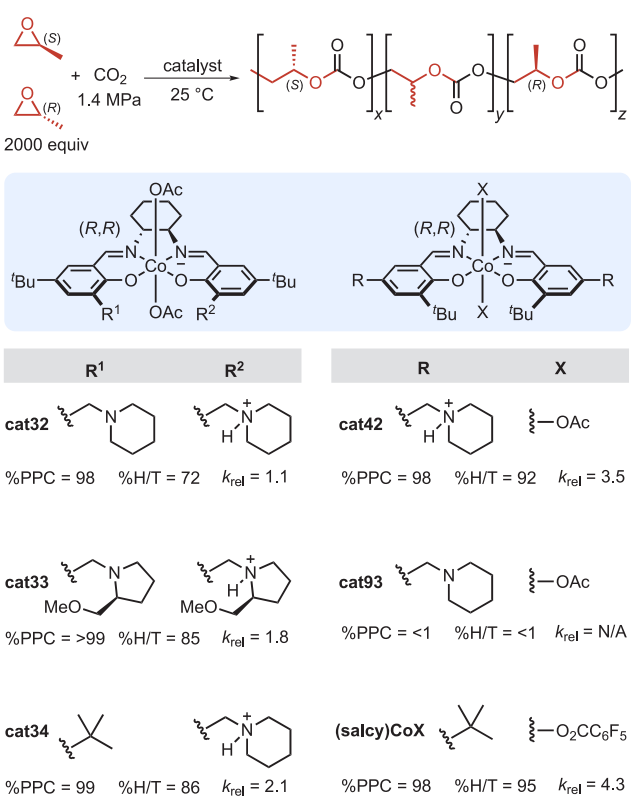

Figure 38. Synthesis of stereogradient PPC.

enantiopure (*R*,*R*)-salcy backbone exhibited excellent selectivity for poly(propylene carbonate) over propylene carbonate but achieved only moderate regioselectivity (72% head-to-tail linkages) and poor enantioselectivity for ring-opening (*S*)-PO relative to (*R*)-PO (kinetic resolution coefficient, k_{rel} = 1.1). **cat34** was also highly selective for PPC formation, emphasizing that only one ammonium group is required for suppression of cyclic carbonate formation. Installing (*S*)-proline-derived substituents at the *ortho* (**cat33**) position improved both regio- and enantioselectivity (85% head-to-tail linkages and k_{rel} = 1.8, respectively). However, **cat33** proved less selective for ring-opening the less reactive (*R*)-PO enantiomer at the unsubstituted position, resulting in regioerrors at high conversions. Anticipating that increasing the steric encumbrement around the metal center would improve regioselectivity, the authors installed *o*-*tert*-butyl substituents and attached the ammonium units via the *para* position of the salicylidene. The resulting **cat42** achieved improved regio- and enantioselectivities (92% head-to-tail linkages, k_{rel} = 3.5). These complexes also suppressed backbiting after full consumption of the preferred (*S*)-PO and at high conversions (>90%) of epoxide. The resulting stereogradient poly(propylene carbonate) exhibited a T_d value higher than that of isotactic (*R*)- or (*S*)-poly(propylene carbonate)s or their equimolar mixture. The authors attributed this improved thermal stability to stereocomplex formation between the (*S*)- and (*R*)-poly(propylene carbonate) blocks within a single polymer chain.

Inspired by the thermal robustness of stereogradient PPC, Lu and co-workers adapted their tethered TBD catalyst to incorporate multiple chiral units and promote enantioselective ROCOP (Figure 39a).[140] Lu and co-workers modified the *o*- and *p*-salicylidene substituents to mimic the optimal substitution pattern reported by Nozaki (vide supra). As anticipated, the complex featuring an *o*-*tert*-butyl substituent and *p*-alkyl-tethered TBD **cat90** achieved enantioselectivity (k_{rel} = 5.7) higher than that of the (*S*,*S*) enantiomer of its positional isomer **cat76** (k_{rel} = 3.5) without a significant decrease in activity (TOF = 328 and 370 h^{-1}, respectively). While retaining the alkyl TBD group in the *para* position of one salicylidene moiety, the authors tuned the *ortho* substituents of the opposite salicylidene to improve enantioselectivity. Replacing the opposite salicylidene with axially chiral (*S*)-BINOL (**cat91**) improved selectivity for the preferred (*R*)-epoxide enantiomer ($k_{rel} \geq$ 10.1 with (*S*)-BINOl versus k_{rel} = 5.7 with 3,5-di-*tert*-butylsalicylidene (**cat90**)), provided the BINOL chirality matched that of the (*S*,*S*)-salcy backbone. Installing the mismatched (*R*)-BINOL significantly decreased selectivity for the (*R*)-epoxide (k_{rel} = 1.4). Additional optimization of the (*S*)-BINOL unit revealed that increasing the substitution of the 2′-alkoxy group from methyl to isopropyl (**cat92**) further improved the kinetic resolution ROCOP (k_{rel} = 12.9). As anticipated, decreasing the reaction temperature increased enchainment of the preferred PO enantiomer, while reducing the CO_2 overpressure had no effect on polymer enantio- and regioselectivity. In all cases, almost exclusively head-to-tail linkages were observed. The optimized catalyst copolymerized CO_2 and monosubstituted epoxides bearing other alkyl substituents (Et or ^{n}Bu), although increasing the length of the alkyl chain marginally decreased enantioselectivity.

While monosubstituted epoxides with alkyl groups typically ring-open at the less hindered C_β-methylene position with retention of stereochemistry, epoxides with electron-withdrawing groups (e.g., ECH and SO) also ring-open at the chiral C_α-methine, making stereospecific ROCOP challenging. Darensbourg and Lu therefore sought to adapt the catalyst design insights obtained from ROCOP of alkyl-substituted epoxides to the regioselective, stereoretentive ROCOP of ECH and CO_2 (Figure 39b).[141] To evaluate catalyst regioselectivity, the authors copolymerized enantiopure (*R*)-ECH with CO_2; any stereoerrors observed in the polymer backbone therefore arise from stereoinvertive ring-opening at the methine carbon. As reported for alkyl substituted epoxides, catalysts bearing the alkyl-tethered TBD at the *ortho* position (*S*,*S*-**cat75**) of the salicylidene achieved only modest enantioselectivity (k_{rel} = 2.4). Exchanging the *ortho*-tethered substituent from TBD to a tethered diethyl methylammonium cocatalyst (*S*,*S*-**cat35**) produced similar results (k_{rel} = 2.3). The authors then synthesized a (salcy)CoX complex *S*,*S*-**cat40** incorporating more sterically encumbered *ortho*-tethered dicyclohexyl methylammonium cocatalyst. As anticipated, increasing the steric bulk of the tethered cocatalyst improved enantioselectivity (k_{rel} = 2.8–3.3 at 0 °C). Copolymerizing enantiopure (*R*)-ECH and CO_2 produced highly isotactic PECH with T_g and T_m values of 42 °C and 108 °C, respectively; by contrast, atactic PECH is amorphous, with a T_g value of 31 °C. The isotactic material also exhibited yield and tensile strengths over a magnitude higher than those of the atactic analogue and greater elongation at break.

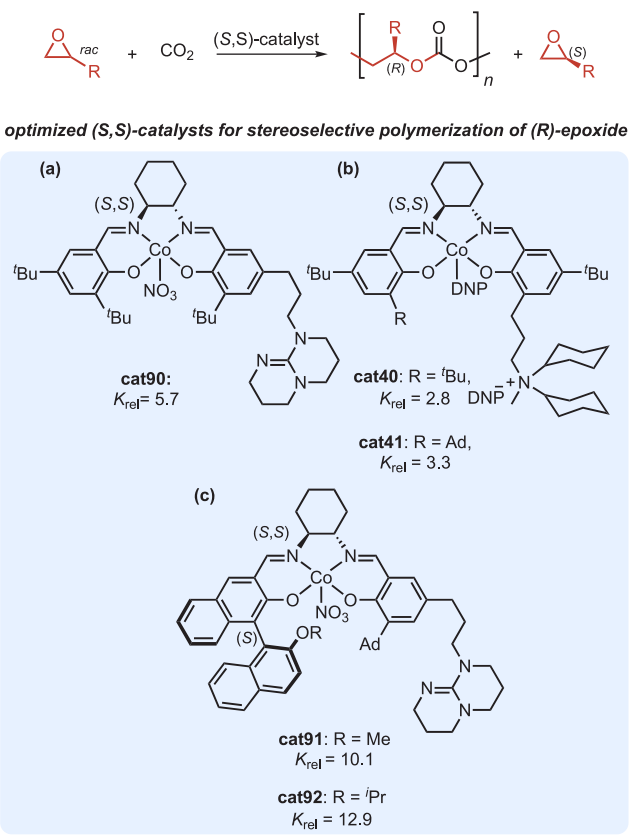

Figure 39. Kinetic resolution copolymerization of (*R*)-PO and CO_2 by chiral multifunctional complexes.

7. OUTLOOK AND CONCLUSIONS

The development of multifunctional catalysts for epoxide copolymerization has enabled the synthesis of well-defined polyesters and polycarbonates at low catalyst loadings while

limiting side reactions and expanding monomer scope. Some challenges remain, as synthetic accessibility, industrial viability, and catalyst efficiency in ambient conditions is still limited. Notably, the low catalyst loading enabled by tethered catalysts, as well as the demonstrated recovery and recyclability of some multifunctional catalysts, mitigates the upfront investment of demanding catalyst syntheses and stability concerns. There is a continued need to improve the tensile and thermal properties of generally amorphous polyesters and polycarbonates, although multifunctional catalysts do exhibit unprecedented stereo- and regiocontrol and an enhanced monomer scope that enable the synthesis of advanced polymer architectures and tougher, often semicrystalline, materials.

These advances in catalyst efficiency and selectivity are largely due to the mechanistic changes encoded by tethering two usually distinct catalytic functions. As opposed to binary catalysts, covalently linking the catalyst and cocatalyst allows epoxide ring-opening and chain-end control to come together in one rate-limiting step. This mechanistic change curbs dilution effects, enabling the formation of high molecular-weight polymers at low loadings that are inaccessible in corresponding binary systems. Further, nucleophilic chain ends remain more readily coordinated to an active Lewis acid center, reducing cyclic carbonate formation, epoxide homopolymerization, transesterification, and epimerization. Finally, the geometric constraints enforced by multifunctional catalysts generally allow improved stereo- and regiocontrol toward high-molecular weight advanced polymer architectures. Ultimately, the use of multifunctional catalysts enables unprecedented activity and selectivity in epoxide ring-opening copolymerization, providing a controlled, sustainable route toward polycarbonates and polyesters.

AUTHOR INFORMATION

Corresponding Author

Geoffrey W. Coates − *Department of Chemistry and Chemical Biology, Baker Laboratory, Cornell University, Ithaca, New York 14853-1301, United States;* orcid.org/0000-0002-3400-2552; Email: coates@cornell.edu

Authors

Claire A. L. Lidston − *Department of Chemistry and Chemical Biology, Baker Laboratory, Cornell University, Ithaca, New York 14853-1301, United States*

Sarah M. Severson − *Department of Chemistry and Chemical Biology, Baker Laboratory, Cornell University, Ithaca, New York 14853-1301, United States;* orcid.org/0000-0001-9305-6270

Brooks A. Abel − *Department of Chemistry and Chemical Biology, Baker Laboratory, Cornell University, Ithaca, New York 14853-1301, United States;* orcid.org/0000-0002-2288-1975

ACKNOWLEDGMENTS

This research was supported by the Center for Sustainable Polymers, a National Science Foundation (NSF) Center for Chemical Innovation (CHE-1901635).

REFERENCES

(1) Odian, G. Step Polymerization. In *Principles of Polymerization*, 4th ed.; John Wiley & Sons: Hoboken, NJ, 2004; pp 39−197.

(2) Lecomte, P.; Jérôme, C. Recent Developments in Ring-Opening Polymerization of Lactones. In *Synthetic Biodegradable Polymers*; Rieger, B.; Künkel, A.; Coates, G. W.; Reichardt, R.; Dinjus, E.; Zevaco, A. T., Eds.; Advances in Polymer Science, Vol. *245*; Springer-Verlag: Berlin, Germany, 2012; pp 173−217; DOI: 10.1007/978-3-642-27154-0.

(3) Brannigan, R. P.; Dove, A. P. Synthesis, Properties, and Biomedical Applications of Hydrolytically Degradable Materials Based on Aliphatic Polyesters and Polycarbonates. *Biomaterials Sci.* **2017**, *5*, 9−21.

(4) Carothers, W. H.; Dorough, G. L.; Van Natta, F. J. Studies of the Polymerization and Ring-Formation. X. The Reversible Polymerization of Six-Membered Cyclic Esters. *J. Am. Chem. Soc.* **1932**, *54*, 761−772.

(5) Chen, G. Q.; Patel, M. K. Plastics Derived from Biological Sources: Present and Future: A Technical and Environmental Review. *Chem. Rev.* **2012**, *112*, 2082−2099.

(6) Zhang, X.; Dai, Y. Cationic Polycarbonates *via* Ring-Opening Polymerization: Design, Synthesis, and Applications. *Polym. Chem.* **2019**, *10*, 296−305.

(7) Feng, J.; Zhuo, R. X.; Zhang, X.-Z. Construction of Functional Aliphatic Polycarbonates for Biomedical Applications. *Prog. Polym. Sci.* **2012**, *37*, 211−236.

(8) Zhang, X.; Fevre, M.; Jones, G. O.; Waymouth, R. M. Catalysts as an Enabling Science for Sustainable Polymers. *Chem. Rev.* **2018**, *118*, 839−885.

(9) Haque, F. M.; Ishibashi, J. S. A.; Lidston, C. A.; Shao, H.; Bates, F. S.; Chang, A. B.; Coates, G. W.; Cramer, C. J.; Dauenhauer, P. J.; Dichtel, W. R.; Ellison, C. J.; Gormong, E. A.; Hamachi, L. S.; Hoye, T. R.; Jin, M.; Kalow, J. A.; Kim, H. J.; Kumar, G.; LaSalle, C. J.; Liffland, S.; Lipinski, B. M.; Pang, Y.; Parveen, R.; Peng, X.; Popowski, Y.; Prebihalo, E. A.; Reddi, Y.; Reineke, T. M.; Sheppard, D. T.; Swartz, J. L.; Tolman, W. B.; Vlaisavljevich, B.; Wissinger, J.; Xu, S.; Hillmyer, M. A. Defining the Macromolecules of Tomorrow through Synergistic Sustainable Polymer Research. *Chem. Rev.* **2022**, *122*, 6322−6373.

(10) Luinstra, G. A.; Borchardt, E. Material Properties of Poly(Propylene Carbonates). In *Synthetic Biodegradable Polymers*; Rieger, B.; Künkel, A.; Coates, G. W.; Reichardt, R.; Dinjus, E.; Zevaco, T. A., Eds.; Advances in Polymer Science, Vol. *245*; Springer-Verlag: Berlin, Germany, 2012; pp 173−217; DOI: 10.1007/978-3-642-27154-0.

(11) Yu, W.; Maynard, E.; Chiaradia, V.; Arno, M. C.; Dove, A. P. Aliphatic Polycarbonates from Cyclic Carbonate Monomers and Their Application as Biomaterials. *Chem. Rev.* **2021**, *121*, 10865−10907.

(12) Tong, R. New Chemistry in Functional Aliphatic Polyesters. *Ind. Eng. Chem. Res.* **2017**, *56*, 4207−4219.

(13) Poland, S.; Darensbourg, D. A Quest for Polycarbonates Provided *Via* Sustainable Epoxide/CO_2 Copolymerization Processes. *Green Chem.* **2017**, *19*, 4990−5011.

(14) Lu, X.-B.; Ren, W.-M.; Wu, G.-P. CO_2 Copolymers from Epoxides: Catalyst Activity, Product Selectivity, and Stereochemistry Control. *Acc. Chem. Res.* **2012**, *45*, 1721−1735.

(15) Luo, M.; Zhang, X. H.; Darensbourg, D. J. Poly(monothiocarbonate)s from the Alternating and Regioselective Copolymerization of Carbonyl Sulfide with Epoxides. *Acc. Chem. Res.* **2016**, *49*, 2209−2219.

(16) Zhang, C. J.; Wu, H. L.; Li, Y.; Yang, J. L.; Zhang, X. H. Precise Synthesis of Sulfur-Containing Polymers via Cooperative Dual

Organocatalysts with High Activity. *Nat. Commun.* **2018**, *9*, 2137−2147.
(17) Zhang, C.-J.; Zhang, X. H. Recent Progress on COS-Derived Polymers. *Chin. J. Polym. Sci.* **2019**, *37*, 951−958.
(18) Longo, J. M.; Sanford, M. J.; Coates, G. W. Ring-Opening Copolymerization of Epoxides and Cyclic Anhydrides with Discrete Metal Complexes: Structure-Property Relationships. *Chem. Rev.* **2016**, *116*, 15167−15197.
(19) Paul, S.; Zhu, Y.; Romain, C.; Brooks, R.; Saini, P. K.; Williams, C. K. Ring-Opening Copolymerization (ROCOP): Synthesis and Properties of Polyesters and Polycarbonates. *Chem. Commun.* **2015**, *51*, 6459.
(20) Wang, L.-Y.; Ren, W.-M. Synthesis of Polythioesters. In *Sulfur-Containing Polymers: From Synthesis to Functional Materials*; Zhang, X.-H.; Theato, P.; Eds.; Wiley-VCH GmbH, 2021; pp 171−190. DOI: 10.1002/9783527823819.
(21) Zhang, C.-J.; Yang, J.-L.; Cao, X.-H.; Zhang, X.-H. Carbonyl Sulfide Derived Polymers. In *Sulfur-Containing Polymers: From Synthesis to Functional Materials*; Zhang, X.-H.; Theato, P.; Eds.; Wiley-VCH GmbH, 2021; pp 81−145. DOI: 10.1002/9783527823819.
(22) Luinstra, G. A. Poly(Propylene Carbonate), Old Copolymers of Propylene Oxide and Carbon Dioxide with New Interests: Catalysis and Material Properties. *Polym. Rev.* **2008**, *48*, 192−219.
(23) Qin, Y.; Sheng, X.; Liu, S.; Ren, G.; Wang, X.; Wang, F. Recent Advances in Carbon Dioxide Based Copolymers. *J. CO_2 Util.* **2015**, *11*, 3−9.
(24) Lustoň, J.; Maňásek, Z. Copolymerization of Epoxides with Cyclic Anhydrides Catalyzed by Tertiary Amines in the Presence of Proton-Donating Compounds. *J. Macromol. Sci., Chem.* **1979**, *13*, 853−867.
(25) Lustoň, J.; Vašš, F. Anionic Copolymerization of Cyclic Ethers with Cyclic Anhydrides. *Adv. Polym. Sci.* **1984**, *56*, 91−133.
(26) Masters, J. E. Epoxide-Anhydride-Hydroxy Polymer Composition and Method of Making Same. U.S. Patent US 2908663, 1959.
(27) Nagata, N.; Taniguchi, S. Copolymers of Epoxy Resins, Unsaturated Carboxylic Acids or Anhydrides, and other Copolymerizable Monomers for Use as Coatings and Sizing agents. Patent GB 108129519670831, 1967.
(28) Sakai, S.; Ito, H.; Ishii, Y. Reactivity and Polymerizability of Cyclic Compounds. IX. Copolymerization of Epoxides with Succinic Anhydride Catalyzed by Organotin Compounds. *Kogyo Kaguku Sasshi.* **1968**, *71*, 186−187.
(29) Inoue, S.; Kitamura, K.; Tsuruta, T. Copolymerization of Carbon Dioxide and Epoxide. *J. Polym. Sci., Part B.: Polym. Lett.* **1969**, *7*, 287−292.
(30) Tsuruta, T.; Matsuura, K.; Inoue, S. Preparation of Some Polyesters by Organometallic-Catalyzed Ring-Opening Polymerization. *Kuzmitteilung* **1964**, *75*, 211−214.
(31) Inoue, S.; Kitamura, K.; Tsuruta, T. Alternating Copolymerization of Phthalic Anhydride and Propylene Oxide by Dialkylzinc. *Die Makromol. Chem.* **1969**, *126*, 250−265.
(32) Sebastian, J.; Srinivas, D. Double-Metal Cyanide Catalyst Design in CO_2/Epoxide Copolymerization. In *Sustainable Polymers from Biomass*; Tang, C.; Ryu, C. Y., Eds.; Wiley-VCH Verlag GmbH & Co. KGaA, 2017; pp 315−345. DOI: 10.1002/9783527340200.ch13.
(33) Ree, M.; Hwang, Y.; Kim, J.-S.; Kim, H.; Kim, G.; Kim, H. New Findings in the Catalytic Activity of Zinc Glutarate and Its Application in the Chemical Fixation of CO_2 into Polycarbonates and Their Derivatives. *Catal. Today.* **2006**, *115*, 134−145.
(34) Klaus, S.; Lehenmeier, M. W.; Herdtweck, E.; Deglmann, P.; Ott, A. K.; Rieger, B. Mechanistic Insights into Heterogeneous Zinc Dicarboxylates and Theoretical Considerations for CO_2-Epoxide Copolymerization. *J. Am. Chem. Soc.* **2011**, *133*, 13151−13161.
(35) Inoue, S. Immortal Polymerization: The Outset, Development, and Application. *Polym. Sci. Part A* **2000**, *38*, 2861−2871.
(36) Inoue, S.; Takeda, N. Reaction of Carbon Dioxide with Tetraphenylporphinato-Aluminium Ethyl in Visible Light. *Bull. Chem. Soc. Jpn.* **1977**, *50*, 984−986.
(37) Jacobsen, E. N.; Tokunaga, M.; Larrow, F. J. PCT Int. Appl. 2000, WO 00/09463.
(38) Coates, G. W.; Jeske, R. C. Homogeneous Catalyst Design for the Synthesis of Aliphatic Polycarbonates and Polyesters. *Angew. Chem., Int. Ed.* **2004**, *43*, 6618−6639.
(39) Wang, Y.; Darensbourg, D. Carbon Dioxide-Based Functional Polycarbonates: Metal Catalyzed Copolymerization of CO_2 and Epoxides. *Coord. Chem. Rev.* **2018**, *372*, 85−100.
(40) Darensbourg, D. J.; Wilson, S. J. What's New With CO_2? Recent Advances in its Copolymerization with Oxiranes. *Green Chem.* **2012**, *14*, 2665−2671.
(41) Kozak, C. M.; Ambrose, K.; Anderson, T. S. Copolymerization of Carbon Dioxide and Epoxides by Metal Coordination Complexes. *Coord. Chem. Rev.* **2018**, *376*, 565−587.
(42) Darensbourg, D. J. Salen Metal Complexes as Catalysts for the Synthesis of Polycarbonates from Cyclic Ethers and Carbon Dioxide. *Adv. Polym. Sci.* **2011**, *245*, 1−27.
(43) Lu, X. B.; Darensbourg, D. J. Cobalt Catalysts for the Coupling of CO_2 and Epoxides to Provide Polycarbonates and Cyclic Carbonates. *Chem. Soc. Rev.* **2012**, *41*, 1462−1484.
(44) Coates, G. W.; Moore, D. R. Discrete Metal-Based Catalysts for the Copolymerization of CO_2 and Epoxides: Discovery, Reactivity, Optimization, and Mechanism. *Angew. Chem., Int. Ed.* **2004**, *43*, 6618−6639.
(45) Darensbourg, D. J. Making Plastics from Carbon Dioxide: Salen Metal Complexes as Catalysts for the Production of Polycarbonates from CO_2. *Chem. Rev.* **2007**, *107*, 2388−2410.
(46) Nakano, K.; Kamada, T.; Nozaki, K. Selective Formation of Polycarbonate over Cyclic Carbonate: Copolymerization of Epoxides with Carbon Dioxide Catalyzed by a Cobalt(III) Complex with a Piperidinium End-Capping Arm. *Angew. Chem., Int. Ed.* **2006**, *45*, 7274−7277.
(47) Noh, E. K.; Na, S. J.; S, S.; Kim, S.-W.; Lee, B. Y. Two Components in a Molecule: Highly Efficient and Thermally Robust Catalytic System for CO_2/Epoxide Copolymerization. *J. Am. Chem. Soc.* **2007**, *129*, 8082−8083.
(48) Ren, W.-M.; Liu, Z.-W.; Wen, Y.-Q.; Zhang, R.; Lu, X.-B. Mechanistic Aspects of the Copolymerization of CO_2 with Epoxides Using a Thermally Stable Single-Site Cobalt(III) Catalyst. *J. Am. Chem. Soc.* **2009**, *131*, 11509−11518.
(49) Trott, G.; Saini, P. K.; Williams, C. K. Catalysts for CO_2/Epoxide Ring-Opening Copolymerization. *Philos. Trans. R. Soc., A* **2016**, *374*, 20150085.
(50) Kember, M.; Buchard, A.; Williams, C. K. Catalysts for CO_2/Epoxide Copolymerisation. *Chem. Commun.* **2011**, *47*, 141−163.
(51) Gruszka, W.; Garden, J. A. Advances in Heterobimetallic Ring-Opening (Co)polymerisation Catalysis. *Nat. Commun.* **2021**, *12*, 3252−3255.
(52) Liang, X.; Tan, F.; Zhu, Y. Recent Developments in Ring-Opening Copolymerization of Epoxides with CO_2 and Cyclic Anhydrides for Biomedical Applications. *Front. Chem.* **2021**, *9*, 647245.
(53) Cao, H.; Liu, S.; Wang, X. Environmentally Benign Metal catalyst for the Ring-Opening Copolymerization of Epoxides and CO_2: State-of-the-art, Opportunities, and Challenges. *Green Chemical Engineering* **2022**, *3*, 111−124.
(54) Liu, J.; Ren, W.-M.; Lu, X.-B. Kinetic Study on the Coupling of CO_2 and Epoxides Catalyzed by Co(III) Complex with an Inter- or Intramolecular Nucleophilic Cocatalyst. *Macromolecules* **2013**, *46*, 1343−1349.
(55) Ren, W.-M.; Zhang, X.; Liu, Y.; Li, J.-F.; Wang, H.; Lu, X.-B. Highly Active, Bifunctional Co(III)-Salen Catalyst for Alternating Copolymerization of CO_2 with Cyclohexene Oxide and Terpolymerization with Aliphatic Epoxides. *Macromolecules* **2010**, *43*, 1396−1402.

(56) (a) Abel, B. A.; Lidston, C. A. L.; Coates, G. W. Mechanism-Inspired Design of Bifunctional Catalysts for the Alternating Ring-Opening Copolymerization of Epoxides and Cyclic Anhydrides. *J. Am. Chem. Soc.* **2019**, *141*, 12760−12769. (b) Lidston, C. A. L.; Abel, B. A.; Coates, G. W. Bifunctional Catalysis Prevents Inhibition in Reversible-Deactivation Ring-Opening Copolymerizations of Epoxides and Cyclic Anhydrides. *J. Am. Chem. Soc.* **2020**, *142*, 20161−20169.

(57) Zhang, H.; Liu, B.; Ding, H.; Chen, J.; Duan, Z. Polycarbonates Derived from Propylene Oxide, CO_2, and 4-Vinyl Cyclohexene Oxides Terpolymerizations Catalyzed by Bifunctional SalcyCo^{III}NO$_3$ and its Post-Polymerization Modification. *Polymer* **2017**, *129*, 5−11.

(58) Duan, Z.; Wang, X.; Gao, Q.; Zhang, L.; Liu, B.; Kim, I. Highly Active Bifunctional Cobalt-Salen Complexes for the Synthesis of Poly(ester-*block*-carbonate) Copolymer *via* Terpolymerization of Carbon Dioxide, Propylene Oxide, and Norbornene Anhydride Isomer: Roles of Anhydride Conformation Consideration. *J. Poly. Sci. Part A: Polym. Chem.* **2014**, *52*, 789−795.

(59) Darensbourg, D. J.; Chung, W.-C.; Arp, C. J.; Tsai, F.-T.; Kyran, S. J. Copolymerization and Cycloaddition Products Derived from Coupling Reactions of 1,2-Epoxy-4-cyclohexene and Carbon Dioxide. Postpolymerization Functionalization via Thiol-Ene Click Reactions. *Macromolecules* **2014**, *47*, 7347−7353.

(60) Darensbourg, D. J.; Kyran, S. J. Carbon Dioxide Copolymerization Study with a Sterically Encumbering Naphthalene-Derived Oxide. *ACS Catal.* **2015**, *5*, 5421−5430.

(61) Darensbourg, D. J.; Chung, W.-C.; Wilson, S. J. Catalytic Coupling of Cyclopentene Oxide and CO_2 Utilizing Bifunctional (salen)Co(III) and (salen)Cr(III) Catalysts: Comparative Processes Involving Binary (salen)Cr(III) Analogs. *ACS Catal.* **2013**, *3*, 3050−3057.

(62) Darensbourg, D. J.; Chung, W.-C. Availability of Other Aliphatic Polycarbonates Derived from Geometric Isomers of Butene Oxide and Carbon Dioxide Coupling Reactions. *Macromolecules* **2014**, *47*, 4943−4948.

(63) Wu, G.-P.; Xu, P.-X.; Lu, X.-B.; Zu, Y.-P.; Wei, S.-H.; Ren, W.-M.; Darensbourg, D. J. Crystalline CO_2 Copolymer from Epichlorohydrin via Co(III)-Complex-Mediated Stereospecific Polymerization. *Macromolecules* **2013**, *46*, 2128−2133.

(64) Darensbourg, D. J.; Wilson, S. J. Synthesis of CO_2-Derived Poly(indene carbonate) from Indene Oxide Utilizing Bifunctional Cobalt(III) Catalysts. *Macromolecules* **2013**, *46*, 5929−5934.

(65) S, S.; Min, J. K.; Seong, J. E.; Na, S. J.; Lee, B. Y. A Highly Active and Recyclable Catalytic System for CO_2/Propylene Oxide Copolymerization. *Angew. Chem., Int. Ed.* **2008**, *47*, 7306−7309.

(66) Na, S. J.; S, S.; Kim, B. E.; Yoo, J.; Kang, Y. K.; Han, S. J.; Lee, C.; Lee, B. Y. Elucidation of the Structure of a Highly Active Catalytic System for CO_2/Epoxide Copolymerization: A Salen-Cobaltate Complex of an Unusual Binding Mode. *Inorg. Chem.* **2009**, *48*, 10455−10465.

(67) Wu, W.; Qin, Y.; Wang, X.; Wang, F. New Bifunctional Catalyst Based on Cobalt-Porphyrin Complex for the Copolymerization of Propylene Oxide and CO_2. *J. Poly. Sci., Part A: Polym. Chem.* **2013**, *51*, 493−498.

(68) Wu, W.; Sheng, X.; Qin, Y.; Qiao, L.; Miao, Y.; Wang, X.; Wang, F. Bifunctional Aluminum Porphyrin Complex: Soil Tolerant Catalyst for Copolymerization of CO_2 and Propylene Oxide. *J. Poly. Sci., Part A: Polym. Chem.* **2014**, *52*, 2346−2355.

(69) Sheng, X.; Wang, Y.; Qin, Y.; Wang, X.; Wang, F. Aluminum Porphyrin Complexes *via* Delicate Ligand Design: Emerging Efficient Catalysts for High Molecular Weight Poly(propylene carbonate). *RSC Adv.* **2014**, *4*, 54043−54050.

(70) Deng, J.; Ratanasak, M.; Sako, Y.; Tokuda, H.; Maeda, C.; Hasegawa, J.-y.; Nozaki, K.; Ema, T. Aluminum Porphyrins with Quaternary Ammonium Halides as Catalysts for Copolymerization of Cyclohexene Oxide and CO_2: Metal-ligand Cooperative Catalysis. *Chem. Sci.* **2020**, *11*, 5669−5675.

(71) Ohkawara, T.; Suzuki, K.; Nakano, K.; Mori, S.; Nozaki, K. Facile Estimation of Catalytic Activity and Selectivities in Copolymerization of Propylene Oxide with Carbon Dioxide Mediated by Metal Complexes with Planar Tetradentate Ligand. *J. Am. Chem. Soc.* **2014**, *136*, 10728−10735.

(72) Fieser, M. E.; Sanford, M. J.; Mitchell, L. A.; Dunbar, C. R.; Mandal, M.; Van Zee, N. J.; Urness, D. M.; Cramer, C. J.; Coates, G. W.; Tolman, W. B. Mechanistic Insights into the Alternating Copolymerization of Epoxides and Cyclic Anhydrides Using a (Salph)AlCl and Iminium Salt Catalytic System. *J. Am. Chem. Soc.* **2017**, *139*, 15222−15231.

(73) Bures, J. A Simple Graphical Method to Determine the Order in Catalyst. *Angew. Chem., Int. Ed.* **2016**, *55*, 2028−2031.

(74) Yoo, J.; Na, S. J.; Park, H. C.; Cyriac, A.; Lee, B. Y. Anion Variation on a Cobalt(III) Complex of Salen-Type Ligand Tethered by Four Quaternary Ammonium Salts for CO_2/Epoxide Copolymerization. *Dalton Trans.* **2010**, *39*, 2622−2630.

(75) Kim, B. E.; Varghese, J. K.; Han, Y.; Lee, B. Y. Cobalt(III) Complexes of Various Salen-Type Ligand Bearing Four Quaternary Ammonium Salts and Their Reactivity for CO_2/Epoxide Copolymerization. *Bull. Korean Chem. Soc.* **2010**, *31*, 829−834.

(76) Yang, G.-W.; Zhang, Y.-Y.; Xie, R.; Wu, G.-P. Scalable Bifunctional Organoboron Catalysts for Copolymerization of CO_2 and Epoxides with Unprecedented Efficiency. *J. Am. Chem. Soc.* **2020**, *142*, 12245−12255.

(77) Yang, G.-W.; Zhang, Y.-Y.; Wu, G.-P. Modular Organoboron Catalysts Enable Transformations with Unprecedented Reactivity. *Acc. Chem. Res.* **2021**, *54*, 4434−4448.

(78) Zhang, D.; Boopathi, S. K.; Hadjichristidis, N.; Gnanou, Y.; Feng, X. Metal-Free Alternating Copolymerization of CO_2 with Epoxides: Fulfilling "Green" Synthesis and Activity. *J. Am. Chem. Soc.* **2016**, *138*, 11117−11120.

(79) Zhang, Y.-Y.; Yang, G.-W.; Xie, R. X.; Yang, L.; Li, B.; Wu, G.-P. Scalable, Durable, and Recyclable Metal-Free Catalysts for the Efficient Conversion of CO_2 to Cyclic Carbonates. *Angew. Chem., Int. Ed.* **2020**, *59*, 23291−23298.

(80) Darensbourg, D. J.; Mackiewicz, R. M. Role of the Cocatalyst in the Copolymerization of CO_2 and Cyclohexene Oxide Utilizing Chromium Salen Complexes. *J. Am. Chem. Soc.* **2005**, *127*, 14026−14038.

(81) Lu, X. B.; Shi, L.; Wang, Y.-M.; Zhang, R.; Zhang, Y.-J.; Peng, X.-J.; Zhang, Z.-C.; Li, B. Design of Highly Active Binary Catalyst Systems for CO_2/Epoxide Copolymerization: Polymer Selectivity, Enantioselectivity, and Stereochemistry Control. *J. Am. Chem. Soc.* **2006**, *128*, 1664−1674.

(82) Iksi, S.; Aghmiz, A.; Rivas, R.; González, M. D.; Cuesta-Aluja, L.; Castilla, J.; Orejón, A.; El Guemmout, F.; Masdeu-Bultó, A. M. Chromium Complexes with Tridentate NN'O Schiff Base Ligands as Catalysts for the Coupling of CO_2 and Epoxides. *J. Mol. Catal. A: Chem.* **2014**, *383*−*384*, 143−152.

(83) DiCiccio, A. M.; Longo, J. M.; Rodríguez-Calero, G. G.; Coates, G. W. Development of Highly Active and Regioselective Catalysts for the Copolymerization of Epoxides with Cyclic Anhydrides: An Unanticipated Effect of Electronic Variation. *J. Am. Chem. Soc.* **2016**, *138*, 7107−7113.

(84) Cohen, C. T.; Chu, T.; Coates, G. W. Cobalt Catalysts for the Alternating Copolymerization of Propylene Oxide and Carbon Dioxide: Combining High Activity and Selectivity. *J. Am. Chem. Soc.* **2005**, *127*, 10869−10878.

(85) Tokunaga, M.; Larrow, J. F.; Kakiuchi, F.; Jacobsen, E. N. Asymmetric Catalysis with Water: Efficient Kinetic Resolution of Terminal Epoxides by Means of Catalytic Hydrolysis. *Science* **1997**, *277*, 936−938.

(86) Jacobsen, E. N. Asymmetric Catalysis of Epoxide Ring-Opening Reactions. *Acc. Chem. Res.* **2000**, *33*, 421−431.

(87) Cohen, C. T.; Thomas, C. M.; Peretti, K. L.; Lobkovsky, E. B.; Coates, G. W. Copolymerization of Cyclohexene Oxide and Carbon Dioxide Using (salen)Co(III) Complexes: Synthesis and Characterization of Syndiotactic Poly(cyclohexene carbonate). *Dalton Trans.* **2006**, 237−249.

(88) Lu, X.-B.; Liang, B.; Zhang, Y.-J.; Tian, Y.-Z.; Wang, Y.-M.; Bai, C.-X.; Wang, H.; Zhang, R. Asymmetric Catalysis with CO_2: Direct Synthesis of Optically Active Propylene Carbonate from Racemic Epoxides. *J. Am. Chem. Soc.* **2004**, *126*, 3732−3733.
(89) Nishinaga, A.; Kondo, T.; Matsuura, T. Reduction of Hydroxocobalt(III) Schiff Base Complexes with Alcohols. *Chem. Lett.* **1985**, *14*, 1319−1322.
(90) Xia, W.; Salmeia, K. A.; Vagin, S. I.; Rieger, B. Concerning the Deactivation of Cobalt(III)-Based Porphyrin and Salen Catalysts in Epoxide/CO_2 Copolymerization. *Chem.-Eur. J.* **2015**, *21*, 4384−4390.
(91) Darensbourg, D. J.; Chung, W.-C.; Wilson, S. J. Catalytic Coupling of Cyclopentene Oxide and CO_2 Utilizing Bifunctional (salen)Co(III) and (salen)Cr(III) Catalysts: Comparative Processes Involving Binary (salen)Cr(III) Analogues. *ACS Catal.* **2013**, *3*, 3050−3057.
(92) Gu, G.-G.; Yue, T.-J.; Wan, Z.-Q.; Zhang, R.; Lu, X.-B.; Ren, W.-M. A Single-Site Iron(III)-Salan Catalyst for Converting COS to Sulfur-Containing Polymers. *Polymers* **2017**, *9*, 515−523.
(93) Ren, W.-M.; Liu, Y.; Xin, A.-X.; Fu, S.; Lu, X.-B. Single-Site Bifunctional Catalysts for COX (X = O or S)/Epoxides Copolymerization: Combining High Activity, Selectivity, and Durability. *Macromolecules* **2015**, *48*, 8445−8450.
(94) Darensbourg, D. J.; Yeung, A. D. A Concise Review of Computational Studies of the Carbon Dioxide-Epoxide Copolymerization Reactions. *Polym. Chem.* **2014**, *5*, 3949−3962.
(95) Darensbourg, D. J.; Yeung, A. D. Thermodynamics of the Carbon-Dioxide-Epoxide Copolymerization and Kinetics of the Metal-Free Degradation: A Computational Study. *Macromolecules.* **2013**, *46*, 83−95.
(96) Qin, Y.; Wang, X.; Zhang, S.; Zhao, X.; Wang, F. Fixation of Carbon Dioxide into Aliphatic Polycarbonate, Cobalt Porphyrin Catalyzed Regio-Specific Poly(propylene carbonate) with High Molecular Weight. *J. Polym. Sci., Part A: Polym. Chem.* **2008**, *46*, 5959−5967.
(97) Whiteoak, C. J.; Kielland, N.; Laserna, V.; Castro-Gómez, F.; Martin, E.; Escudero-Adán, E. C.; Bo, C.; Kleij, A. W. Highly Active Aluminum Catalysts for the Formation of Organic Carbonates from CO_2 and Oxiranes. *Chem.-Eur. J.* **2014**, *20*, 2264−2275.
(98) De la Cruz-Martínez, F.; Martínez, J.; Gaona, M. A.; Fernández-Baeza, J.; Sánchez-Barba, L. F.; Rodríguez, A. M.; Castro-Osma, J. A.; Otero, A.; Lara-Sánchez, A. Bifunctional Aluminum Catalysts for the Chemical Fixation of Carbon Dioxide into Cyclic Carbonates. *ACS Sustainable Chem. Eng.* **2018**, *6*, 5322−5332.
(99) Ren, Y.; Jian, O.; Zeng, H.; Mao, Q.; Jiang, H. Lewis Acid-Base Bifunctional Aluminum-Salen catalysts: Synthesis of Cyclic Carbonates from Carbon Dioxide and Epoxides. *RSC Adv.* **2016**, *6*, 3243−3249.
(100) Luo, R.; Zhang, W.; Yang, Z.; Zhou, X.; Ji, H. Synthesis of Cyclic Carbonates from Epoxides Over Bifunctional Salen Aluminum Oligomers as a CO_2-Philic Catalyst: Catalytic and Kinetic Investigation. *J. CO_2 Util.* **2017**, *19*, 257−265.
(101) Liu, B.; Gao, Y.; Zhao, X.; Yan, W.; Wang, X. Alternating Copolymerization of Carbon Dioxide and Propylene Oxide Under Bifunctional Cobalt Salen Complexes: Role of Lewis Base Substituent Covalent Bonded on Salen Ligand. *J. Polym. Sci., Part A: Polym. Chem.* **2010**, *48*, 359−365.
(102) Darensbourg, D. J.; Wilson, S. J. Synthesis of Poly(indene carbonate) from Indene Oxide and Carbon Dioxide - A Polycarbonate with a Rigid Backbone. *J. Am. Chem. Soc.* **2011**, *133*, 18610−18613.
(103) Darensbourg, D. J.; Fang, C. C.; Rodgers, J. L. Catalytic Coupling of Carbon Dioxide and 2,3-Epoxy-1,2,3,4-tetrahydronaphthalene in the Presence of a (Salen)Cr^{III}Cl Derivative. *Organometallics* **2004**, *23*, 924−927.
(104) Darensbourg, D. J.; Kyran, S. J. Carbon Dioxide Copolymerization Study with a Sterically Encumbering Naphthalene-Derived Oxide. *ACS Catal.* **2015**, *5*, 5421−5430.
(105) Wu, G.-P.; Wei, S.-H.; Ren, W.-M.; Lu, X.-B.; Xu, T.-Q.; Darensbourg, D. J. Perfectly Alternating Copolymerization of CO_2 and Epichlorohydrin Using Cobalt(III)-Based Catalyst Systems. *J. Am. Chem. Soc.* **2011**, *133*, 15191−15199.
(106) Wu, G.-P.; Wei, S.-H.; Lu, X.-B.; Ren, W.-M.; Darensbourg, D. J. Highly Selective Synthesis of CO_2 Copolymer from Styrene Oxide. *Macromolecules* **2010**, *43*, 9202−9204.
(107) Ema, T.; Miyazaki, Y.; Koyama, S.; Yano, Y.; Sakai, T. A Bifunctional Catalyst for Carbon Dioxide Fixation: Cooperative Double Activation of Epoxides for the Synthesis of Cyclic Carbonates. *Chem. Commun.* **2012**, *48*, 4489−4491.
(108) Maeda, C.; Taniguchi, T.; Ogawa, K.; Ema, T. Bifunctional Catalysts Based on *m*-Phenylene-Bridged Porphyrin Dimer and Trimer Platforms: Synthesis of Cyclic Carbonates from Carbon Dioxide and Epoxides. *Angew. Chem., Int. Ed.* **2015**, *54*, 134−138.
(109) Ema, T.; Miyazaki, Y.; Shimonishi, J.; Maeda, C.; Hasegawa, J.-Y. Bifunctional Porphyrin Catalysts for the Synthesis of Cyclic Carbonates from Epoxides and CO_2: Structural Optimization and Mechanistic Study. *J. Am. Chem. Soc.* **2014**, *136*, 15270−15279.
(110) Liu, B.; Zhao, X.; Guo, H.; Gao, Y.; Yang, M.; Wang, X. Alternating Copolymerization of Carbon Dioxide and Propylene Oxide by Single-Component Salen Complexes with Various Axial Groups. *Polymer* **2009**, *50*, 5071−5075.
(111) Luo, M.; Zhang, X.-H.; Du, B.-Y.; Wang, Q.; Fan, Z.-Q. Regioselective and Alternating Copolymerization of Carbonyl Sulfide with Racemic Propylene Oxide. *Macromolecules.* **2013**, *46*, 5899−5904.
(112) Yue, T. J.; Ren, W.-M.; Liu, Y.; Wan, Z.-Q.; Lu, X.-B. Crystalline Polythiocarbonate from Stereoregular Copolymerization of Carbonyl Sulfide and Epichlorohydrin. *Macromolecules* **2016**, *49*, 2971−2976.
(113) Van Zee, N. J.; Sanford, M. J.; Coates, G. W. Electronic Effects of Aluminum Complexes in the Copolymerization of Propylene Oxide with Tricyclic Anhydrides: Access to Well-Defined, Functionalizable Aliphatic Polyesters. *J. Am. Chem. Soc.* **2016**, *138*, 2755−2761.
(114) Wang, L.-Y.; Gu, G.-G.; Ren, B.-H.; Yue, T.-J.; Lu, X.-B.; Ren, W.-M. Intramolecularly Cooperative Catalysis for Copolymerization of Cyclic Thioanhydrides and Epoxides: A Dual Activation Strategy to Well-Defined Polyesters. *ACS Catal.* **2020**, *10*, 6635−6644.
(115) Wang, L.-Y.; Gu, G.-G.; Yue, T.-J.; Ren, M.-W.; Lu, X.-B. Semiaromatic Poly(thioesters) from the Copolymerization of Phthalic Thioanhydride and Epoxide: Synthesis, Structure, and Properties. *Macromolecules* **2019**, *52*, 2439−2445.
(116) Liang, X.; Tan, F.; Zhu, Y. Recent Development in Ring-Opening Copolymerization of Epoxides with CO_2 and Cyclic Anhydrides for Biomedical Applications. *Front. Chem.* **2021**, *9*, 647245.
(117) Xia, Y.; Zhao, J. Macromolecular Architectures Based on Organocatalytic Ring-Opening (Co)polymerization of Epoxides. *Polymer* **2018**, *143*, 343−361.
(118) Xie, R.; Zhang, Y.-Y.; Yang, G.-W.; Zhu, X.-F.; Li, B.; Wu, G.-P. Record Productivity and Unprecedented Molecular Weight for Ring-Opening Copolymerization of Epoxides and Cyclic Anhydrides Enabled by Organoboron Catalysts. *Angew. Chem., Int. Ed.* **2021**, *60*, 19253−19261.
(119) Kummari, A.; Pappuru, S.; Chakraborty, D. Fully Alternating and Regioselective Ring-Opening Copolymerization of Phthalic Anhydride with Epoxides using Highly Active Metal-Free Lewis Pairs as a Catalyst. *Polym. Chem.* **2018**, *9*, 4052−4062.
(120) Tong, Y.; Cheng, R.; Dong, H.; Liu, Z.; Ye, J.; Liu, B. Highly Active Bifunctional Dual-Arm Organoboron Catalysts Bearing Cooperative Intramolecular Structures for the Copolymerization of CO_2 and Epoxides. *J. CO_2 Util.* **2022**, *60*, 101979.
(121) Yang, G.-W.; Xu, C. K.; Xie, R.; Zhang, Y.-Y.; Zhu, X. F.; Wu, G.-P. Pinwheel-Shaped Tetranuclear Organoboron Catalysts for Perfectly Alternating Copolymerization of CO_2 and Epichlorohydrin. *J. Am. Chem. Soc.* **2021**, *143*, 3455−3465.
(122) Asano, S.; Aida, T.; Inoue, S. 'Immortal' Polymerization. Polymerization of Epoxide catalysed by an Aluminium Porphyrin-Alcohol System. *J. Am. Chem. Soc., Chem. Commun.* **1985**, 1148−1149.

(123) Cyriac, A.; Lee, S. H.; Varghese, J. K.; Park, E. S.; Park, J. H.; Lee, B. Y. Immortal CO_2/Propylene Oxide Copolymerization: Precise Control of Molecular Weight and Architecture of Various Block Copolymers. *Macromolecules* **2010**, *43*, 7398−7401.
(124) Tsai, F.-T.; Wang, Y.; Darensbourg, D. J. Environmentally Benign CO_2-Based Copolymers: Degradable Polycarbonates Derived From Dihydroxybutyric Acid and Their Platinum-Polymer Conjugates. *J. Am. Chem. Soc.* **2016**, *138*, 4626−4633.
(125) Ren, W.-M.; Yue, T.-J.; Li, M.-R.; Wan, Z.-Q.; Lu, X.-B. Crystalline and Elastomeric Poly(monothiocarbonate)s Prepared from Copolymerization of COS and Achiral Epoxide. *Macromolecules* **2017**, *50*, 63−68.
(126) Seong, J. E.; Na, S. J.; Cyriac, A.; Kim, B.-W.; Lee, B.-Y. Terpolymerizations of CO_2, Propylene Oxide, and Various Epoxides Using a Cobalt(III) Complex of Salen-Type Ligand Tethered by Four Quaternary Ammonium Salts. *Macromolecules* **2010**, *43*, 903−908.
(127) Zhang, H.; Liu, B.; Deng, H.; Chen, J.; Duan, Z. Polycarbonates Derived from Propylene Oxide, CO_2, and 4-Vinyl Cyclohexene Oxides Terpolymerization Catalyzed by Bifunctional SalcyCo^{III}NO$_3$ Complex and its Post-Polymerization Modification. *Polymer* **2017**, *129*, 5−11.
(128) Duan, Z.; Wang, X.; Gao, Q.; Liu, B.; Kim, I.; Zhang, L. Highly Active Bifunctional Cobalt-Salen Complexes for the Synthesis of Poly(ester-*block*-carbonate) Copolymer *via* Terpolymerization of Carbon Dioxide, Propylene Oxide, and Norbornene Anhydride Isomer: Roles of Anhydride Conformation Consideration. *J. Poly. Sci. Part A: Polym. Chem.* **2014**, *52*, 789−795.
(129) Jeon, J. Y.; Eo, S. C.; Varghese, J. K.; Lee, B. Y. Copolymerization and Terpolymerization of Carbon Dioxide/Propylene Oxide/Phthalic Anhydride Using a (salen)Co(III) Complex Tethering Four Quaternary Ammonium Salts. *Beilstein J. Org. Chem.* **2014**, *10*, 1787−1795.
(130) Jeske, R. C.; Rowley, J. M.; Coates, G. W. Pre-Rate-Determining Selectivity in the Terpolymerization of Epoxides, Cyclic Anhydrides, and CO_2: A One-Step Route to Diblock Copolymers. *Angew. Chem., Int. Ed.* **2008**, *47*, 6041−6044.
(131) Wu, G.-P.; Darensbourg, D. J.; Lu, X.-B. Tandem Metal-Coordination Copolymerization and Organocatalytic Ring-Opening Polymerization via Water to Synthesize Diblock Copolymers of Styrene Oxide/CO_2 and Lactide. *J. Am. Chem. Soc.* **2012**, *134*, 17739−17745.
(132) Darensbourg, D. J.; Wu, G.-P. A One-Pot Synthesis of a Triblock Copolymer from Propylene Oxide/Carbon Dioxide and Lactide: Intermediacy of Polyol Initiators. *Angew. Chem., Int. Ed.* **2013**, *52*, 10602−10606.
(133) Varghese, J. K.; Cyriac, A.; Lee, B. Y. Incorporation of Ether Linkage in CO_2/Propylene Oxide Copolymerization by Dual Catalysis. *Polyhedron* **2012**, *32*, 90−95.
(134) Zhang, Y.-Y.; Yang, G.-W.; Wu, G.-P. A Bifunctional β-Diiminate Zinc Catalyst with CO_2/Epoxides Copolymerization and RAFT Polymerization Capacities for Versatile Block Copolymers Construction. *Macromolecules* **2018**, *51*, 3640−3646.
(135) Denk, A.; Kernbichl, S.; Schaffer, A.; Kränzlein, M.; Pehl, T.; Rieger, B. Heteronuclear, Monomer-Selective Zn/Y Catalyst Combines Copolymerization of Epoxides and CO_2 with Group-Transfer Polymerization of Michael Type Monomers. *ACS Macro Lett.* **2020**, *9*, 571−575.
(136) Cyriac, A.; Lee, S. H.; Lee, B. Y. Connection of Polymer Chains using Diepoxide in CO_2/Propylene Oxide Copolymerizations. *Polym. Chem.* **2011**, *2*, 950−956.
(137) Snyder, R. L.; Lidston, C. A. L.; De Hoe, G. X.; Parvulescu, M. J. S.; Hillmyer, M. A.; Coates, G. W. Mechanically Robust and Reprocessable Imine Exchange Networks from Modular Polyester Pre-Polymers. *Polym. Chem.* **2020**, *11*, 5346−5355.
(138) Childers, M. I.; Longo, J. M.; Van Zee, N. J.; LaPointe, A. M.; Coates, G. W. Stereoselective Epoxide Polymerization and Copolymerization. *Chem. Rev.* **2014**, *114*, 8129−8152.
(139) Nakano, K.; Hashimoto, S.; Nakamura, M.; Kamada, T.; Nozaki, K. Stereocomplex of Poly(propylene carbonate): Synthesis of Stereogradient Poly(propylene carbonate) by Regio- and Enantioselective Copolymerization of Propylene Oxide with Carbon Dioxide. *Angew. Chem., Int. Ed.* **2011**, *50*, 4868−4871.
(140) Ren, W.-M.; Liu, Y.; Wu, G.-P.; Liu, J.; Lu, X.-B. Stereoregular Polycarbonate Synthesis: Alternating Copolymerization of CO_2 with Aliphatic Terminal Epoxides Catalyzed by Multichiral Cobalt(III) Complexes. *J. Poly. Sci. Part A: Polymer Chem.* **2011**, *49*, 4894−4901.
(141) Wu, G.-P.; Xu, P.-X.; Lu, X.-B.; Zu, Y.-P.; Wei, S.-H.; Ren, W.-M.; Darensbourg, D. J. Crystalline CO_2 Copolymer from Epichlorohydrin via Co(III)-Complex-Mediated Stereospecific Polymerization. *Macromolecules* **2013**, *46*, 2128−2133.